# VLÁKNA a TEXTIL

2

Volume 24.
June
2017

ISSN1335-0617

## FIBRES AND TEXTILES

Indexed in:

Chemical Abstracts,

World Textile Abstracts

EMDASE

Elsevier Biobase

Elsevier GeoAbstracts

VÚTCH CHEMITEX

Trenčianska univerzita Alexandra Dubčeka v Trenčíne
Fakulta priemyselných technológií v Púchove

VÚCHV

Spoločnosť priemyselnej chémie ZSVTS

TECHNICAL UNIVERSITY OF LIBEREC
Faculty of Textile Engineering

STU FCHPT

# Fibres and Textiles
# Vlákna a textil

*Published by* / *Vydáva*

- Slovak University of Technology in Bratislava, Faculty of Chemical and Food Technology
- Technical University of Liberec, Faculty of Textile Engineering
- Alexander Dubček University of Trenčín, Faculty of Industrial Technologies
- Slovak Society of Industrial Chemistry, Bratislava
- Research Institute of Man-Made Fibres, JSC, Svit
- VÚTCH – CHEMITEX, Ltd., Žilina
- Chemosvit Fibrochem, JSC, Svit

- Slovenská technická univerzita v Bratislave, Fakulta chemickej a potravinárskej technológie
- Technická univerzita v Liberci, Fakulta textilní
- Trenčianska univerzita Alexandra Dubčeka v Trenčíne, Fakulta priemyselných technológií
- Slovenská spoločnosť priemyselnej chémie, Bratislava
- Výskumný ústav chemických vlákien, a.s. Svit
- VÚTCH – CHEMITEX, spol. s r.o., Žilina
- Chemosvit Fibrochem, a.s., Svit





*Editorial Office and distribution of the journal*
*(Redakcia a distribúcia časopisu)*

Ústav prírodných a syntetických polymérov
Fakulta chemickej a potravinárskej technológie
Slovenská technická univerzita v Bratislave
Radlinského 9, 812 37 Bratislava, SK
Tel: 00 421 2 59 325 575
e-mail: marcela.hricova@stuba.sk

*Order and advertisement of the journal*
*(Objednávka a inzercia časopisu)*

Slovenská spoločnosť priemyselnej chémie,
člen Zväzu vedecko-technických spoločností
Radlinského 9, 812 37 Bratislava, SK
Tel: 00 421 2 59 325 575
e-mail: marcela.hricova@stuba.sk

*Order of the journal from abroad – excepting Czech Republic*
*Objednávka časopisu zo zahraničia – okrem Českej Republiky*
SLOVART G.T.G, s.r.o. EXPORT-IMPORT
Krupinská 4, P.O.Box 152, 852 99 Bratislava, SK
Tel: 00421 2 839 471-3, Fax: 00421 2 839 485
e-mail: info@slovart-gtg.sk

*Typeset and printing at* / *Sadzba a tlač*

FOART, s.r.o., Bratislava

Journal is published 4x per year / Časopis vychádza 4x ročne
Subscription 60 EUR / Ročné predplatné 60 EUR

**ISSN 1335-0617**

Evidenčné číslo MKCR SR Bratislava EV 4006/10

# Fibres and Textiles (2) 2017
# Vlákna a textil (2) 2017
June 2017

**Content**

# DEVELOPMENT AND INVESTIGATION OF NONWOVEN WOUND DRESSINGS WITH ANTIMICROBIAL PROPERTIES ON THE BASIS OF NATURAL FIBERS

**N.P. Suprun, S.Ya. Brichka and O.I. Litvinova**

*Kyiv National University of Technologies & Design, N.-Danchenko str. 2, 01011 Kyiv, Ukraine*
suprun.knutd@mail.ru

***Abstract:*** *This article presents results of the study of elaborated nonwoven materials for wound dressings on the basis of silk and cotton fibers treated at eco-safe processing with water solutions of silver nitrate. The study of structure and surface changes in the obtained nanomodified nonwovens has been carried out with the use of methods of energy dispersive spectroscopic chemical analysis, TG-DSC spectroscopy and infrared spectroscopy.*

***Keywords*** *wound dressings, nanosilver, cotton fibres, silk fibres, ecosafe processing.*

## 1 INTRODUCTION

During the whole history of mankind wound dressings have been and remain the first aid means for stopping the bleeding and wound protection that is caused by their available and simple use under different conditions. Long since people used textile materials for covering wounds supplementing them with natural curative substances. Such dressings should not only protect a wound from contamination, but also reduce a pain. However a role of textile material in treatment of wounds has remained passive protective. “Therapy under dressings” even now remains one of the basic methods of conservative wound treatment, and in some cases (at concurrent diseases, extensive lesions, surgical contra-indications) practically the only one. A timely stop of bleeding, processing of open wounds with antimicrobial substances, covering of the surface of burnt skin, removal of pain and edema, and also other actions in emergency situations help to save a life and to minimize consequences of wounds and traumas.

Last years in the world practice the use of wound dressings of a new type having a prolonged medical and antimicrobial action has become widespread. Modern wound coverings should provide a complex impact on a wound: delete effectively excess wound exudate and its toxic components, provide adequate gas exchange between a wound and air, prevent secondary wound infection and contamination of objects of the environment, assist in creation of optimum dampness of a wound surface, have low-adherence and sufficient mechanical strength [1-3]. A distinctive feature of a new generation of wound dressings is provision of targeted transport of drugs to wound with their controllable release of required concentration. A prolonged curative action of such materials excludes a necessity of frequent change of dressings, does not affect the process of wound healing, facilitates work of medical staff and enables first self-help to a wounded or injured person.

Issues on production of wound coverings of a new generation are in the center of attention of leading manufacturing companies of the USA, Germany, Great Britain and other developed countries.

Present-day wound dressings with a prolonged curative and antimicrobial action are in fact composites comprised at least of three components: a textile basis, a polymeric layer and a pharmaceutical drug. At this a textile basis is considered not as an inert substrate – it is selected proceeding from set mechanical and physical properties, and also from provision of a required prolonged action of antiseptic agents and medicines. Among different textile structures used as bases for wound dressings, nonwoven materials [1, 3] are considered to be the most promising ones. They have high absorptive ability enabling to facilitate a procedure of their processing with pharmaceutical drugs, to provide ease of passing and sorption of sweat and wound excretions. They are easily cut in any directions without affecting the structure, can contact freely with open wound surfaces. Nonwovens are easy- and convenient-to-use, pleasant- and soft- to-touch, and they are characterized with low cost - unlike woven and knitted fabric, their manufacture does not require the use of complex equipment.

Wound dressings have many performance criteria, such as the need to protect the wound surface, the ability to absorb wound exudate, the ease of application and removal, but the main is its antimicrobial function, desirably, with a prolonged action. For this purpose different groups of antimicrobial substances belonging to different classes of organic and inorganic compounds are used. At present there is an obvious tendency to the use of low-toxicity antimicrobial additives among which special attention is paid to nanosilver processing. Silver has a long history as an antimicrobial agent [4]. In recent years it has been successfully used as an effective antimicrobial agent for wound management and silver-containing wound dressings are now widely used throughout the world. Silver is more universally effective than antibiotics, more broadly powerful than chlorine and blocks the growth of gram negative and gram positive bacteria, fungi, viruses and yeast. An important feature of ionic silver is that it kills detrimental microbes but it is non-cytotoxic to proliferating granulation tissue, in the right concentrations [5-7]. Also silver is deprived in many respects of lacks connected with a problem of resistance of pathogenic microorganisms [8].

With the development of nanotechnologies scientists of the world evidenced coming back of a “silver era” in medical practice. An active use of silver nanocomposites for textile impregnation is determined by significant and incontestable advantages over all existing antimicrobial means due to it wide range of antimicrobial activity. Disinfecting properties of nanosilver reveal themselves through its surface contacting with microorganisms. In the form of nanoparticles silver gets unique properties due to extremely big specific area of the surface which increases an area of contact with bacteria, improves an antimicrobial action and enables to reduce silver concentration by hundred times preserving all bactericidal properties [9].

The purpose of the work is to develop nonwoven materials on the bases of natural fibers for wound dressings with bactericidal properties provided due to nanosilver processing.

## 2 EXPERIMENTAL AND METHODS

With the use of cotton and silk fibres by means of a needle-punching method we have obtained two types of nonwoven materials for their further use as a textile basis for wound dressing. To provide antibacterial properties the process of silver recovery from water solution of silver nitrate in the presence of a surface-active substance with the use of glucose as a reducer has been used for introduction of silver nanoparticles in nonwovens [10]. Such conditions provide eco-safety of the process which is important for materials contacting with open wounds.

Antibacterial properties of the obtained colloidal solution were checked with the use of reference strains *S. aureus* UKM V-904 (ATSS 25923), *E. coli* UKM V-906 (ATSS-25922) and *P. aeruginosa* UKM V-907 (ATSS-27853) by Gratsia method [11]. The presence of antimicrobial properties as to the used test strains of microorganisms was determined according to occurrence of areas of absence of growth on the place of solution application. Correctness of the carried out experiment was estimated by presence of a clarification zone on the place of application of a positive control sample and by absence – on the place of application of a negative control sample. The carried out experiments evidenced that starting sol of silver nanoparticles depresses in a different measure the growth of microorganism strains studied. *S. aureus* turned out to be the most sensitive to a sol action, *E. coli* – the least sensitive.

The structure of initial and silver nanomodified materials was characterized by a method of scanning electronic microscopy with the use of microscope MIRA3 LMU, Tescan with the resolution of ±1 nm and with the energy dispersive spectroscopic chemical analysis system Oxford X-MAX 80 $mm^2$; uncertainty of the device - ±1%. Information on qualitative composition of samples and interaction between components of material was received from the analysis of arrangement and intensity of maxima in infrared spectra measured at an ambient air temperature with spectrometer IR Affinity-1, Shimadzu within 4000-550 $cm^{-1}$ with the use of multiple attenuated total internal reflection attachment with a diamond tip and uncertainty of the device of ±2 $cm^{-1}$. TG-DSC spectra of materials were measured with the thermal analyzer SDT Q600, Intertech within 25-800°C in the airflow with a heat rate of 10 K/min; uncertainty of the device ±2% (DSC), ±0.001 mg (TG). UV visible spectra of silk and cotton materials were registered on UV-VIS-NIR-spectrophotometer UV-3600, Shimadzu in the transmission mode within 220-800 nm with uncertainty of the device of ±1 nm.

## 3 RESULTS AND DISCUSSION

Images of the fibre surface of silk nonwoven samples under study before and after modification with colloidal silver obtained by a method of scanning electronic microscopy are given in Figure 1. Original fibers of silk with distribution by a diameter of 10-50 μm look like flat formations more often twisted in a tubular form (Figure 1a).

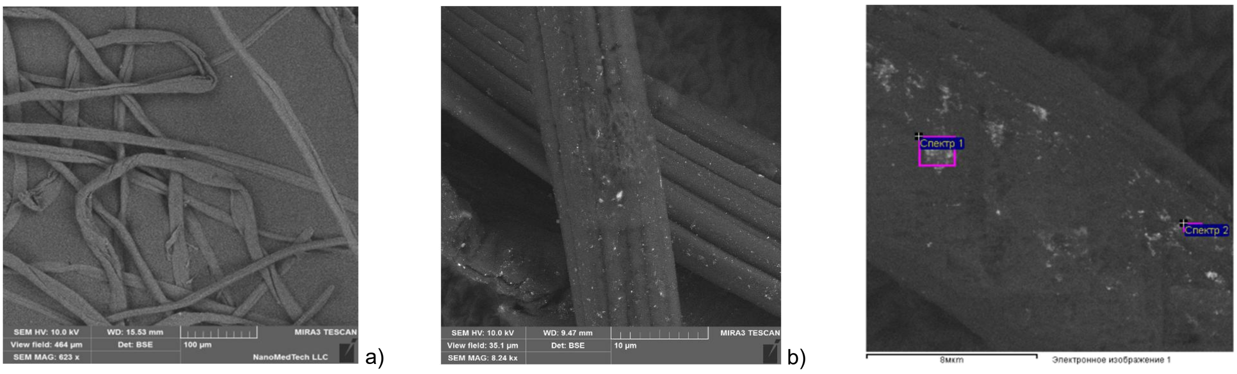


a) b) c)

**Figure 1** Photos of scanned electronic images of the nonwoven silk surface: (a) - original, (b) - modified with silver nanoparticles, (c) - areas selected for chemical energy dispersive analysis

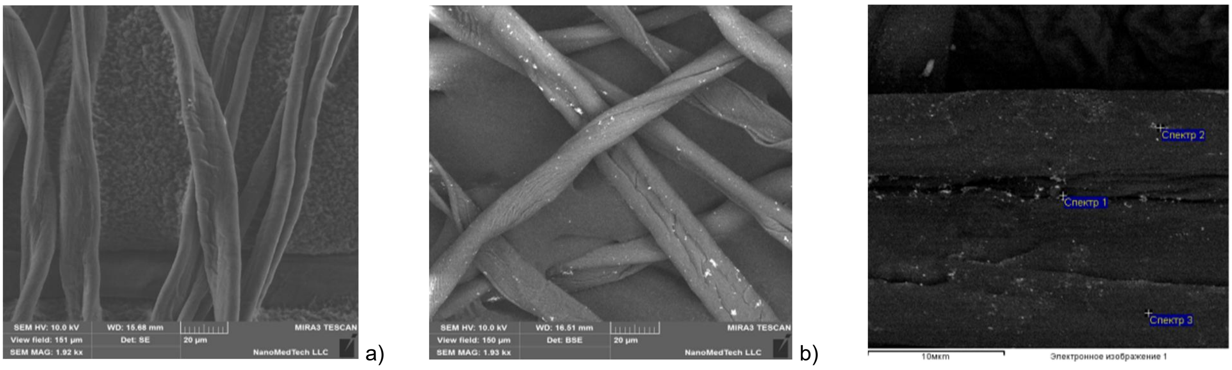


a) b) c)

**Figure 2** Photos of scanned electronic images of the nonwoven cotton surface: (a) - initial, (b) - modified with silver nanoparticles, (c) - areas selected for chemical energy dispersive analysis

Their length exceeds obviously millimetric indices. After application of particles of synthesized colloidal solution the light areas which relate to a modifier appeared on SEM images. Contrast is caused by heavier silver atoms. 5-15 nm particles can be observed next to agglomerates which we have related to silver nanoparticles.

The evidence of modification with silver nanoparticles is chemical elemental analysis in the selected area (Figure 1c). In spectra such elements as carbon, oxygen and silver (only in modified silk) have been registered. It should be noted that the content of elements less than 1% is not registered in energy dispersive analysis. C/O ratio for all samples is of the same order which mean that the state of silver is ionic; its content on different sites differs significantly y times (Table 1).

**Table 1** Results of chemical energy dispersive analysis of initial and Ag-modified silk in the selected areas

| Elements / the area of analysis | C | O | Ag |
|---|---|---|---|
| | content [%] | | |
| initial | 75.78 | 24.22 | - |
| initial | 72.85 | 27.15 | - |
| range 1 | 73.93 | 21.10 | 4.97 |
| range 2 | 71.26 | 14.95 | 13.79 |

Nanosilver particles are also registered on the surface of cotton fibres of nonwoven samples (Figure 2). In spectra of chemical energy dispersive analysis such elements as carbon, oxygen and silver have been registered only in modified cotton (Table 2).

**Table 2** Results of chemical energy dispersive analysis of starting and nanosilver-modified cotton nonwovens in the selected areas

| Elements / the area of analysis | Content [%] | | |
|---|---|---|---|
| | C | O | Ag |
| Initial | 75.33 | 24.67 | - |
| Initial | 78.6 | 21.4 | - |
| range 1 | 26.36 | 17.53 | 56.11 |
| range 2 | 95.85 | 0 | 4.15 |
| range 3 | 78.63 | 21.37 | - |

For development of effective technology for creation of wound dressing it is important to determine changes in the thermal behavior of fibers after modification. TG-DSC analysis of spectra testifies to the fact that initial and nanosilver-modified silk samples (Figure 3) have a similar two-stage mechanism of burning with mass loss and exothermic enthalpy of 1331-1338 and 1226-1765 J/g.

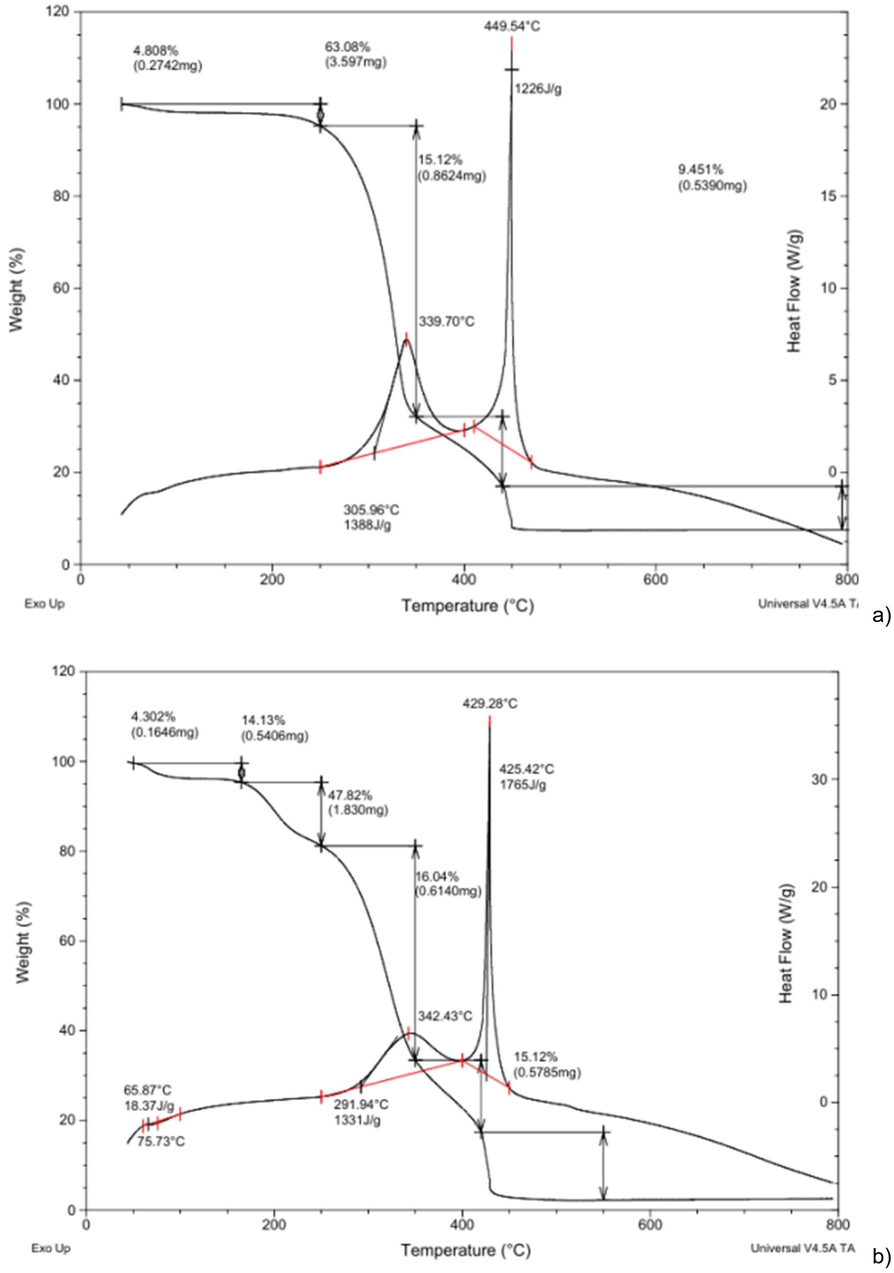


**Figure 3** TG-DSC spectra of nonwoven silk samples: a - initial, b - modified with silver nanoparticles

Divergence in a thermal effect of high temperature maximum of more than 20% may relate to participation of modifiers - silver, surface-active substances and other impurities during burning. It is also confirmed with much bigger mass loss about 5.5% at more intensive thermal destruction of material. Maxima of exothermic effects make 339.7, 342.43 and 449.54, 429.28°C respectively for silk and silk/Ag. There were no significant changes in thermal stability (Figure 3 for DSC curves). Samples lose mass equally 4.302-4.808% up to 200°C with an endothermic effect that, as a rule, is connected with desorption of adsorbed water. The unexpected strongly pronounced stage of mass loss without a pronounced thermal effect (Figure 3 for TG curves) can be observed within 200-250°C in the modified sample. Similar studies were done for the nonwoven cotton samples (Figure 4).

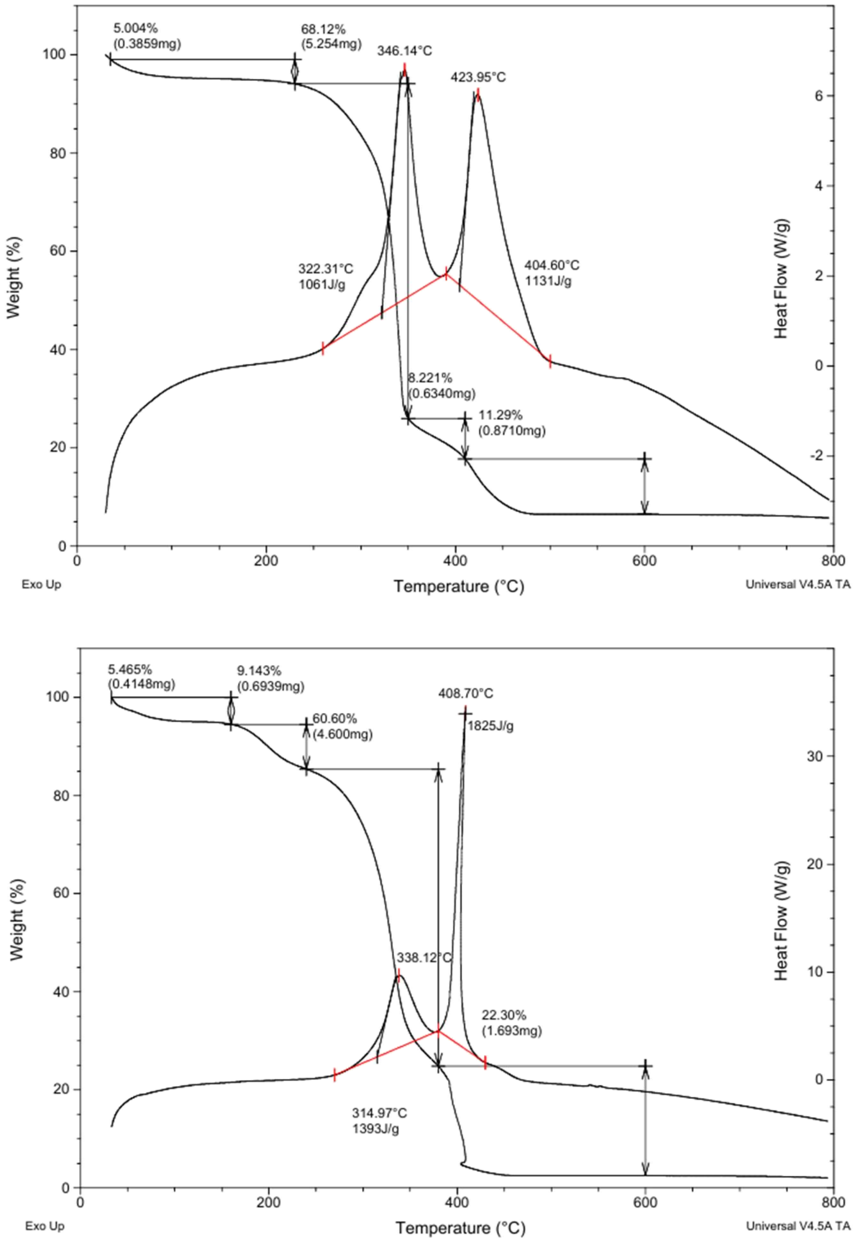

a)

b)

**Figure 4** TG-DSC spectra of nonwoven cotton samples: a - initial, b - modified with silver nanoparticles

Information on qualitative composition of samples and interaction between components of material has been received from the analysis of arrangement and intensity of maxima in infrared spectra. By comparing the obtained IR spectra of samples of initial (a) and silver-modified silk fibres (Figure 5) we can see that valence vibrations of OH- and NH-groups have not changed significantly at 3335 and 3302 $cm^{-1}$. It is obvious that physical or chemical interaction between the modifier and fibres is not set. Mechanical interaction between silver nanoparticles and silk has not been shown spectroscopically because of a small number of contacts between hydroxyl groups and silver with surface-active substances. A number of bands of valence vibrations of the -CH groups at 2895 $cm^{-1}$ testify to an energetically unequivalent condition of groups relating to linear and aromatic structural fragments. There were no redistributions of maxima and intensities and it was logical because of strength of polar covalent weak C-H bonds. A wide band with maximum of 1648 $cm^{-1}$ relates to valence vibration C=O. Deformation vibrations of -NH2 and -NH groups can contribute to this sphere. A number of bands in the range of 1450-591 $cm^{-1}$ frame vibrations relate to single and collective valence vibrations C-C, C-O and deformation vibrations -CH. Insignificant weakly intensive divergences of two samples can be explained by the influence of organic modifiers or silk heterogeneity.

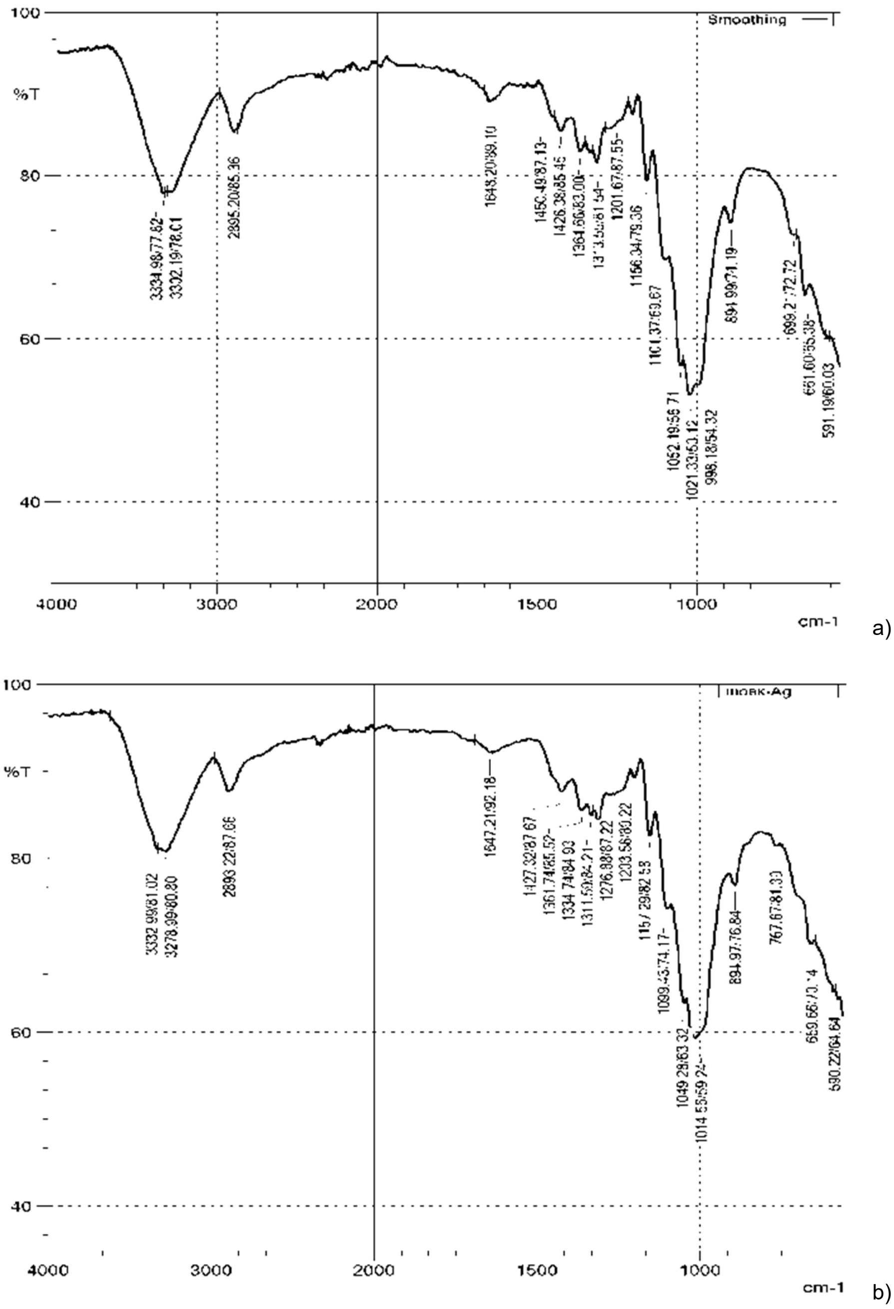


**Figure 5** IR spectra of nonwoven silk samples: a - initial, b - modified with silver nanoparticles

Cotton is a biopolymer to which the basic absorption bands of deformation and valence vibrations characteristic for polysaccharides correspond. In the spectrum of starting cotton in the field of 3600 $cm^{-1}$ there are bands of valence vibrations of –OH bond of different groups (primary, secondary, tertiary). This wide band has two maxima of 3332 $cm^{-1}$ primary –OH and 3279 $cm^{-1}$ – secondary -OH. Valence vibrations C-O of different groups (C-OH - primary, OH - secondary, C-O-C - cyclic, C-O-C - intercycle (glycosidic linkage) are shown in the field of 900-1200 $cm^{-1}$ in the form of a complex band with several maxima which correspond to these bonds, respectively: 1000 $cm^{-1}$, 1028 $cm^{-1}$, 1054 $cm^{-1}$, 1106 $cm^{-1}$, 1159 $cm^{-1}$. There are also bands of valence and deformation vibrations C-H in the spectrum - linkage of different groups. A strip with the maximum of 2895 $cm^{-1}$ corresponds to valence vibrations of -CH- group, and in the field of 1300-1500 $cm^{-1}$ to deformation vibrations -CH both of a cyclic and a skeletal type.

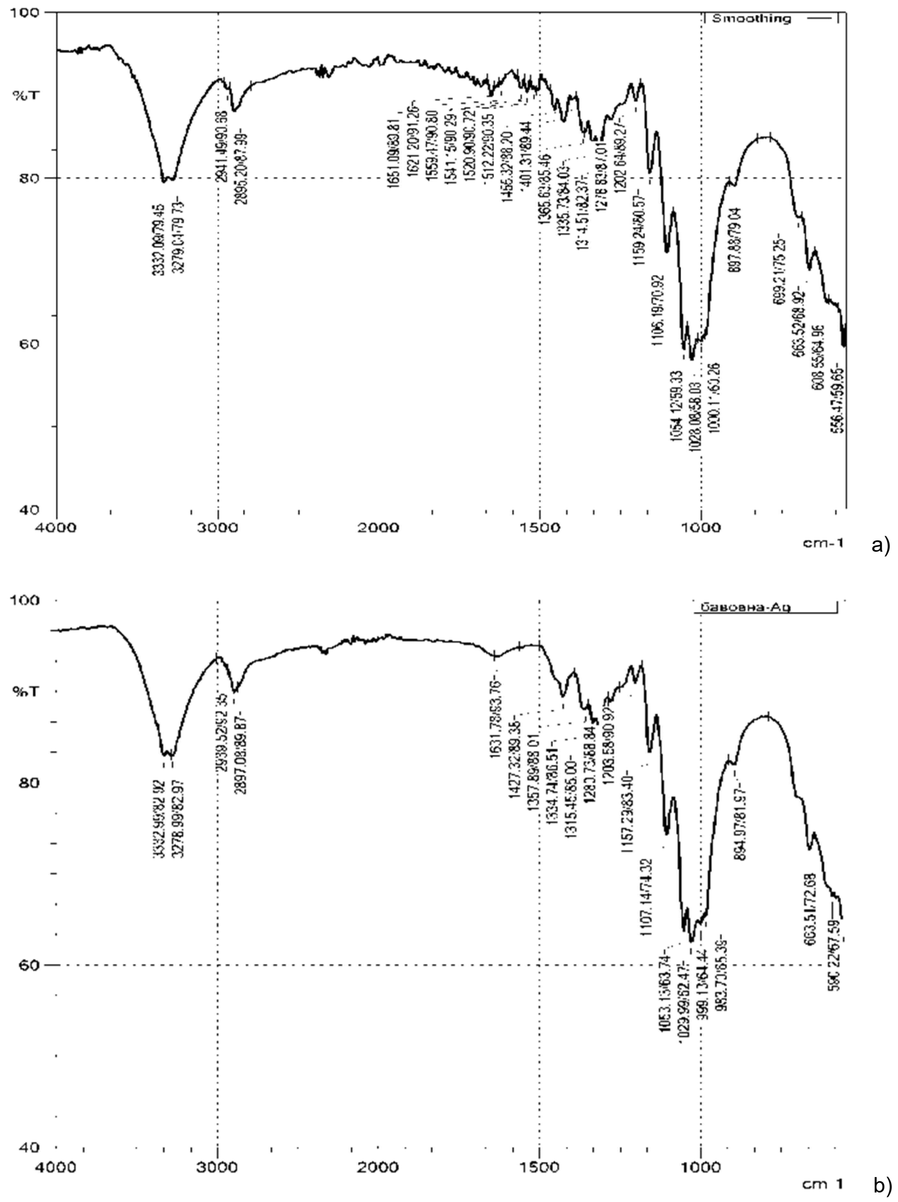


**Figure 6** IR spectra of nonwoven cotton samples: a - initial, b - modified with silver nanoparticles

So the analysis has confirmed that samples of nanomodified cotton contain primary and secondary OH- groups having properties to form a hydrogen bond of different force. Primary groups form such a bond faster, but it is weaker as regards interacting force, and secondary groups do it slower, but the bond is stronger. Just this provides ability of silver particles to be sorbed well at processing of nonwoven cotton cloth with $AgNO_3$ solution due to hydrogen bonds and to stay on the surface and inside the molecules. It is obvious that physical or chemical interactions between a modifier (silver) and fibres are not set; neither chemical nor physical nature of polysaccharide does not change.

## 4 CONCLUSIONS

Silver-containing fibrous nonwoven fabrics on the basis of cotton and silk fibres have been obtained for their use as a bactericidal textile basis for wound dressings. Experiments evidenced that sols of silver nanoparticles used for nonwoven materials processing depresses the growth of microorganism strains studied. The study of the structure and properties of obtained fabrics has been carried out with the use of methods of scanning electronic microscopy, energy dispersive spectroscopic chemical analysis and infrared spectroscopy.

## 5 REFERENCES


1. Advanced textiles for wound care. Edited by Rajendran S.: Woodhead Publishing Limited, 2009
2. Boateng J.S., Matthews K.H., Stevens H.N., Gillian M.E.: Wound Healing Dressings and Drug Delivery Systems. A Review, Journal of Pharmaceutical Sciences 97(8), August 2008, pp. 2892-2923
3. Handbook of Medical Textiles. Edited by Bartels V.T.: Woodhead Publishing Limited, 2011
4. Klasen H.J.: Historical review of the use of silver in the treatment of burns. I .Early uses, Burns 26(2), 2000, pp. 117-130
5. Landage S.M., Wasif A.I.: Nanosilver - an effective antimicrobial agent for finishing of textiles, International Journal of Engineering Sciences & Emerging Technologies 4(December), 2012, pp. 66-78
6. Alexander J.W.: History of the medical use of silver, Surgical Infections 10(3), 2009, pp. 289-292
7. Chen A.X.; Schluesener H.J.: Nanosilver: a nanoproduct in medical application, Toxicology Letters, 176(1), 2009, pp. 1-12
8. Supotnitskiy M.V.: Mechanisms of Antibiotic Resistance in Bacteria, Biopreparaty 2, 2011, pp. 4-44
9. Chmielowiec-Korzeniowska A., Krzosek L., Tymczyna L., Pyrz M., Drabik A.: Bactericidal, fungicidal and virucidal properties of nanosilver. Mode of action and potential application. A review, Annales Universitatis Mariae Curie-Skłodowska, XXXI (2), Sectio EE. 2013
10. Vishnyakova E.A., Saykova S.V., Zharkov S.M., Likhatskaya M.N., Mikhlin J.L.: Determination of conditions for the formation of silver nanoparticles in the reduction of glucose in aqueous solutions, Journal of Siberian Federal University, Chemistry 1(2), 2009, pp. 48-55
11. Elfarash A., Dingemans J., Ye L., Hassan A.A., Craggs M., Reimmann C., Thomas M.S., Cornelis P.: Pore-forming pyocin S5 utilizes the FptA ferripyochelin receptor to kill Pseudomonas aeruginosa, Microbiology 2, 2014, pp. 261-269

# RESEARCH OF TOPOGRAPHY OF INFLUENCE AND CLASSIFICATION OF THE REQUIREMENTS FOR UNIFORM OF PASSENGER CAR ATTENDANTS

**I.O. Prykhodko-Kononenko, O.V. Kolosnichenko, N.V. Ostapenko, M.S. Vinnichuk and M.V. Kolosnichenko**

*Kyiv National University of Technology and Design, Nemirovicha-Danchenka str. 2, 01011 Kyiv, Ukraine*
*3212793@gmail.com*

***Abstract:*** *The article investigates the theoretical foundations of the study of reliability indicators in order to identify priorities in development of efficient uniform for the passenger car attendants with predictable properties. Thus, functional and constructive design is carried out, taking into account the topography of influence by defining zones of influence on different parts of the garment, what enables development of variable constructive and functional solutions for the uniform in accordance with the quality requirements.*

***Keywords:*** *uniform of passenger car attendants, reliability indicators, list of hazardous and harmful operational factors, predictable properties.*

## 1 INTRODUCTION

At present, departmental uniform is used by the customs officers, taxmen, prosecutors, bailiffs, foresters, transport workers and other officials. The main requirements in design of the uniform of any department have always been and still are the following: aiming for maximum comfort, practicability, versatility and originality. At the same time, development of new and unique collections set an objective for the designers: to promote imaginative perception of the personnel of the departments as professionals, inspiring confidence, whose appearance should inform about respectability and reliability of the company as a whole. That is why the railwaymen, who never take off their uniforms (unlike many departments, which historically diverged from wearing uniforms), are still considered to be a reputable company.

Among the employees of the rolling stock of passenger rail transport passenger car attendants are the largest group, but their working conditions and health status have been poorly examined. Railway professions are classified as hazardous. Work of the passenger car attendants of the railroad passenger service is associated with permanent influence of a number of physical, chemical, biological, psychological and other factors on the body: temperature jumps, noise, vibration, dust, high levels of microbial contamination of air and cars, disturbance of sleep and rest regime, physiological and emotional stress, etc. [1-4].

## 2 EXPERIMENTAL

Accidents arising in connection with the use of poor quality, out-dated equipment and violation of the procedure for carrying out hazardous works, etc., pose threat to work and health of the personnel and passengers. The analysis of the operating activity of the passenger car attendants resulted in development of the list of hazardous and harmful occupational factors (HHOF). Development of industrial technologies enhances the influence of the HHOF, what requires increased level of protection of a person through the use of new structural and technological solutions and materials for clothes. Therefore, it is advisable to constantly improve the design and manufacturing process of the uniforms in order to improve its quality.

Based on the analysis of professional activity and developed list of hazardous and harmful occupational factors, the topography of their influence on the uniform of the passenger car attendants has been studied (Figure 1).

The topography of influence includes the effect of perspiration, light weather, residual deformation (stretching, bending), industrial pollution, wearing in the plane, destruction of materials and joint places of clothes (breaking), what requires extra attention in the process of design of reliable and durable articles.

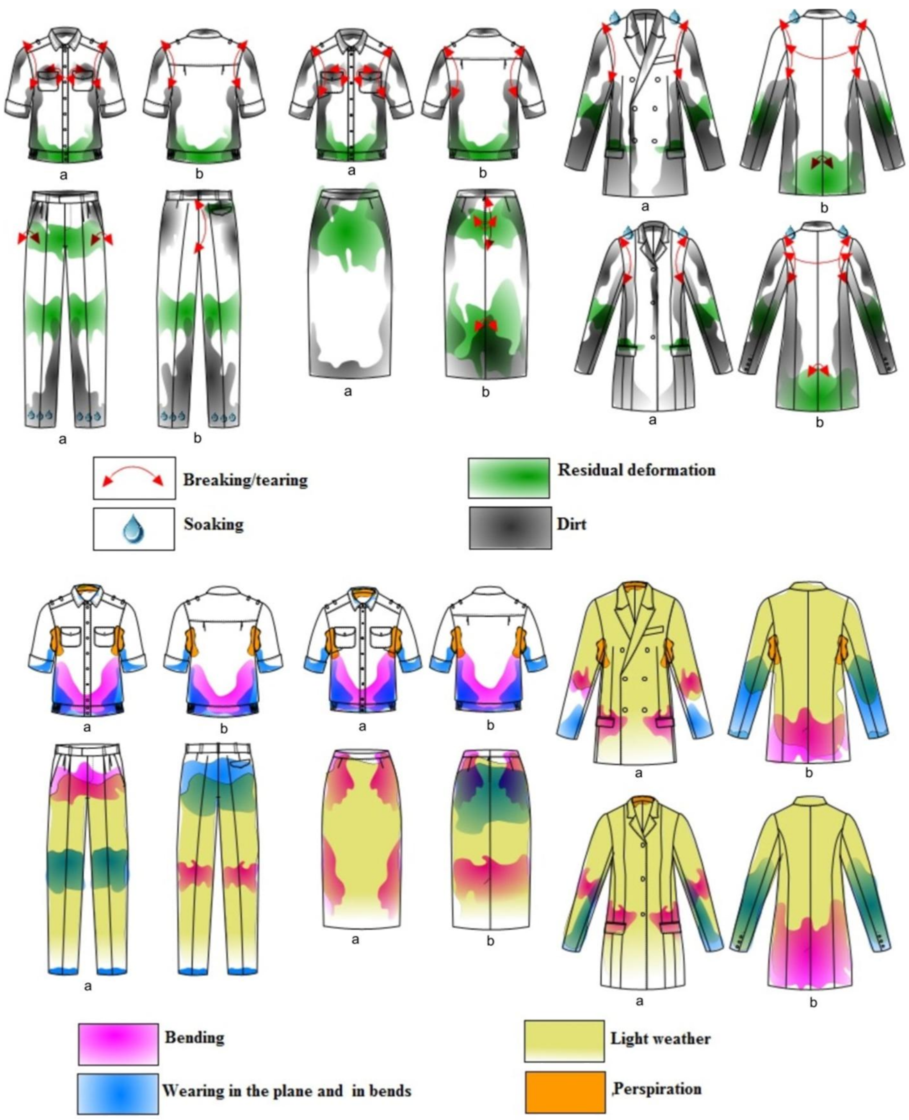


**Figure 1** The topography of influence of the HHOF on women`s and men`s uniform (shirt, trousers, jacket, blouse, skirt, coat) of the Ukrzaliznytsia passenger car attendants: a - front view, b - back view

The data provided in Figure 2 have been obtained by the research wearing of the uniform by the customers; the analysis has been carried out by the expert estimation method. The results have been processed by application of the mathematical statistics methods. A range of disadvantages have been revealed; the demand of the employees has been studied for the purpose of further application of the results of the survey in the course of designing the reliable and comfortable clothing.

The main requirements to be met by the uniform include protection from hazardous and harmful occupational factors (HHOF) (Figure 2), ensuring occupational safety, maintenance of normal functional state of a human and his/her performance, and, of course, clothing must not have a toxic effect on a human body while its use and production. The content of the questionnaire also included the issues of the main and additional requirements for the materials, model and technological peculiarities of clothing, and requirements for the design and ergonomics, as well.

The survey results have showed that the current uniform has a range of disadvantages: the construction of armhole (creates discomfort during moves) and neck hole (quickly becomes dirty) do not meet the requirements for comfort; are not comfortable (at the placement) and have unreliable pockets (tear off quickly); insufficient number of pockets in clothing; deficient tailoring of longitudinal sections (vent); lower sewn underplacket (in a blouse) creates inconveniences; materials are unpleasant to the touch, air-impermeable and electrifiable.

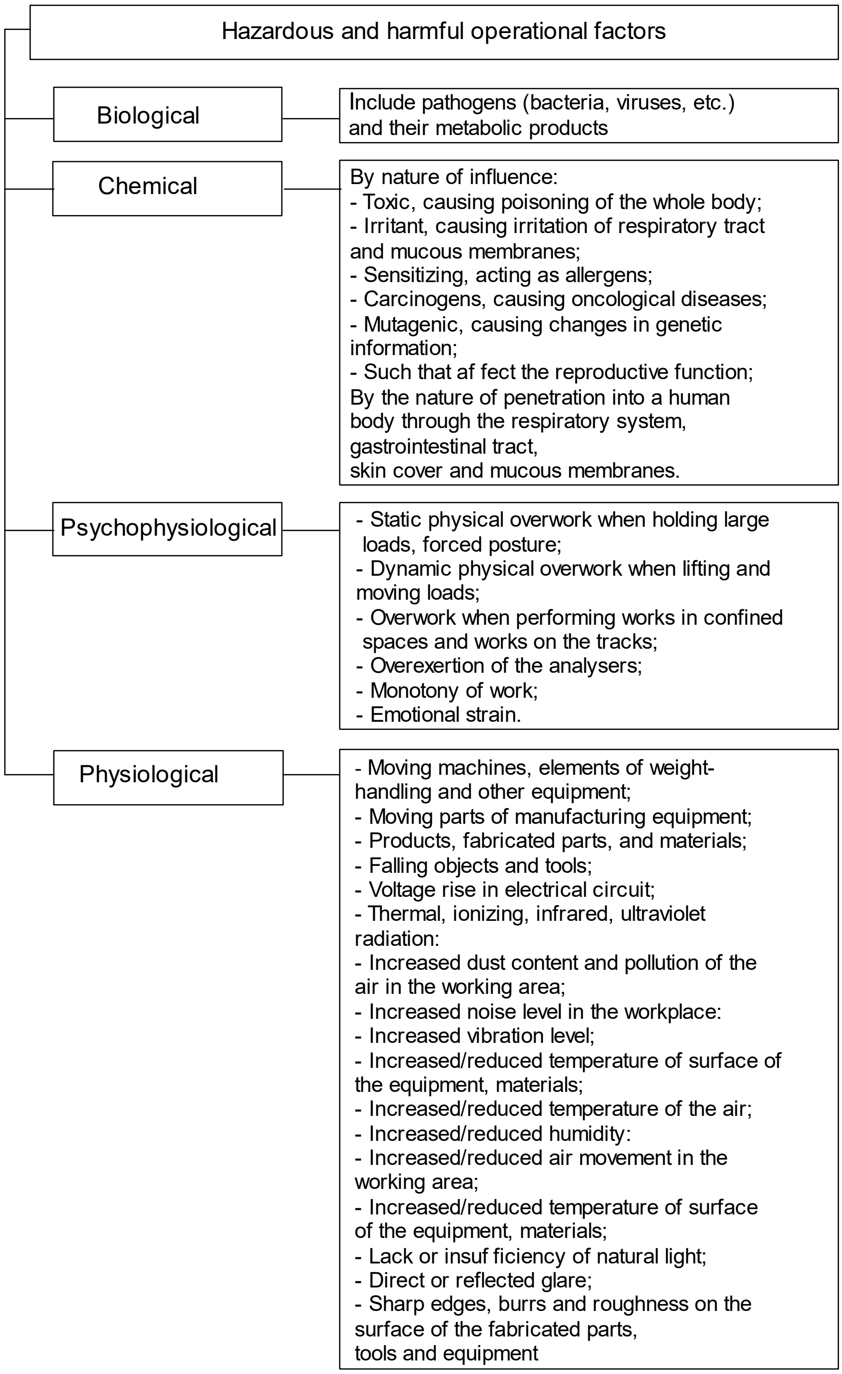


**Figure 2** List of hazardous and harmful operational factors

Specificity of working environment and climatic conditions, HHOF types, their intensity, frequency became the basis for development of the theoretical foundations of the study of reliability indicators in order to identify priorities in development of efficient uniform for the passenger car attendants with predictable properties. Thus, functional and constructive design is carried out, taking into account the topography of influence by defining zones of influence on different parts of the garment, which enables the development of variable structural and functional solutions for the uniform in accordance with the quality requirements.

A critical review of the current state of the problem of development of the current uniforms revealed the necessity for its improvement. Before starting to design the uniforms, it is necessary to develop scientifically grounded requirements for such design [5-7]. The requirements for the uniforms must satisfy certain aspects of consumption and manufacturing. In this relation, they may be divided into consumer and manufacturing. Feasibility of manufacturing and marketing of an article determines social qualities of such article.

## 3 RESULTS AND DISCUSSION

The uniform of the passenger car attendants shall meet a set of stringent and contradictory requirements, conditioned by its functional use. Analysis of the current uniforms of the Ukrzaliznytsia passenger car attendants allowed to establish that it does not fully take into account the actual working conditions and hinders movements. It should also be noted that the current package of the materials has not been differentiated in accordance with the topography of influence of different HHOF and their intensity, etc. A key component of the design process for new types of the uniform of the Ukrzaliznytsia passenger car attendants shall be development of constructive and technological solutions in each project case. So, uniform of the Ukrzaliznytsia passenger car attendants shall have ergonomic and aesthetic design in order to ensure the highest possible level of protection, convenience and good appearance.

The uniform of the Ukrzaliznytsia passenger car attendants must: ensure adequate protection level against all types of hazards; have such structure that would provide the maximum possible level of ergonomics and aesthetics; not to create obstacles for the person performing the work; ensure "harmlessness", i.e. will not create additional risk factors; ensure the highest possible level of comfort; have a maximum permissible limitation of movements, position or sensory perception of the passenger car attendant and not cause movements that may pose a threat to him or passengers; provide perfect fitting of the garment and fixation on the body in the process of its use regardless of environmental conditions, movements and posture of the passenger car attendant; be compatible with other existing articles; carry information about the position, field of application; provide easy recognition among the employees; ensure extension of the period of its use, provided by the possibility of reparability or replacement of separate components of the uniform, provide fixed sizes and shape for a given period of use; have such structure that would provide its easy and correct wearing; provide comfortable microclimate and space under clothes. Compliance with these requirements in the process of design and manufacturing of the uniform for the Ukrzaliznytsia passenger car attendants provides high efficiency of work and reduces negative impact of environmental factors on a person. Uniform of the passenger car attendants shall conform to its functional use, not hinder the movements, ensure easy care (laundry); fabric shall be resistant to abrasion, mechanical damage, etc.

Analysis of uniforms and requirements made it possible to establish product range, which consists of jackets, coats, blouses, shirts, trousers, skirts, etc. Depending on the conditions, these products are used as a particular set of clothes. On the basis of the carried out analysis, the list of the quality indicators of men`s and women`s uniform of the passenger car attendants has been suggested separately for the upper body garments and lower body garments. According to the results of the previous calculations, we singled out 19 significant indicators for the upper body garments (jacket, coat) (Table 1) out of 39 suggested indicators, 16 significant indicators out of 38 – for blouse and shirt, 16 out of 30 – for men's lower body garment (trousers), 15 out of 29 - for women`s lower body garment (skirt).

The reliability indicators characterize the ability of the material or clothing to perform the specified functions while keeping their operational indicators within the set limits for a specified period of time.

Ergonomics indicators characterize the system "worker – uniform – occupational environment" containing the elements that interact with each other, namely, a person, set of the uniform and environment in which the worker carried out his activity. Structural and technological indicators determine manufacturability of design of the article, labour costs and terms for manufacturing of the article. Manufacturability of the clothes is determined by the possibility of using optimal, economic and technological methods during manufacturing process, the most efficient techniques and articles processing methods. Aesthetics indicators play an important role in assessing the appearance, artistic and coloristic decoration of the material or uniform.

The following indicators should be noted among the cost effectiveness indicators: product cost and expenses for garment care. Based on these very indicators, the railway personnel limited imagination of the designers: only assemblies of summer and winter clothes and cost of the materials and accessories of suitable quality. Therefore, we proposed a list of the quality indicators of men`s and women`s uniform for the passenger car attendants (Table 2).

Among consumptive qualities of a set of the uniform, significance of the indicator or requirement is characterized by the coefficient. Value of the coefficients of the significance indicators is established by the expert assessment method by significance ranking n of the indicator (requirement). The most significant indicator is denominated with a rank $R = 1$, and the least significant – $R = n$. Having analysed the obtained coefficients of significance and statistic criteria we established the ranking of significance of the quality indicators, represented in Table 2.

**Table 1** List of the quality indicators of the uniform of the passenger car attendants

| Group of requirements significance [%] | Property | Quality indicator and means for its ensuring (M*, S*, T*) |
|---|---|---|
| 1 | 2 | 3 |
| **1. Ergonomic 33%** | Sanitary conformance | 1.1 Water permeability coefficient, M |
| | | 1.2 Water-absorption quality, M |
| | | 1.3 Air permeability coefficient, M |
| | | 1.4 Thermal conductivity coefficient, M |
| | | 1.5 Content of natural fibre in raw material components, M |
| | Psychophysiological conformance | 1.6 Ease of using, S, T |
| | | 1.7 Surface resistivity, M |
| | Anthropometric conformance | 1.9 Dynamic conformance, S |
| | | 1.10 Static conformance, S |
| **2. Reliability 27%** | Durability of materials and structures | 2.1 Dyeing fastness (dry-cleaning, wet processing, light weather, perspiration) M |
| | | 2.2 Number of lint, M |
| | | 2.3 Breaking strength of seam, T |
| | | 2.4 Number of cycles of wearing in the plane and in bends, M |
| | | 2.5 Dust content coefficient, M |
| | | 2.6 Change in linear dimensions after wet processing and dry-cleaning, M |
| | | 2.7 Thread shifting, M |
| | | 2.8 Number of launderings and dry-cleanings before loss of market condition, M |
| | | 2.9 Remaining strain, M |
| **3. Aesthetic 20%** | Composition perfection degree | 3.1 Availability of distinguishing features, S, M |
| | | 3.2 Conformance of decoration to appearance, S, M |
| | | 3.3 Artistic and coloristic decoration of fabrics, M |
| | Market condition | 3.4 Conformity to structural and harmonious image and aesthetics, S, M |
| | | 3.5 Level of technical performance of the garment, T |
| | | 3.6 Degree of bleaching, M |
| | | 3.7 Crease resistance coefficient, M |
| | | 3.8 Fitting, S |
| | | 3.9 Dimensional stability of the garment, S, T |
| **4. Economic 13%** | Conformance of the finished product to the proposed price | 4.1 Product cost, M, T, S |
| | | 4.2 Expenses for garment care, M |
| | | 4.3 Expenses for repair, M, T, S |
| | | 4.4 Garment quality/price ratio, M, T |
| **5. Structural and technological** | Conformance to structural and technological solution | 5.1 Total labour intensity, S, T |
| | | 5.2 Flaking of cuttings, M |
| | | 5.3 Availability of lining, S, M |
| | | 5.4 Structural segmentation of the form, S |
| | | 5.5 Maintainability, S, M |
| | | 5.6 Availability of elements for fixation of belt and differentiating marks, S, T |
| | | 5.7 Quality of processing treatment S, T |
| | | 5.8 Elasticity of busting seam, T |
| | | 5.9 Direction and position of segmentation lines, S, T |
| | | 5.10 Availability of inside pockets T |
| | | 5.11 Quality of fabric-to-fabric bonding, T |

*M – materials, *S – structure, *T - technology

Table 2 shows that 19 significant indicators have been identified out of 39 suggested indicators for the upper body garments (jacket, coat); similar calculations have been carried out for all items used in a set of the uniform. 16 significant indicators have been identified out of 38 indicators for blouses and shirts in the course of the analysis, 16 out of 30 – for men's lower body garment (trousers), 15 out of 29 – for women`s lower body garment (skirt).

Analysis of the estimates obtained from the experts required concordance of their opinions by a number of factors affecting the final result. It was suggested to estimate the concordance of the expert opinions through the concordance coefficient *W*, which is common rank correlation coefficient for the group consisting of m experts. The sequence of calculation involves first calculating the sum of the grades (ranks) for each separate factor obtained from all experts, and then calculating the difference between this sum and the average sum of the ranks. For this purpose, it is necessary to calculate the sum of the estimates (ranks) for each factor obtained from all experts $\sum_{j=1}^{m} x_{ij}$, and then calculate the difference between this sum and the average sum of the ranks

$$\Delta_i = \sum_{j=1}^{m} x_{ij} - T \tag{1}$$

where the value $T$ shall be calculated by the following formula:

$$T = \frac{\sum_{i=1}^{n}\sum_{j=1}^{m} a_{ij}}{n} \tag{2}$$

and separate estimations $a_{ij}$ shall be calculated by:

$$a_{ij} = -\frac{1}{2}m(n+1) \quad (3)$$

Further calculation provides for determination of the parameter $S$ by the following formula:

$$S = \sum_{i=1}^{n}\left\{\sum_{j=1}^{m} x_{ij} - \frac{1}{2}m(n+1)\right\}^2 \quad (4)$$

The value $S$ is considered to be maximum if all experts put the same ranks. Under these conditions, the average square deviation for total ranking factors in case of the best match is considered to be the maximum value if all experts give the same estimates.

$$S_{\max} = \frac{1}{12}nm^2(n^2-1) \quad (5)$$

The concordance coefficient $W$ shall be determined as the ratio of the actual obtained value to its maximum value:

$$W = \frac{S}{S_{max}} \quad (6)$$

Value of the calculated concordance coefficients have been calculated within $W$=0.54÷0.93 for all indicators, pointing out to the level of concordance of the expert opinions. Under these conditions the table value of Pearson fitting criterion $\chi^2_P$ is less than the calculated $\chi^2_P$, namely $\chi^2_T$ = 1.1÷19.7<$\chi^2_P$ = 19.24÷73.59. Thus, as a result of the expert estimation a number of indicators of reliability, ergonomics and aesthetics have been singled out for further research.

**Table 2** Ranking of significance of the quality indicators of the uniform for passenger car attendants

| Code and name of the requirement, name of the indicator | Ranking by the expert | Coefficient of significance | Mentioned coefficient of significance |
|---|---|---|---|
| 1 | 2 | 3 | 4 |
| **1. Reliability** | **2** | **0.27** | |
| 1.1 Resistance to light weather | 5 | 0.17 | 0.0459 |
| 1.2 Crease resistance coefficient | 3 | 0.21 | 0.0567 |
| 1.3 Pilling | 8 | - | - |
| 1.4 Seam strength | 9 | - | - |
| 1.5 Number of cycles of wearing in the plane | 4 | 0.18 | 0.0486 |
| 1.6 Resistance to ripping at seams | 2 | 0.21 | 0.0567 |
| 1.7 Change of linear dimensions after wet processing | 7 | - | - |
| 1.8 Thread shifting | 10 | - | - |
| 1.9 Number of launderings before loss of market condition | 1 | 0.23 | 0.0621 |
| 1.10 Remaining strain | 6 | - | - |
| **2. Ergonomic** | **1** | **0.33** | |
| 2.1 Water permeability coefficient | 6 | - | - |
| 2.2 Textile porosity | 7 | - | - |
| 2.3 Breathability | 4 | 0.18 | 0.0594 |
| 2.4 Water penetration | 9 | - | - |
| 2.5 Permissible terms for continuous use | 3 | 0.21 | 0.0693 |
| 2.6 Vapour permeability coefficient | 5 | 0.17 | 0.0561 |
| 2.7 Ease of using | 1 | 0.23 | 0.0759 |
| 2.8 Surface resistivity | 8 | - | - |
| 2.9 Dynamic conformance | 2 | 0.21 | 0.0693 |
| 2.10 Static conformance | 10 | - | - |
| **3. Aesthetics** | **3** | **0.2** | |
| 3.1 Availability of distinguishing features | 2 | 0.29 | 0.058 |
| 3.2 Colouring and decoration | 4 | 0.15 | 0.03 |
| 3.3 Artistic and coloristic decoration of fabrics | 5 | - | - |
| 3.4 Conformity to structural and harmonious image and aesthetics | 1 | 0.35 | 0.07 |
| 3.5 Quality of processing treatment | 3 | 0.21 | 0.042 |
| **4. Structural and technological** | **5** | **0.07** | |
| 4.1 Complete set | 3 | 0.2 | 0.014 |
| 4.2 Flaking of cuttings | 5 | 0.11 | 0.0077 |
| 4.3 Availability of lining | 4 | 0.15 | 0.0105 |
| 4.4 Structural segmentation of the form | 6 | - | - |
| 4.5 Maintainability | 2 | 0.25 | 0.0175 |
| 4.6 Availability of elements for fixation of clothes | 1 | 0.29 | 0.0203 |
| **5. Economic** | **4** | **0.13** | |
| 5.1 Product cost | 1 | 0.5 | 0.065 |
| 5.2 Expenses for garment care | 2 | 0.33 | 0.0429 |
| 5.3 Expenses for repairmen | 3 | 0.17 | 0.0221 |

The main feature of the developed list is a summary and content of all requirements of the consumer, characterized by a set of parameters defined as directly social and individual values for the consumer. Functional and ergonomic substantiation of the design solutions plays dominant role in the bringing the uniform of the passenger car attendants into conformity with the conditions of its use. In the process of development of the requirements we applied an approach, that took into account the study of existing types of domestic and foreign analogues, distinctive features of operating activity, nature of injuries and occupational diseases, working conditions, existing hazardous and harmful factors that directly affect the employee.

The list of quality indicators is represented separately for upper body garments and lower body garments. Such approach makes it possible to determine the level of quality indicators during project design of the sets of the uniform.

## 4 CONCLUSION

Hazardous and harmful operational factors which play dominant role in bringing the uniforms in conformity with the conditions of its use have been examined and systematized. In the process of development of the requirements we applied an approach, that took into account the study of existing types of domestic and foreign analogues, distinctive features of operating activity, nature of injuries and occupational diseases, working conditions, existing hazardous and harmful factors that directly affect the employee.

Significance of quality indicators and means for their ensuring in the uniforms of the passenger car attendants has been assessed. The necessity of theoretical research of reliability indicators has been substantiated by establishing integrated ranking of the indicators in accordance with their incommensurability and lack of standards for comparisons. An expert assessment has been carried out; reliability, ergonomics and aesthetics indicators, among which requirements for quality of the materials and process and design solutions of the articles is of top priority, has been determined.

Prospects of relevant researches highlight the fact that at present there is a necessity to develop uniforms for the employees of the postal departments, some of which are separate legal entities. In the process of work each of them shall give its employees a particular workwear, which differs from the workwear of the personnel of the state-owned post service "Ukrposhta". Development of generalized requirements for this type of uniform requires creation of its own corporate style of the employees of postal departments of Ukraine. However, centralization of the tasks in relation to design, materials, complete sets and traditions by categories of the officers, standards and terms of usage will allow to reduce its cost. These issues are also quite urgent for private transport companies, where the uniforms are in the first place most widely used by aviation companies that are the subject of some further scientific researches.

## 5 REFERENCES


1. Kolosnichenko M.V., Ostapenko N.V.: Hygiene clothing: Annotated lecture notes for students of "Design and Technology of garments" specialization "Designing garments" direction 6.051602 "Technology of light industry" full-time, KNUTD, 2012, 16 p
2. Hygiene. Terms and definitions of basic concepts: DSTU 3038-95, [Chynnyy vid 1996-01-01], Derzhavnyy standart Ukrayiny, 1996, 62 p (Natsional'nyy standart Ukrayiny)
3. Rudenko L.A.: Incidence of temporary disability leaders carriages railway transport, Praktyka i dosvid 3, 2011, pp. 54-56
4. Pohorel'chuk Y.S., V. Ya. Umans'kyy, V. H. Tsurkan: The internal environment of carriages and morbidity conductor rail transport, Nova knyha, 2008, 40 p
5. Semykoz E.A.: Morphofunctional health indicators railroad, Zdorov"ya naselennya: tendentsiyi ta prohnozy 1(5), 2008, pp. 33-35
6. Kolosnichenko M.V., Ostapenko N.V.: Design special clothing. Regulatory requirements for special protective clothing, Guidance for laboratory works for students of specialty 7.091801, Ready-made garments for the direction 0918 "Light industry", KNUTD, 2008, 128 p
7. Legal documents of Ukraine [electronic resource]/Cabinet of Ministers of Ukraine of 27 August 2008, Number 761 on the approval of the Technical Regulations of personal protective equipment in accordance with Article 14 of the Law of Ukraine "On standards, technical regulations and conformity assessment procedures", Access: http://zakon2.rada.gov.ua/laws/show/761-2008-%D0%BF

# DEVELOPMENT OF AN OBJECTIVE METHOD FOR THE ASSESSMENT OF NYLON SUTURES KNOT SECURITY

**Samar Turki and Saber Ben Abdessalem**

*Monastir University, National Engineering School of Monastir,*
*Textile Materials and Processes Research Unit, 5000, Tunisia*
samar.turki@hotmail.fr

***Abstract:*** *A perfect wound healing requires sutures having many handling characteristics such as good knot security and flexibility. Knot security characteristics are influenced by a variety of physical and mechanical parameters including the friction coefficient, bending rigidity and compressibility of the suture. Knot security and other handling characteristics are evaluated only by surgeons during the implantation. There are no standard tests to evaluate these qualities. We present in this paper an objective method to assess knot security of nylon sutures. This method is based on a fuzzy-logic model which correlates suture physical parameters and the knot security.*

***Keywords:*** *Nylon braided sutures, handling characteristic, knot security, physical parameters, fuzzy-logic model.*

## 1 INTRODUCTION

Sutures are used in all surgical operations and are the most implanted biomaterials. Linen sutures are the first sutures used by Egyptians [1]. There are several types of sutures which present different physical and chemical properties. These sutures can be classified according to their origins: natural or synthetic, according to their behavior in tissue: absorbable or non-absorbable and in terms of their physical configurations, suture materials can be classified into monofilaments or multifilaments.

In order to ensure a perfect and complete healing of a wound, sutures should always meet certain requirements and characteristics. These characteristics can be classified into three types: physiological, physical and handling qualities. Handling characteristics are generally appreciated subjectively by the surgeon. It's the category of suture characteristics related to the 'feel' of suture materials by surgeons during wound healing. These characteristics including pliability, flexibility, knot tie down and knot security are the most difficult to be evaluated objectively. In fact, industrially, only the diameter and the tensile strength of the suture are tested.

Handling characteristics are related to physical and mechanical characteristics [2]. For example, "knot security" which describes the ability of the knot to stay in position without untying or slippage is related to the coefficient of friction, stiffness or bending rigidity, size, compressibility of the suture and tying technique. The present study aims to lay some assessment parameters for handling characteristics. Multifilament sutures such as braided sutures are generally easier to handle and tie than monofilament sutures. They provide a better knot security due to their higher coefficient of friction [2, 3]. A linear relationship between knot security and coefficient of friction was reported by Herman [4]. A high coefficient of friction makes the knot tying difficult but leads to a more secure knot thanks to additional frictional forces which hold the knot ears together.

Determining the knot security of the sutures is the subject of many researches in orthopedic surgery [5, 6]. This literature focuses on knot security because it plays an important role in the successful wound healing but reported results are not usually approved clinically. Indeed, there are no conventional procedures for objectively evaluating the handling properties of sutures [7].

We propose, in this paper, an objective method for evaluating knot security based on the correlation between subjective evaluation of sutures and objective measurements based on physical tests by using fuzzy logic method. The purpose of this modeling is to predict handling properties of sutures from physical measured parameters.

## 2 EXPERIMENTAL PART

Braided nylon sutures "Polyamide T Noir" commercialized by Adhe-els were evaluated. They are made from multifilament yarns and have different USP sizes: 2 - 1/0 - 2/0 - 3/0. The size 3/0 correspond to the smallest diameter. Suture sizes are defined by the United States Pharmacopeia (U.S.P.). For a given USP size, the diameter of thread differs depending on the suture material class (Absorbable, Non-absorbable…). Sutures diameters are mentioned in Table 1.

**Table 1** Sutures diameters measured with microscope

| Size (USP) | 2 | 1/0 | 2/0 | 3/0 |
|---|---|---|---|---|
| Diameter [mm] | 0.782 | 0.469 | 0.421 | 0.342 |

### *2.1 Objective evaluation*

In order to evaluate knot security, friction coefficient, bending rigidity and compressibility can be used [2, 8]. We determined friction coefficient by twist method proposed by Lindberg and Gralen and adopted by Gupta [8]. An experimental device composed of six pulleys was developed and fixed to the lower jaws of a tensile tester. Two identical sutures are fixed to the upper jaws and passed around pulleys and two identical masses are attached to the two sutures as shown in Figure 1.

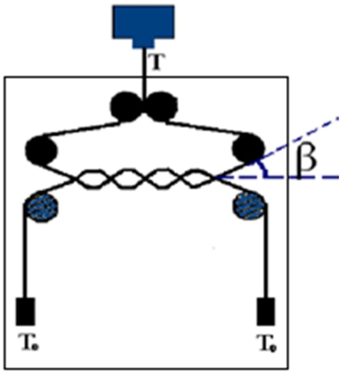


**Figure 1** Schematic presentation of the developed device for the measurement of friction coefficient

Equation 1 allows the calculation of friction coefficient $\mu$:

$$\mu = \frac{log(T/T_0)}{\pi\, n\, \beta} \qquad (1)$$

The variables $T$, $T_0$, $n$ and $\beta$ are respectively friction force registered by the load cell, normal force, number of twists and angle between sutures.

$T_0$ was equal to 0.2 N and $n$ is equal to 1 corresponding to a single twist simulating a surgical knot. The test was performed at a speed of 12.7 mm/min with a load cell of 10 N. When the test starts, sutures are tightened, then slip, producing a stick-slip phenomena. The force-displacement curve provided by the test shows maximum and minimum peaks corresponding to maximum and minimum friction coefficients levels.

Gupta [8] considered the difference between these levels ($\mu_s$-$\mu_k$) as the magnitude of stick-slip phenomena reflecting the ease or difficulty encountered by the suture to slip in the knot.

Available literature related textile flexure concerns mainly fabrics and fibers. Today, there are no conventional methods or standards for the measurement of yarns bending rigidity. Ghane et al. [9] showed that we can assimilate yarn to a beam and determine the flexural rigidity using a two-support beam system and classic elastic equations in the case of small deflection. The yarn is fixed at one end, supported at the other and loaded in middle to measure deflection. We tried this method but results were not reproducible in the case of our braids. Inspired by this method, we had the idea to fix the two ends of sutures in order to avoid random slip of suture and apply a force $F$ in the middle of the suture as shown in Figure 2. The distance $l$ between two supports is 6 cm.

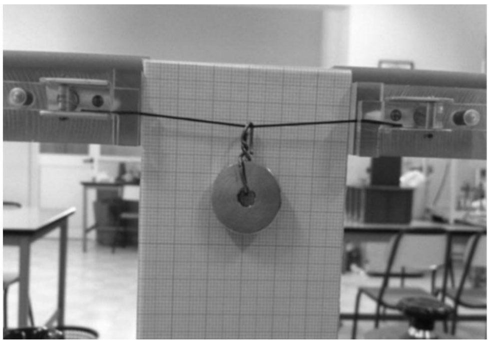

**Figure 2** The two-support beam device

The deflection $f$ is measured and bending stiffness $EI_{Gz}$ is calculated from equation 2:

$$f = \frac{F.l^3}{192E.I_{Gz}} \qquad (2)$$

The determination of compression behavior of the suture requires the study of compressive stresses occurring inside the knot in order to evaluate important parameters such as knot security. During, this study, compressibility of the suture was measured by determining the lateral deformation of the suture at different pressures. This deformation corresponds to the difference between the suture diameter measured with the microscope and image processing and diameter under pressure measured with thickness measurement gauge (Figure 3). Five samples from each diameter were tested in each test.

**Figure 3** Thickness gauge

### *2.2 Subjective evaluation*

In order to evaluate sutures subjectively we did a survey of 15 surgeons. Every surgeon was request to use our sutures in surgical operations and assign a score to the knot security which varies between -2 and 2. The score -2 corresponds to a very low knot security and 2 corresponds to an excellent knot security as shown in Figure 4.

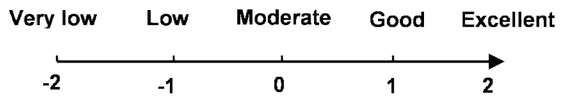


**Figure 4** Evaluation criteria

The influence of the tying technique on the knot security was reported by many studies [2, 3, 10]. The highest knot security was found with square knots. We performed tests with this knot type (Figure 5).

**Figure 5** Square knot

### *2.3 Modeling the relationship between objective tests and subjective evaluation*

Subjective or sensory evaluation gives an idea about surgeon perception towards sutures handling characteristics but it is difficult to use because of the lack of standards describing interpretation of human evaluation. On the other side, objective tests provide precise quantitative data which describe sutures hand. In literature, some researchers studied the relationship between objective tests and subjective evaluation mainly in the case of knitted fabric hand [11-13].

The prediction of knot security from objective tests requires correlation between subjective evaluation of handling characteristics and physical parameters obtained from objective tests. Relationship between physical parameters and knot security is complex. For the correlation, we used fuzzy logic technique which has been often used in the field of fabric hand evaluation [14-17]. This method has shown many advantages in characterizing some complex concepts related to sensory and instrumental evaluation of hand properties. Fuzzy logic is flexible and tolerant of imprecise data that can model non-linear functions. A fuzzy Inference system can be described via the diagram shown in Figure 6.

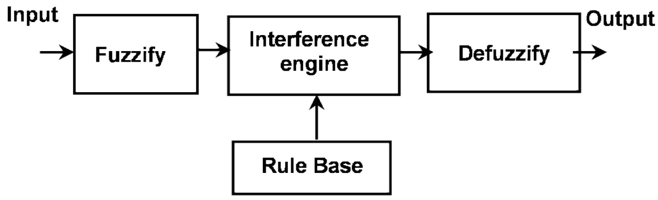


**Figure 6** Diagram of Fuzzy Interference System

In our case, the inputs are physical parameters and the output is the score attributed by the surgeon. We used the Java Eclipse software to program Fuzzy Interference System.

## 3 RESULTS AND DISCUSSION

### *3.1 Objective evaluation*

Figure 7 presents an example of force-displacement diagrams registered by the tensile tester according to the twist method. This diagram shows maximum and minimum peaks. These peaks were used to calculate the term ($\mu_s$ $-\mu_k$) corresponding to the difference between successive friction coefficients by using a program developed on Matlab software.

Figure 8 shows mean values of these differences for different sutures sizes. Confidence intervals are calculated with an error margin of 5%.

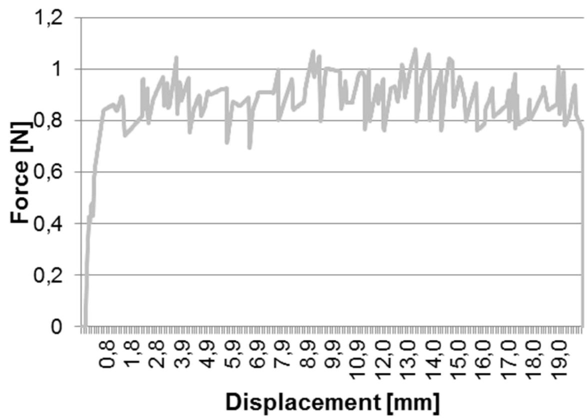


**Figure 7** Example of force-displacement diagram

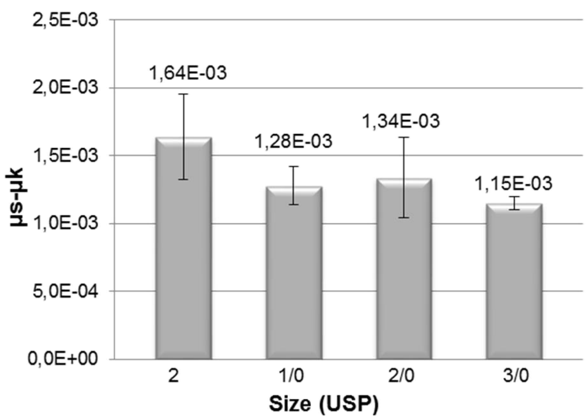


**Figure 8** Variation of $\mu_s$-$\mu_k$ with suture diameter

As can be seen from Figure 8, friction coefficient is overall proportional to suture diameter. Suture having the highest diameter (USP 2) shows the highest friction coefficient. This is explained by the fact that when the diameter increases, filaments are more inclined relatively to braid axis and are more opposed to tangential movement of braid surface. During suture slippage tensile tester load cell records consecutive maximum and minimum forces which are different.

Figure 9 shows results of bending rigidity test. It is quite obvious that when the diameter of the braid increases, the bending stiffness increases. Sutures having low bending rigidities are more flexible and allow easy handling by the surgeon.

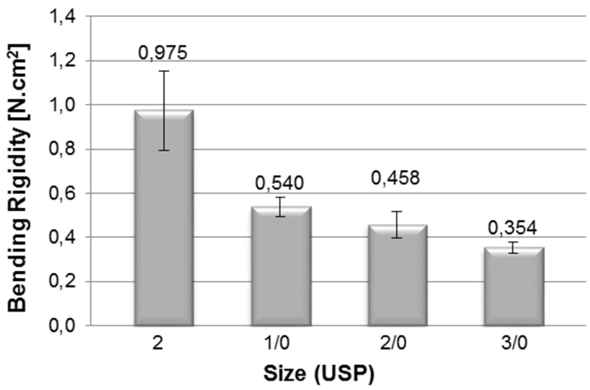


**Figure 9** Variation of bending rigidity with suture diameter

For sutures compressibility evaluation, we determined sutures diameters by using a microscope and image processing (Table 1), then, lateral deformation with the following pressures [kPa]: 1 - 3.05 - 4.2 - 5.09 - 8.97 – 16.05. Results are shown in Figure 10. We can see that suture have the smallest diameter (USP 3/0) has the highest lateral deformation.

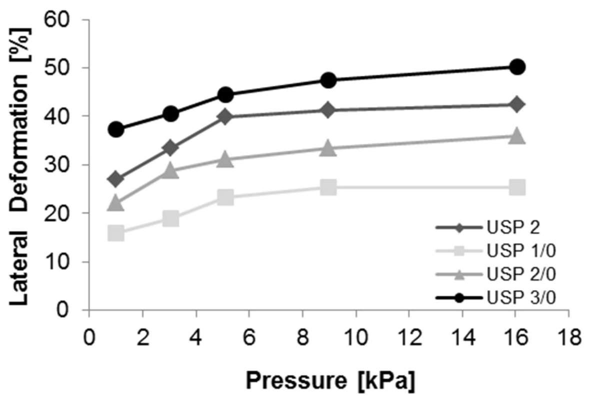


**Figure 10** Lateral deformation of sutures under different pressures

### *3.2 Subjective evaluation*

We collected scores attributed by surgeons for the different sutures used in different surgeries (Table 2). Results are presented in term of percentage relatively to the total number of evaluations. We can notice that sutures which have low diameter (USP 2/0 and 3/0) present good knot security.

**Table 2** Results of the surgeons sensory evaluation

| Size (USP) | 2 | 1/0 | 2/0 | 3/0 |
|---|---|---|---|---|
| Very Low [%] | 13 | 0 | 0 | 0 |
| Low [%] | **50** | 19 | 0 | 0 |
| Moderate [%] | 37 | **56** | 11 | 25 |
| Good [%] | 0 | 19 | **78** | **50** |
| Excellent [%] | 0 | 6 | 11 | 25 |

### 3.3 *Development of the fuzzy-logic based model for correlating objective tests and knot security*

The Table 3 summarizes the numeric data of inputs and outputs of the model.

$E_1$, $E_2$ and $E_3$ are respectively bending rigidity, lateral deformation (under a pressure of 1 kPa) and friction coefficient.

**Table 3** Numeric data of inputs and outputs of the model

| N USP | $E_1$ [N.cm$^2$] | $E_2$ [%] | $E_3$ (μs-μk) | Output Knot security |
|---|---|---|---|---|
| 2 | 0.975 | 26.85 | 1.64E-03 | -1 |
| 1/0 | 0.54 | 15.99 | 1.28E-03 | 0 |
| 2/0 | 0.458 | 22.09 | 1.34E-03 | 1 |
| 3/0 | 0.354 | 37.43 | 1.15E-03 | 1 |

A fuzzy inference system contains four components: the fuzzifier, inference engine, rule base and defuzzifier (Figure 6) [13, 16]. The fuzzifier maps the inputs numbers into corresponding fuzzy memberships in order to activate rules that are in terms of linguistic variables. Then, the fuzzifier determines for a given input the degree of membership to the fuzzy sets via the membership functions.

The rule base contains linguistic rules provided by experts. In our case, there are no experts able to provide rules which describe the relationship between physical parameters and knot security of sutures. So, we have to extract the rules of the model from numerical data.

The inference engine consists in passing from input fuzzy sets to output fuzzy ones. Every activated rule has an output fuzzy set using fuzzy operators. It is possible that one or more rules are kept out. The used method for the implication is the minimum. Then, all rules are aggregated to obtain only one output set.

To defuzzify is to return a number from the output fuzzy set. There are several methods used for defuzzification but the most used is the centroid. It calculates and returns the center of gravity of the aggregated fuzzy sets.

For the extraction of rules, we used the method of clustering map [18, 19]. From Table 3, we obtain Figure 11 which corresponds to the mapping of each two mechanical parameters together.

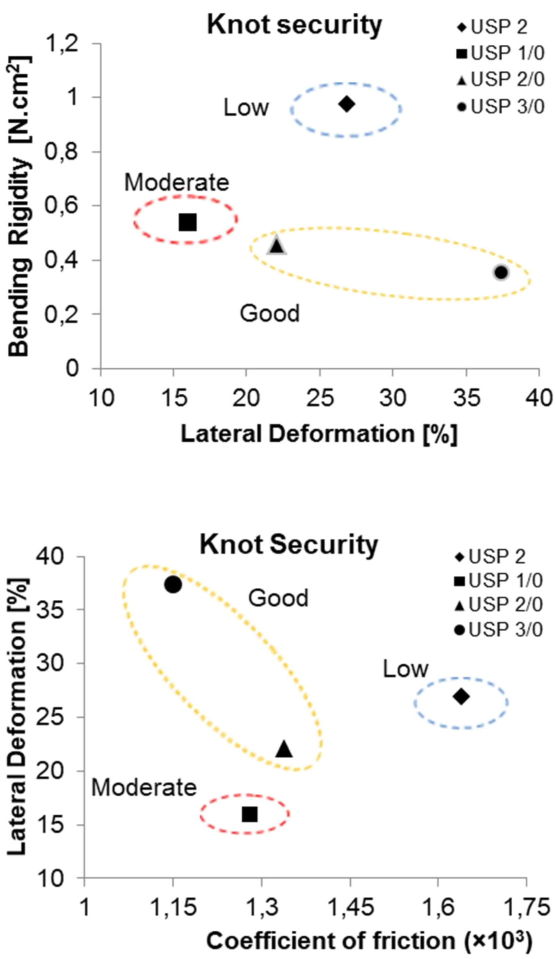


**Figure 11** Mapping of the inputs: $E_1$ and $E_2$ (top), $E_2$ and $E_3$

The obtained maps show 3 clusters: low, moderate and good. Our sutures were divided into 3 subsets and the following rules were extracted.

*Rules extracted from objevtive and subjective data*

*Cluster 1:* **If** $0.4 \leq E_1 \leq 0.7$ **&** $15 \leq E_2 \leq 20$ **&** $1.25 \leq E_3 \leq 1.35$ **then** knot security is moderate

*Cluster 2:* **If** $0.8 \leq E_1 \leq 1.2$ **&** $25 \leq E_2 \leq 30$ **&** $1.6 \leq E_3 \leq 1.7$ **then** knot security is low

*Cluster 3:* **If** $0.2 \leq E_1 \leq 0.6$ **&** $20 \leq E_2 \leq 40$ **&** $1 \leq E_3 \leq 1.45$ **then** knot security is good

*Fuzzy Inference System*

The steps of fuzzy modeling procedure are described as following:

- *Step 1*: Fuzzification of input variables

Based on Figure 11, the bending rigidity was divided into three fuzzy values named: Low, medium and high on the scale of 0.2-1.2 $N.cm^2$ (Figure 12). The scale of physical parameters was decided according to minimum and maximum values of these parameters among our samples.

The lateral Deformation was divided into four fuzzy values named: Very Low, low, medium and high (Figure12). By referring to Figure 11 the coefficient of friction (*µs-µk*) was divided into four fuzzy values named: Low, medium and high (Figure12).

- *Step 2*: Fuzzification of output variable

The sensory scores were divided into five fuzzy values as shown in Figure 12.

- *Step 3*: Reformulation of the rules

After determination of membership functions, we reformulate the rules linguistically in order to be used later in the programming.

**If** $E_1$ is medium **&** $E_2$ is very low **&** $E_3$ is medium **then** knot security is moderate.

**If** $E_1$ is high **&** $E_2$ is medium **&** $E_3$ is high **then** knot security is low.

**If** $E_1$ is low **&** $E_2$ is high **&** $E_3$ is low **then** knot security is good.

**If** $E_1$ is medium **&** $E_2$ is low **&** $E_3$ is medium **then** knot security is good.

The Mandami method was used to aggregate these rules and compute the output from input values.

- *Step 4*: Defuzzification of output

This goal of this step is to calculate a score by calculating the center of gravity of the output fuzzy set.

The fuzzy model calculates the score related to knot security from the three entered physical data.

*Fuzzy system programming*

In the beginning of the program, we have to declare input and output variables and enter input and output membership functions described in the fuzzification step. Then we introduce rules describing used fuzzy operators. We use the operator 'minimum' to calculate the intersection between predicates and activate rules; we used the operator 'maximum' to aggregate or accumulate rules. The transition from the fuzzy "world" to the real "world" requires the calculation of the center of gravity of output fuzzy set.

Figure 13 gives an overview of the calculation program. We can see that, for a suture non evaluated by surgeons having a bending rigidity of 0.69 $N.cm^2$, a lateral deformation of 20% and a coefficient of friction of 1.43 E-03 ($E_1$=0.69, $E_2$=20, $E_3$=1.43), the output Knot_security is the aggregate output fuzzy set built by the aggregation of fuzzy sets obtained by each rule. The calculation of the center of gravity of the output fuzzy set leads to a Knot_security equal to 0.5.

The output equal to 0.5 obtained after defuzzification means that we have a suture having a moderate to good knot security. This same suture was then evaluated by surgeons; half of them assigned a 0 as a score and the other half a score of 1 for the knot security. Finally, we can say that developed Fuzzy-logic method and subjective evaluation done by the surgeons converge to similar results.

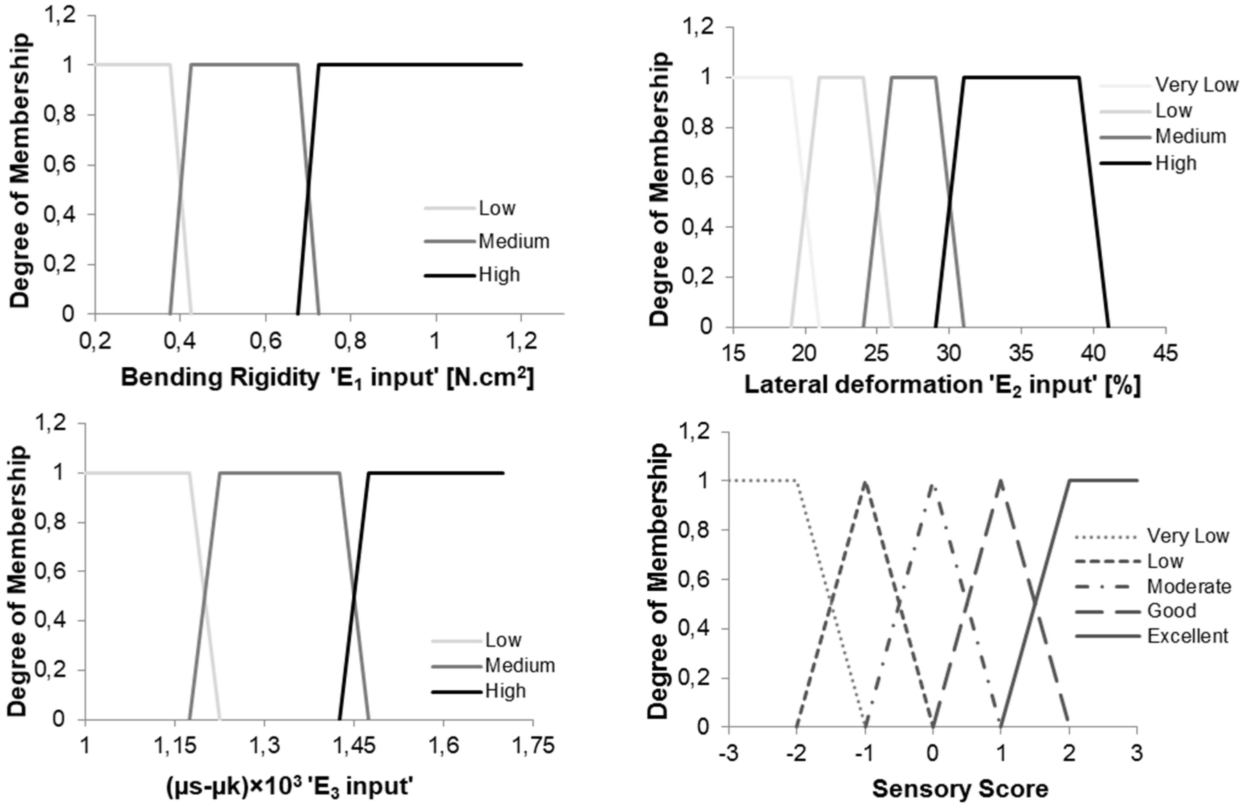


**Figure 12** Membership functions of the different inputs and the output

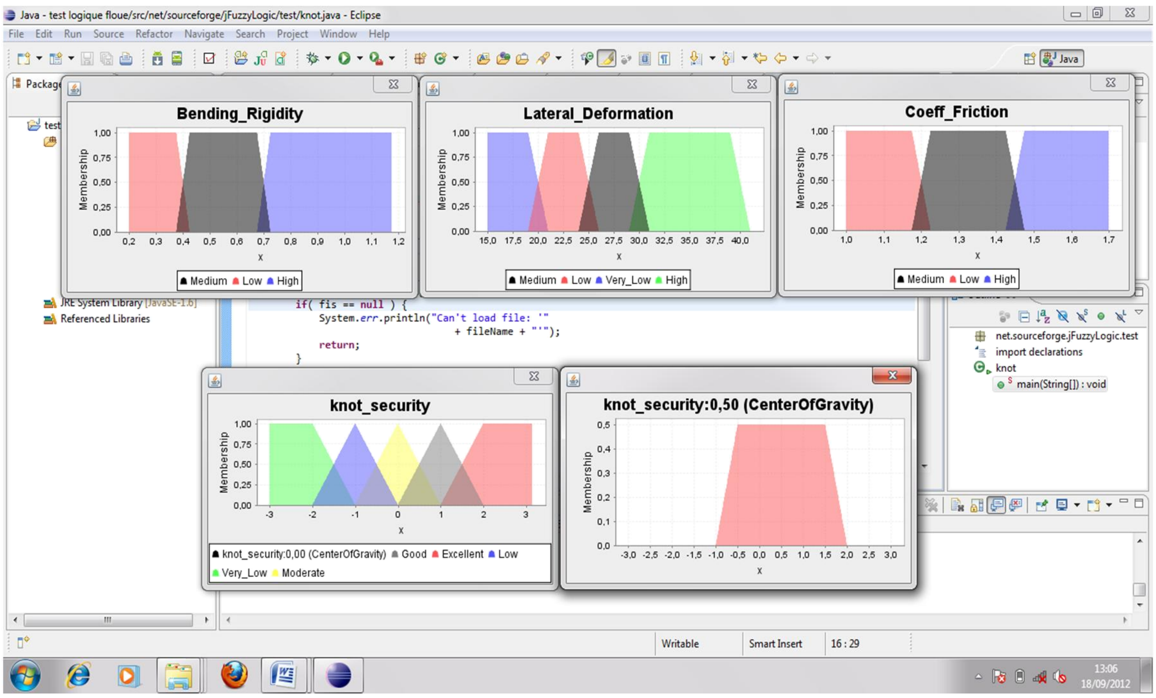


**Figure13** Overview of the calculation program interface

## 4 CONCLUSION

In this work, we propose an objective method to evaluate knot security of braided sutures made of nylon multifilament yarns. Knot security is a handling characteristic which can be evaluated only subjectively by surgeons during implantation. The developed method is based on a fuzzy model which correlates physical parameters determined by objective tests and knot security of sutures evaluated by surgeons.

We showed that it is possible to reproduce, reliably, surgeons appreciation of sutures. In fact, we developed a fuzzy model allowing the prediction of knot security from three physical parameters of the suture: bending rigidity, lateral deformation and friction coefficient.

Further work will focus on the evaluation of knot security of other sutures available in the market in order to generalize results obtained in this work.

## 5 REFERENCES


1. Tremblay S., Mantovani D.: Les fils de suture: de fil en aiguille, Le Médecin du Québec 38(10), 2003, pp. 105-108
2. Chu C.C.: Classification and General Characteristics of Suture Materials, Chapter 4. In C.C. Chu, J. A. Fraunhofer, and H.P. Greisler (Eds), Wound Closure: Biomaterials and Devices, CRC Press, 1997, pp. 39-64, ISBN 0-8493-4964-8
3. Fraunhofer J.A., Chu C.C.: Mechanical properties, Chapter 6. In: C.C. Chu, J. A. Fraunhofer, and H.P. Greisler (Eds), Wound Closure: Biomaterials and Devices, CRC Press 1997, pp. 107-130, ISBN 0-8493-4964-8
4. Herman J.B.: Tensile strength and knot security of surgical suture materials, Am. Surg. 37, 1971, pp. 209-217
5. Lo I.K.Y., Burkhart S.S., Chan K.C., Athanasiou K.: Arthroscopic knots: determining the optimal balance of loop security and knot security, The Journal of Arthroscopic and Related Surgery 20(5), 2004, pp. 489-502
6. Hassinger S.M., Wongworawat M.D., Hechanova J.W.: Biomechanical characteristics of 10 arthroscopic knots, The Journal of Arthroscopic and Related Surger 22(8), 2006, pp. 827-83
7. Ben Abdessalem S., Debbabi F., Jedda H., Elmarzougui S., Mokhtar S.: Tensile and Knot Performance of Polyester Braided Sutures, Textile Research Journal 79(3), 2009, 247-252
8. Gupta B.S.: Frictional Properties of Textile Materials, In: Pastore C.M. and Kiekens P. (Eds), Surface characteristics of fibers and textiles, New York, Les Etats Unis: Marcel Dekker, 2001, pp.59-92, ISBN 0824700023
9. Ghane M., Sheikhzadeh M., Halabian A.M., Khaburi S.: Bending Rigidity of Yarn Using a Two Supports Beam System, FIBRES & TEXTILES in Eastern Europe 68(3), 2008, pp. 30-32
10. Debbabi F., Ben Abdessalem S., Limem S.: New test methods to evaluate the performance of dermatological braided sutures from both the doctor and the patient sides, Journal of Textile Institute 102(6), 2011, pp. 548-557
11. Park S.W., Hwang Y.G., Kang B.C., Yeo S.W.: Applying Fuzzy Logic and Neural Networks to Total Hand Evaluation of Knitted Fabrics, Textile Research journal 70(8), 2000, pp. 675-681
12. Jeguirim S.G., Sahnoun M., Babay D.A., Cheikhrouhou M., Schacher L.M., Adolphe D.C.: Predicting compression and surfaces properties of knits using fuzzy logic and neural networks techniques, International Journal of Clothing Science and Technology 23(5), 2011, pp. 294-309
13. Agarwal G., Koehl L., Perwuelz A.: Interaction of wash-ageing and use of fabric softener for drapeability of knitted fabrics, Textile Research Journal 81(11), 2011, pp. 1100-1112
14. Raheel M., Liu J.: An Empirical Model for Fabric Hand: Part I: Objective Assessment of Light Weight Fabrics, Textile Research Journal 61(31), 1991, pp. 31-38
15. Zeng X., Koehl L.: Representation of the Subjective Evaluation of the Fabric Hand Using Fuzzy Techniques, International Journal Of Intelligent Systems 18, 2003, pp. 355-366
16. Agarwal G., Koehl L., Perwuelz A., Lee K.S.: Interaction of Textile Parameters, Wash-ageing and Fabric Conditioner with Mechanical Properties and Correlation with Textile-hand. II. Relationship between Mechanical Properties and Textile-hand. Fibers and Polymers 12(6), 2011, pp. 795-800
17. Jeguirim S.G., Adolphe D.C., Sahnoun M., Babay D.A., Schacher L.M., Cheikhrouhou M.: Intelligent Techniques for Modelling the Relationships between Sensory Attributes and Instrumental Measurements of Knitted Fabrics, Journal of Engineered Fibers and Fabrics 7(3), 2012, pp. 88-97
18. Agarwal G.: Interaction of textile parameters, wash ageing and use of fabric softener during the laundry with mechanical properties of the knitted fabrics and correlation with textile hand, Ph.D. Thesis, University of science and Technology, Lille1, 2011, p. 206
19. Zhu Y.: Contribution à l'évaluation et à la modélisation du bien-être des matériaux textiles habillement par l'utilisation des techniques de calcul avancé, Ph.D Thesis, Universitey of Lille 1, 2010

# SORPTION ABILITY & WICKING ON KNITTED FABRICS: EXPERIMENTAL AND THEORETICAL STUDIES

**Nesma Sawsen Achour[1], Mohamed Hamdaoui[1] and Sassi Ben Nasrallah[2]**

[1]Textile Materials and Processes Research Unit (MPTex), National Engineering School of Monastir (ENIM), Tunisia
[2]Laboratory of Thermal and Energy Systems Studies, National Engineering School of Monastir (ENIM), Tunisia

***Abstract:*** *The main idea of this work is to study the effect of knitted fabric characteristics on capillary rise and sorption ability by combining experimental and mathematical approaches. An experimental device performing the vertical suspension of fabric-liquid surface and permitting the penetration of water molecules through the tested samples is used. Experimental values of vertical wicking were gravimetrically measured using an electronic microbalance, and theoretically studied using the linear logarithmic model (LLM). The results show that the theoretical predictions are in reasonable agreement with the experimental data with high correlation coefficients values. It is also demonstrated that capillary rise kinetics are influenced by knitted fabric features, such as composition, knit structure, type of yarn and of couliering depth value.*

*Water sorption kinetics of cotton fabrics have also been studied and modeled by using mass measurements of the water absorbed by the textile and the LLM equation in order to interpret the experimental data in terms of sorption ability.*

***Keywords:*** *Knitted fabric, capillary rise, linear logarithmic model, water sorption kinetics, sorption ability.*

## 1 INTRODUCTION

The process of making textiles can require several dozen gallons of water for each pound of clothing, especially during the dyeing process. In fact, water is the most common solvent: All dyes, specialty chemicals and finishing chemicals are applied to textiles in water baths. Most fabric preparation steps, including desizing, scouring, bleaching and mercerizing, require the use of water. Textile dyes consume 10.95 billion liters of water each day, a huge amount of water for a highly polluting activity. Thus, it is necessary to optimize and control the sorption kinetics of this natural resource in textile materials during the industrial textile wet processing.

On the other hand, global demand for knitwear is growing at a faster rate. Currently around 50% of clothing needs in the developed countries is met by knit goods. So, ensuring the required quality in a knitted fabric is a vital issue for the manufacturer. In fact, liquid transfer through knitted fabrics is a critical factor affecting physiological comfort especially in sportswear, underwear, working garment or protective clothing [1, 2]. When the metabolism is very high, people sweat and perspiration spreads all over the skin, that's why, knitted clothes should transfer quickly the sweat outside to provide tactile and sensorial comfort for the wearer and even to prolong sport exercise performance [3, 4]. So, it is so important to understand moisture and liquid transport mechanisms.

That's why, in recent years, experimental and theoretical studies of the wicking rate in porous media have received significant attention. Extensive publications on liquid flow through porous media are available [5-22] and many investigations [15-18] were used the well-known equation of Lucas [24] and Washburn [25] to study dynamic invasion of fluid into straight, vertical circular capillaries. They showed that a liquid which has a viscosity $\mu$ and surface tension $\gamma$ rises in a vertical tube of radius $r$ according to the following law:

$$h^2\ (t) = Dt \tag{1}$$

where $h$ is the distance penetrated by the liquid and $D$ is the capillaries rate coefficient which is related at the same time to the surface properties, capillaries radius and liquid characteristics according the following equation:

$$D = \frac{r\ \gamma\ \cos\theta}{2\mu} \tag{2}$$

where $\theta$ is the contact angle between the liquid and the inside surface of the capillary.

The Lucas-Washburn equation has been tested over the years [26-28] and has been used to characterize porous media which was considered as a bundle of cylindrical capillaries by calculating its mean pore radius $r$ from slope of the curve $h^2$ versus $t$. This approach is very useful. However, it can be applied as long as gravity and evaporation are negligible. Only the viscosity restricts the maximum reachable height. That's why, many researchers [17, 18] focused on this weak point of Lucas-Washburn law and they developed a generalized equation which was applicable for short and long experimental time as shown below:

$$h\dot{h} = \frac{d}{2}\left[1 - \frac{h}{h_e}\right] \quad (3)$$

where $h_e$ is the maximum height attained at the equilibrium.

In order to study experimentally the wicking in textiles, different techniques have been employed: we note, the weight variation measurement of liquid rising in textiles recorded by a microbalance [21, 23, 29]. The direct observation using colored solution [15] which have been enhanced by many researchers [15-18]. They developed another method based on image analysis taken with CCD camera of raised colored liquid in textiles. However, the main deficiency of this method is the fact that the addition of the dye changes the liquid properties and modifies its velocity [29]. It has been demonstrated that kinetic of the dye can be less important than those of the water which can significantly falsify the results.

In this paper, kinetics of the water capillary rise onto cotton knitted fabric is investigated using an ameliorated experimental system (without addition of dye, UV lighting system in a darkroom). And the complete profile of vertical wicking has been predicted using the linear logarithmic model (LLM), which was the simplified linear form of the double exponential model (DEM) [21-23] as a function of the fabric characteristics, i.e. composition and structure. A good fit of the experimental data with the mathematical model was done.

Thereafter, the sorption kinetics of different cotton fabrics has been studied and modelled by using the LLM in order to interpret the experimental data in terms of diffusion parameters and sorption ability.

## 2 EXPERIMENTAL PART

### 2.1 Materials

The fabric samples used in this study were knitted by using the same machine: the STOLL CMS 320 TC automatic straight knitting machine which has a double fall electronic jacquard selection on both needle beds and "*E*" gauge equal to 7.

The samples were knitted with the same yarns properties (yarn count and twist). Nevertheless, in order to investigate the effect of knitted parameters on wicking behaviors, we change fabric structural parameters, the kind and the composition of yarn.

Table 1 gives the knitting parameters and geometrical properties of each sample used in this study.

The dimension of the dry sample used in our experiments was 20 × 30 cm. To remove the natural wax and paraffin oil applied to yarns prior to knitting, a chemical treatment was used.

The fabric was treated for 20 minutes at 65°C with a solution containing 2 mL/L of caustic soda and 2.5 mL/L of wetting agent (Lavotan TBU). We used the distilled water which is used frequently in textile industry.

### 2.2 Methods

Figure 1 shows a sketch of the system prior to wicking experiments. It is composed of a device permitting the vertical suspension of the fabric-surface on the liquid, a UV lighting system and a video camera to record the wicking liquid front height versus time.

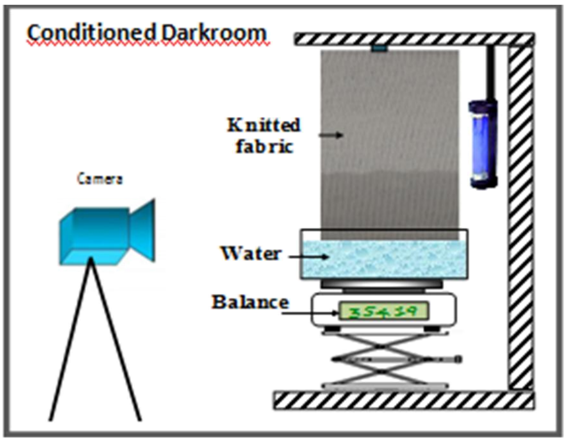


**Figure 1** Experimental device

**Table 1** Characteristics of knitted fabrics tested

| Sample | Composition | Knit structure | Yarn spinning | Couliering depth | Yarn count [m/g] | Thickness [$10^3$ m] | Weight [g/m$^2$] |
|---|---|---|---|---|---|---|---|
| 1 | 100% Cotton | Jersey | Carded | 14 | 12.5 | 1.99 | 359.5 |
| 2 | 80% Cotton/20% PES | Jersey | Carded | 14 | 12.5 | 2.13 | 378.1 |
| 3 | 100% Cotton | Rib 1&1 | Carded | 14 | 12.5 | 2.85 | 461.1 |
| 4 | 100% Cotton | Jersey | Open-end | 14 | 12.5 | 2.03 | 419.2 |
| 5 | 100% Cotton | Jersey | Carded | 12 | 12.5 | 2.33 | 349.0 |

In order to measure the mass of liquid raised, the fabric is attached, in the course direction, to a sensitive electronic balance (AND GX-2000 precision balance) with the accuracy of 0.001 g which has the capability of recording the weight of the total raised water [g] versus time [s] with its special software (RsCom program of WinCT data communication software Version 2.40 compatible with Windows, Window 95, 98 & NT).

All the experiments were done in a conditioning darkroom (20±2°C and 65±4%) which allows us, under UV lamp, to have a good resolution and quality of images without addition of a dye.

Three rinsing baths are applied after scouring; a simple average is calculated on the remaining data.

## 3 RESULTS AND DISCUSSION

### *3.1 Experimental data*

In this section, we are interested in the determination of the height attained by the water raised along tested knits. For this, two knit structures (jersey and Rib1&1), two different fabric compositions (100% Cotton and 80% Cotton – 20% Polyester), two different kinds of yarn spinning (carded and Open-end) and two various tightening (12 and 14) are used.

Figure 2 and Figure 3 describe respectively the evolution of the water raised height and the water absorbed mass along the knitted fabrics as function of time. The values of the height $h_t$ and the mass $m_t$ at each instant $t$ are the average values calculated after three wicking tests.

It is shown that all curves of experimental data of knitted fabric have a positive slope which decreases with time and attains zero at full saturation. So, this result indicates that capillary rise of water into knitted fabrics could be divided into two steps, namely the rapid phase and the slow phase.

<u>Analysis of Capillary Rise Study</u>

In order to study the capillary kinetic of water molecules in cotton knitted fabric, the experimental reached height of water raised in fabrics at each time were curve fitted using MatLab to the double-exponential function (DEM) proposed by Hamdaoui et al. [21-23] in order to interpret the sorption kinetics of vertical capillary rise of water in cotton woven fabrics. This approach, which has a double exponential form, is valid for short and long time and given by the following equations:

– *Mass Approach [22, 23]*

$$m_t = m_e - m_1.exp(-K_1t) - m_2.exp(-K_2t) \tag{4}$$

where $m_e$ is the quantity of water absorbed at equilibrium (saturation of fabric), $m_1$ and $m_2$ are respectively the quantities of water absorbed at the rapid phase and the slow phase, $K_1$ [min$^{-1}$] and $K_2$ [min$^{-1}$] are the sorption kinetic coefficients of the rapid step and the slow step, respectively.

– *Height Approach [24]*

$$h_t = h_e - h_1.exp(-K_1t) - h_2.exp(-K_2t) \tag{5}$$

where $h_e$ is the height attained by the water at equilibrium (saturation of fabric), $m_1$ and $m_2$ are respectively the quantities of water absorbed at the rapid phase and the slow phase, $h_1$ [cm] and $h_2$ [cm] are the heights attained by the water during the rapid step and the slow step, respectively. $K_1$ [min$^{-1}$] is the capillary kinetic coefficient of the rapid step and $K_2$ [min$^{-1}$] of the slow step.

Hamdaoui et al. found that the parallel double exponential kinetics model (DEM) fit well the experimental data with higher determination coefficient.

However, it has been confirmed that $K_1$ was, in the both cases, very larger than $K_2$, which allows considering that the first and rapid process can be assumed to be negligible on the overall vertical capillary kinetics into woven fabrics [22, 23]. Moreover, the exponential term associated with the slow processes and the DEM equations have the same appearance and they are almost confounded. So, the DEM equation can be simplified to be as:

– *Mass Approach [22, 23]*

$$m_t = m_e - m_e.exp(-Kt) \tag{6}$$

– *Height Approach [24]*

$$h_t = h_e - h_e.exp(-K't) \tag{7}$$

where $K$ [min$^{-1}$] and $K'$ [min$^{-1}$] are, respectively, the sorption kinetic coefficient and the capillary kinetic coefficient of the vertical capillary rise of water through fabrics.

To explain the reason of this deceleration of capillary rise velocity over time, we must analyze correctly the porous medium structure and understand by which effects the capillary rise has been restrained.

In fact, for short time, when the extent of the water flow in porous fabric is significantly less important than the maximum equilibrium height, the influence of gravity can be neglected. Consequently, the liquid rises quickly through the macro pores (pores between yarns) and the meso pores (pores between fibers) which are responsible for the diffusion during the first seconds (the rapid process) [24]. After full saturation of pores which have largest radius, liquid tries to enter the fiber in its accessible sites of amorphous regions known by micro pores which makes the diffusion more difficult. Moreover, gravity effect, for long time, shall not be neglected; it limits the inserting of water into these micro pores which are responsible for the long time diffusion (the slow process).

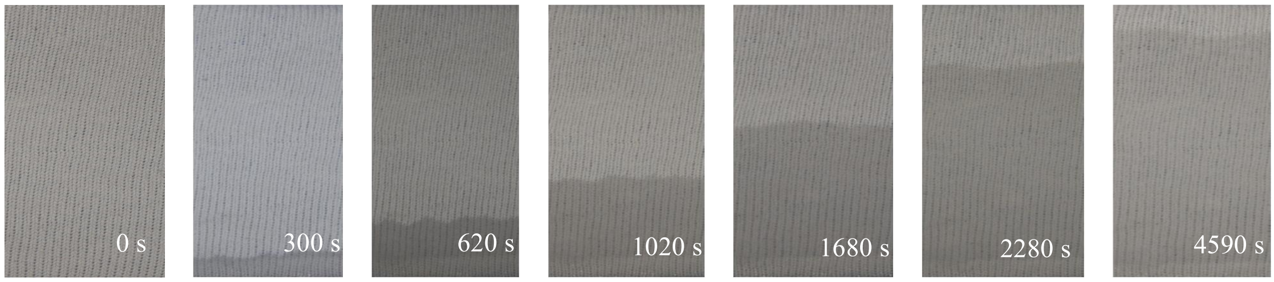


**Figure 2** Wicking of distilled water into jersey - 100% cotton knitted fabric (sample 1)

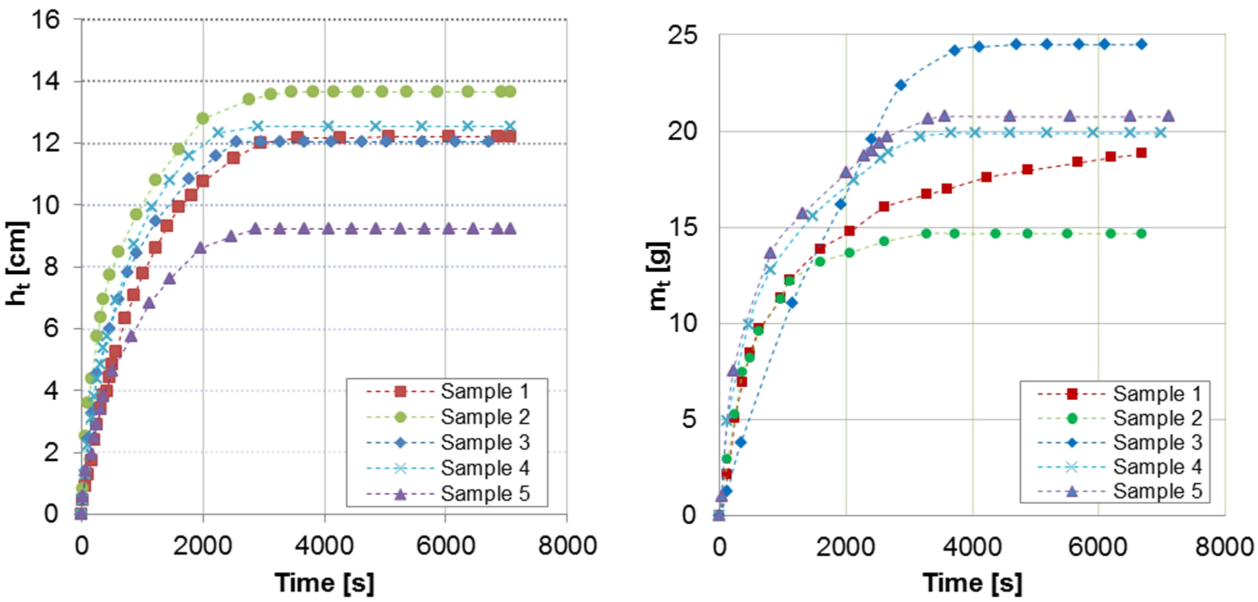


(a) (b)

**Figure 3** Experimental results of capillary rise: (a) water height evolution (b) water absorbed mass evolution

In this work, experimental data of water capillary rise into knitted fabrics will be analyzed directly by the Linear Logarithmic Model (LLM), which is the simplified linear form of the DEM, given by the following equation:

$$Ln\left(h_{e,experimental} - h_t\right) = Ln\ h_{e,theoretical} - Kt \qquad (8)$$

The results of the linear fitting curves of experimental data of capillary rise in five different knitted fabrics are listed in Table 2. The high values of R-square (>0.97) presented in the table indicate that the experimental data of knitted fabrics were well correlated with the LLM equation. Even, the theoretical values of maximum reachable height $h_{e,\ theoretical}$ were approximately equal to those found experimentally. So, we can confirm that the rapid step is negligible in comparison with the slow step also for capillary rise on knitted fabrics.

It is clear from experimental and theoretical results presented in Figure 3(a) and Table 2 that the diffusion parameter of water sorption is influenced by knitted fabric structure, composition and yarns properties.

**Table 2** LLM fitting parameters and R-square coefficients for the tested sample

| Sample N° | $h_{e,\ experimental}$ [cm] | $h_{e,\ theoretical}$ [cm] | K [$min^{-1}$] | R-Square |
|---|---|---|---|---|
| 1 | 12.19 | 12.46 | 0.0012 | 0.9713 |
| 2 | 13.67 | 11.65 | 0.0017 | 0.9845 |
| 3 | 12.03 | 11.64 | 0.0013 | 0.9903 |
| 4 | 12.56 | 12.89 | 0.0016 | 0.9759 |
| 5 | 9.22 | 9.35 | 0.0010 | 0.9838 |

We note that the capillary kinetic coefficients $K$ [$min^{-1}$] of the cotton/polyester fabric (sample 2) are greater than that of 100% cotton fabric (sample 1). And the highest maximum height attained by the water was detected for the cotton/polyester knitted fabric. This is explained by the fact that the polyester is a synthetic fiber which its crystallinity is very important (80-90%), its micro pores occupy a smaller volume which leads to a poor sorption ability and promote the capillary rise of water. However, cotton fiber has a great number of amorphous regions, where water molecules can penetrate and be very well linked to the hydroxyl groups. Consequently, it has better sorption ability than the blended polyester fiber.

We observe also that diffusion parameter of rib knit (sample 3) is more important than the diffusion parameter of jersey fabric (sample 1). In fact, we note that rib fabric contains more quantities of cotton per centimeter than jersey fabric knowing that it is knitted on both needle beds of knitting machines. But, water maximum height reached in this complicated structure is not important.

Concerning the effect of the couliering depth, according to Figure 3(a) and Table 2, it is shown that diffusion parameters and $h_e$ values of samples 5 are less important than those of sample 1. Water diffuses more rapidly into the less tightened knitted fabric (sample 1). Indeed, when couliering depth value decreases, the fabric is, then, tighter, the number of stitches per centimeter of the fabric increases and pores between loops become smaller. Consequently, liquid rises slowly and with difficulty. Moreover, an increasing of the stitches number per centimeter causes the rise of the material amount used for knitting per centimeter which leads to good sorption ability.

It can also be seen that capillary rise of water is influenced by the type of yarn spinning. In fact, open-end yarn is considered a hollow yarn, like cylinders, as seen that the fibers constituting are subjected to a very fast rotation. This increases the fabric meso porosity and explains the high values of capillary kinetic coefficient $K$ and the maximum reached height $h_e$ of sample 4 than those of sample 1 made out carded yarns which are characterized by their good cohesion between fibers.

*Analysis of Sorption Ability using LLM Equation*

As soon as it has been explained previously, capillary rise of water on knitted fabric is strongly influenced by the sorption ability of samples. So, the second goal of this study is to calculate total sorption ability values *SAT* for all knitted fabrics. That can provide information about the sum of macro, meso and micro pores. In fact, from the knowledge of the mass of water absorbed by knits at equilibrium $m_e$, the total sorption ability *SAT* of knitted fabric is given by the following equations [24]:

$$SA_T = \frac{W_v}{F_v} = \frac{m_e}{\rho_w \cdot (L_F \cdot W_F \cdot T_F)} \quad (9)$$

where $W_v$ is the total water volume, $F_v$ is the fabric volume, $\rho_w$ [g/cm$^3$] is the density of water, $L_F$, $W_F$ and $T_F$ are respectively the length, the width and the thickness of fabric.

However, it is shown, previously, that pores intervene at different times of the capillary rise depending on their size. That's why, we propose to determine the evolution of water sorption ability *SAt* of knitted fabrics versus time using the water absorbed mass $m_t$ as function of time (every 30 s), (Fig. 3(b)):

$$SA_t = \frac{m_t}{\rho_w \cdot (L_F \cdot W_F \cdot T_F)} \quad (10)$$

The results of the experimental data are reported in Figure 4, which shows the evolution of the textiles sorption ability versus time. Using the linear form of DEM (equation 6), sorption ability *SAT* equation can be expressed as:

$$SA_t = \frac{m_e - m_e.exp(-Kt)}{\rho_w \cdot (L_F \cdot W_F \cdot T_F)} \quad (11)$$

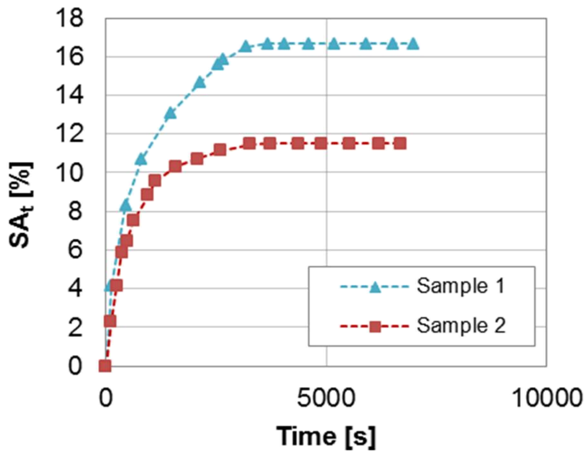


**Figure 4** Experimental data of sorption ability of the sample 1 and 2 versus time

Using equation 9, *SAt* equation takes the following form:

$$SA_t = SA_T - SA_T.exp(-Kt) \quad (12)$$

Then, it can be rearranged in the linear logarithmic form as shown below:

$$Ln\,(SA_T - SA_t) = Ln\,SA_T - Kt \quad (13)$$

Experimental quantities of absorbed water at equilibrium (saturation of the fabric) by all the knitted samples and experimental values of their total sorption ability $SA_{T,exp}$ are presented in Table 3.

**Table 3** Influence of fabric characteristics on linear logarithmic model (LLM) parameters

| Sample | $m_e$ [g] | $\rho_W.(L_F.W_F.T_F)$ [g] | $SA_{T,exp}$ [%] | $SA_{T,the}$ [%] | K [$min^{-1}$] | R-Square |
|---|---|---|---|---|---|---|
| 1 | 19.81 | 119.40 | 16.65 | 14.82 | 0.0008 | 0.9877 |
| 2 | 14.68 | 127.80 | 11.49 | 9.77 | 0.0013 | 0.9909 |
| 3 | 24.49 | 171.00 | 14.32 | 13.64 | 0.0004 | 0.8974 |
| 4 | 18.81 | 121.80 | 15.44 | 15.04 | 0.0010 | 0.9837 |
| 5 | 20.75 | 139.80 | 14.84 | 13.29 | 0.0003 | 0.9897 |

In addition, the best fit model parameters (total sorption ability $SA_{T,the}$ and sorption kinetic coefficient $K$ corresponding to the higher determination coefficient $R^2$ of the LLM fitting curves of experimental kinetic sorption were determined and regrouped in Table 3.

Based on the high values of $R^2$ for all cases as shown in Table 3, we conclude that experimental data of sorption kinetic are well correlated to the linear model equation. In fact, it can be seen that experimental and theoretical values of sorption ability, respectively, $SA_{T,exp}$ and $SA_{T,the}$ are very close. In addition, it is clearly visible that kinetic of water sorption is influenced by the construction parameters, the composition of fabrics materials and their yarn properties.

*Influence of fabric composition*

Experimental and theoretical results presented in Table 3 confirm that sorption ability of 100% cotton knitted fabric (sample1) is greater than that of the blended Cotton/Polyester (sample 2). However, it can be seen that blending cotton with polyester fibers improves the fabric sorption kinetic coefficient $K$. In fact, because of its hydrophobic character, the water does not penetrate into the polyester fiber pores and continue the capillary progression through the other vacant pores. Nevertheless, cotton fiber has more available hydroxyl groups in its amorphous regions which are capable to bind more water molecules. That explains its best sorption ability.

*Influence of fabric structural parameters*

Comparing the sorption ability values of samples 1, 3 and 5, we observe that, as knitted structure is more tightened (sample 5) and more complicated (sample 3), the sorption ability of the fabric is less important. In fact, as the couliering depth value increases and the stitches number per centimeter is more important, macro porosity of the knitted structure raises. As a consequence, sample 1 presents the best sorption kinetic coefficient $K$ and the total sorption ability $SA_T$.

*Influence of yarn spinning type*

Experimental and theoretical results show that capillary sorption kinetic of water on knitted fabric is influenced by the type of yarn spinning: In fact, the $SAT$ of sample 4 made out of open-end yarns has the most important $SAT$ theoretical values and the higher diffusion parameter than those of sample 1 made out of carded yarns. In fact, by changing the cotton carded yarn with cotton open-end yarns, we increase the fabric mesopores rate. As a consequence, the total absorbed water volume improves.

## 4 CONCLUSION

Along this study, mathematical model was established and has been demonstrated to be satisfactory describing the water capillary rise and the sorption ability of knitted fabrics. In fact, the experimental data have been interpreted using the linear logarithmic model (LLM) and have analyzed in terms of diffusion parameter, maximum reached height and total sorption ability.

We conclude that capillary height at equilibrium $h_e$ and capillary kinetics coefficient $K$ of raised water on knitted fabrics are influenced by the size of the pores responsible for water molecules migration. Indeed, we found that the blended fabric with hydrophobic synthetic fibers (polyester) and the knit made out with open-end yarns have the best wickability due to their poor sorption abilities $SA_T$. However, the water rises with difficulty through the more tightened sample and the more complicated structure (Rib 1&1) which have low sorption ability values.

We conclude that the fabric sorption ability $SAT$ can be affected by the way of the arrangement of fibers or yarns in the knitted fabric.

## 5 REFERENCES


1. CSE: Study on pollution of Bandi river by textile industries in pali town, Centre for Science and environment, 2006, New Delhi
2. Stämpfli R., Brühwiler P.A., Rechsteiner I., Meyer V.R., et al.: X-ray tomographic investigation of water distribution in textiles under compression – Possibilities for data presentation, Measurement 46(03), 2013, pp. 1212-1219
3. Youngmin J., Chung H.P., Tae J.K.: Effect of heat and moisture transfer properties on microclimate and subjective thermal comfort of caps, Textile research journal 80(20), 2010, pp. 2195-2203
4. Gat A.D., Vahdani A., Navaz H., Nowakowski A., Gharib M.: Asymmetric Wicking and Reduced Evaporation Time of Droplets. Penetrating a Thin Double-Layered Porous Material, Applied Physics Letters 103(13), 2013, doi: http://dx.doi.org/10.1063/1.4823534
5. Harnett P.R., Mehta P.N.: A survey and comparison of laboratory test methods for measuring wicking, Textile research journal 54(7), 1984, pp. 471-478

6. Princen H.M.J.: Colloid Interf. Sci 1968, 30
7. Dullien F.A.L., El-Sayed M.S., Batra V.K.: J. Colloid and Interface Sci. Vol. 60, 1977
8. Marmur A.J.: Colloid and interface sci 124(1), 1988
9. Wehner J., Miller B., Rebenfeld L.: Text. Res. J. 58, 1988, pp. 581-592
10. Li Y., Luo Z.: Text. Res. J. 69, 1999, pp. 760-768
11. Bayramli E., Powell R.L.: Colloid Surface 56, 1991
12. Deng J.L., Zhu Y.D., Wang J.H., Meng Z.H.J.: Compos. Mater. 249, 2003
13. Zhong W., Xing M.Q.J.: Colloid Interf. Sci 2004
14. Lukas D., Chaloupek J., Kost'akova E., Pan N., Martinkova I.: Morphological transitions of capillary rise in a bundle of two and three solid parallel cylinders, Physica A: Statistical Mechanics and its Applications 37, 2006, pp. 226-248
15. Lukas D., Chaloupek J.: Wetting between parallel fibres; column-unduloid and column disintegration transitions, Proc. Inst. Mech. Eng. H 217(04), 2003, pp. 273-280
16. Perwuelz A., Mondon P., Cazé C.: Experimental Study of Capillary Flow in Yarns, Textile Res. J. 70(04), 2000, pp. 333-339
17. Perwuelz A., Mondon P., Cazé C.: Liquid organization during capillary rise in yarns – influence of yarn torsion. Polymer Testing 20, 2001, pp. 553-561
18. Hamdaoui M., Fayala F., Ben Nasrallah S.: Experimental Apparatus and mathematical model for determination of parameters of capillary rise in fabrics, Journal of Porous Media 09(04), 2006, pp. 381-392
19. Hamdaoui M., Fayala F., Ben Nasrallah S.: J. Porous Media 09, 2007
20. Hamdaoui M., Fayala F., Ben Nasrallah S.: J of porous Media 11(03), 2008, pp. 231-240
21. Hamdaoui M., Fayala F., Ben Nasrallah S.: AUTEX Research Journal 8(2), 2008, pp. 44-48
22. Hamdaoui M., Achour N.S., Ben Nasrallah S.: The Influence of Woven Fabric structures on Kinetics of Water Sorption. Journal of Engineered Fibers and Fabrics 9(1), 2014
23. Achour N.S., Baffoun A., Hamdaoui M., Ben Nasrallah S.: Effect of knitted parameters on wicking behaviours, Industria Textila Magazine 67(2), 2016, pp. 99-102
24. Hamdaoui M., Ben Nasrallah S.: Indian J Fibre Text Res 40(2), 2015
25. Lucas R.: Kolloid Z, 24, 1918, pp. 15-22
26. Washburn EW.: Phys. Rev. 17(3), 1921, pp. 273-283
27. Fisher L.R., Lark P.D.J.: Colloid Interface Sci. 69, 1979, pp. 486
28. Williams R J.: Colloid Interface Sci. 79, 1981, pp. 287
29. Achour N.S., Hamdaoui M., Ben Nasrallah S., Perwuelz A.: Investigation of liquid characteristics effect on wetting and wicking behaviors of knitted fabrics, 6th International Conference of Applied Research in Textile (CIRAT-6), Tunisia 2014, pp. 265-272

# ELECTROBLEACHING OF COTTON FABRICS IN SODIUM CHLORIDE SOLUTION

**F. Vitero[1], P. Monllor[1], M. Bonet-Aracil[1], E. Morallon[2] and C. Quijada[1]**

*[1] Departamento de Ingeniería Textil y Papelera, Universitat Politècnica de València (UPV), Pza Ferrándiz i Carbonell, 03801, Alcoi (Alicante), Spain,*
*[2] Departamento de Química Física e Instituto Universitario de Materiales, Universidad de Alicante, Ap. 99, 03080, Alicante, Spain*
fevipe@doctor.upv.es

***Abstract:*** *The objective of the paper is to describe an alternative method based on electrochemistry to bleach cotton fabrics. Electrolysis of cotton fabrics soaked in proper electrolyte as a bleaching technology has been studied in this work. Some experiments have been conducted by applying this technique to see the whiteness index effect on fabric cotton. The duration of every experiment was two hours, and it has been applied different currents to study the whiteness index, as well as wetting agent has been used. Once the optimal conditions have been established, a treatment with reuse of the electrolyte and wetting agent has been carried out and six samples have been analysed in these conditions. It has been observed how the cotton fabric was bleaching with the same electrolyte and the whiteness index was similar every time and better than the conventional treatment. In addition, resistance and surface morphology did not present any noticeable weakness at fabrics submitted to electrolysis*

***Keywords:*** *electrobleaching, whiteness index, cotton fabrics, sodium hypochlorite.*

## 1 INTRODUCTION

Raw cotton fibers contain a certain amount of natural non cellulosic impurities, such as proteins, wax, fats, pectins hemicelluloses and mineral matter, distributed on their peripheral layers, either the cuticle or the primary wall. In addition to these non cellulose components, raw fibers also contain some colouring matter of uncertain and complex chemical composition that confers a typical yellowish-brown colour. All these components render the cotton fibers hydrophobic and impair effective and uniform dyeability and successful processing into finished apparels.

To avoid the unwanted effects of non-cellulosic constituents, they are removed in a series of pre-treatment or preparation steps prior to the application of further finishing steps like dyeing or printing. One of the central operations in preparation treatments of raw cotton fabrics is bleaching. Conventional techniques for bleaching of cotton are based on oxidative processes. One of them, which was developed long time ago, is chlorine bleaching. This process consists of a batch or pad immersion of the fabric in a solution containing sodium hypochlorite or other oxidizing chlorine compound. This technique has several advantages, like low chemical costs and no heating costs, because it works an ambient temperature. However, it has several disadvantages because it requires the transport, storage and handling of hazardous, unstable chemicals and hence it poses stringent industrial safety and risk prevention concerns.

Electrobleaching is based on the application of a DC voltage between two electrodes in an electrochemical cell to enable the passage of a DC current through an ion conducting medium (the electrolyte) that separates the electrodes. Electrochemical technologies show a unique combination of advantageous features because they can be conveniently operated in situ with inexpensive equipment, at ambient temperature and pressure, with low energy consumption and short time requirements, just by using electrons as the only reagent or driving force [1]. Moreover, these technologies can be advantageously connected and supplied with renewable energies. In the present study, the electrochemical system is devised to electrogenerate the desired oxidants in situ to address more controlled oxidation reactions (indirect electro-oxidation) with high efficiency [2]. As a result, bleaching can be performed without adding oxidants, avoiding their transportation, handling, storage and the generation and management of additional by-products.

The potential application of electrochemical techniques for bleaching fabrics has been reported by Kokot et al. [3] and Fukatsu et al. [4] who analysed bleaching and structural damage in cotton fibers electrolysed using Pt electrodes in alkaline solutions containing $Na_2SO_4$. The effect was attributed to the formation of hydroxyl radicals at both the anode and cathode during the oxygen electrogeneration and the reduction of dissolved oxygen respectively. Also, Fukatsu et al. [5] studied the electrochemistry decoloration of dyed cotton fabrics using a platinum anode. A significant decoloration was observed only when the electrolysis was conducted in a potassium chloride solution, which was attributed to the electrogeneration of hypochlorite. The generation of strongly oxidizing hypohalogenites from electrolysis of solutions containing sodium chloride and potassium bromide was also investigated as a mean for bleaching indigo-dyed denim fabrics [6, 7]. The oxidants were produced on site in an undivided electrolyzer at high current efficiency. The electrolyzer was coupled to a commercial drum washing machine, which received an inflow of the electrogenerated bleaching liquor. The electrogeneration of chlorine compounds has also been proposed as a viable technology for delignification and bleaching of wood pulp in the paper industry [8]. However, to the best of our knowledge, an exhaustive study of bleaching of undyed raw cotton fabrics by chlorine active species generated in situ by electrolysis from a chloride-containing electrolyte has not been carried out to date.

When a chloride-containing electrolyte is electrolyzed by passing through a proper DC current between two electrodes in an undivided electrochemical cell, a set of chlorine-containing oxidants are anodically produced by the oxidation of chloride ions and released into the bulk of the solution according to the following reactions [2]:

Anode:

$$2Cl^{-} \rightarrow Cl_2 + 2e^{-} \tag{1}$$

Solution:

$$Cl_2 + H_2O \rightarrow HClO + Cl^{-} + H^{+} \tag{2}$$

$$HClO \leftrightarrow H^{+} + ClO^{-} \tag{3}$$

While hydrogen and hydroxyl ions are formed at the cathode by the half-reaction:

Cathode:

$$2H_2O + 2e^{-} \rightarrow 2OH^{-} + H_2 \tag{4}$$

The equilibrium outlined in Eq. (3) depends on the pH of the bulk solution, as shown in Figure 1 [9]. Hypochlorous acid is rapidly converted into hypochlorite by reacting with hydroxyl ions from the cathode according to reaction in Eq. 5, which predicts a self-adjusted pH in the region of predominance of the hypochlorite ion:

$$HClO + OH^{-} \rightarrow ClO^{-} + H_2O \tag{5}$$

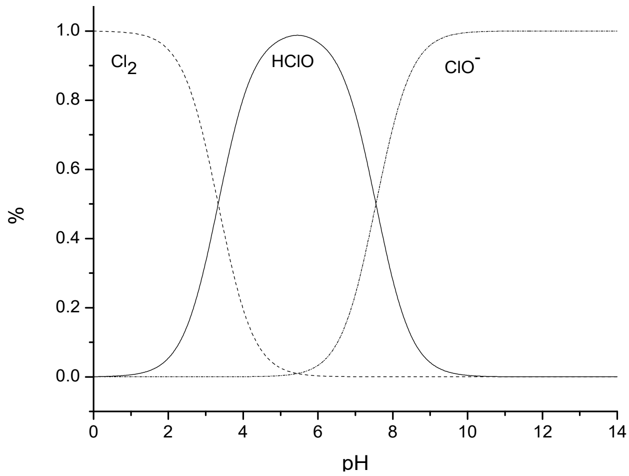


**Figure 1** Distribution of main aqueous chlorine species as a function of pH at 25ºC

One further advantage of the electrobleaching technology based on the hypochlorite electrogeneration over conventional chemical bleaching is the exhausted liquor can be easily regenerated because reaction of hypochlorite with colouring matter and other non-cellulosic impurities mostly gives back the precursor chloride ions:

$$\begin{aligned} &ClO^{-} + H_2O + Coloured\ Matter \rightarrow \\ &\rightarrow Cl^{-} + 2OH^{-} + Bleached\ Matter \end{aligned} \tag{6}$$

Instead, in a conventional bleaching process, hypochlorite must be replenished as it is exhausted, so leading to higher chemical costs and/or discharging higher amounts of wastewaters with higher pollutant loads.

In this work we report the bleaching of woven raw cotton fabrics by hypochlorite liquors electrogenerated on site upon passing a DC current through a sodium chloride electrolyte. Several sample fabrics were successively processed in batchwise mode in the same electrolytic bath and the change in whiteness index measured. The influence of adding a wetting agent at very low concentration was analysed. Furthermore, the effect of the electrobleaching process on the tensile strength and the surface morphology of the cellulose fiber was examined. Similar properties were measured for fabrics submitted to conventional bleaching steps by chemical bleach liquors for the sake of comparison.

## 2 EXPERIMENTAL

The electrochemical generation of the bleaching oxidants was conducted in a filter-press electrochemical cell, which has been used in previous work by our group [10–12], with an electrode projected area of 100 cm$^2$.

The anode was a commercial DSA® electrode, composed of a coating of mixed metal oxides, namely, titanium oxide ($TiO_2$), iridium oxide ($IrO_2$) and ruthenium oxide ($RuO_2$), on a Ti support in the form of expanded mesh. This kind of anodes are known to have very good electroactivity for chlorine evolution as well as excellent long-term mechanical and chemical stability [2]. The cathode was a stainless steel plate electrode.

A sodium chloride (Carlo Ebra Reagents, 99.5%) solution of concentration 0.34 M was used as the supporting electrolyte. Leophen RA by BASF was used as the wetting agent. It has used a concentration of 0.02% v./v. at electrochemical treatment and 0.2% v./v. at conventional treatment. The volume of solution was 1000 mL. Active (free) chlorine production was measured with Spectroquant® test kits by Merck [13].

The fabric used was a 100% cotton twill fabric with 210 g/m$^2$, the initial whiteness index of this raw cotton fabric was 16.41.

The experiments were carried out under galvanostatic conditions using a DC power supply model BL Ausonic FA-325. The applied current was 0.5 and 1.0 A. All electrolyses were run at a self-adjusted pH of 9-9.5 and at 25°C. Up to six pre-washed unscoured cotton fabric samples were processed consecutively in a batch mode for a total duration of two hours each.

For the sake of comparison, raw cotton fabric samples were bleached by conventional chemical treatment consisting of a soaking in bleach (at concentration of 3 g/L) during two hours in alkaline medium at room temperatre. After bleaching, fabrics were submitted to antichlor treatment, washed repeatedly up to neutral pH and dried at 60°C.

The surface morphology of raw and bleached cotton samples were examined by scanning electron microscope (SEM: JEOL JSM 840).

The whiteness index was determined in the CIELAB color space from diffuse reflectance measurements according to ISO 105-J01:1997 and ISO 105-J02:1997, by using the CIE formula [14].

$$W_{10} = Y_{10} + 800(x_{n,10} - x_{10}) + 1700(y_{n,10} - y_{10}) \quad (7)$$

where: $Y_{10}$ is the tri-stimulus value for the sample, $x_{10}$ and $y_{10}$ the color coordinates for the sample as this calculated using the illuminant/observer condition, $x_{n,10}$ and $y_{n,10}$ are the color coordinates of the achromatic point.

The tensile strength was measured according to ISO 13934-1:1999 [15].

## 3 RESULTS AND DISCUSSION

Preliminary electrolysis conducted in the filter-press cell in the absence of fabric showed that the pH rapidly rises from neutral to 9.0-9.5 during the experiment. As expected, the pH levelling-off within this basic range was also observed in the presence of fabrics. According to Figure 1, hypochlorite is therefore the prevalent chlorine species in the electrogenerated bleaching liquor, and hypochlorous acid remains at negligible amounts.

The concentration of electrogenerated active or free chlorine was also monitored during the electrolysis time at 1 A (Figure 2). It is shown that the active chlorine concentration rises during the course of the electrolysis and it reaches a steady value of about 3 g/L after six hours of treatment.

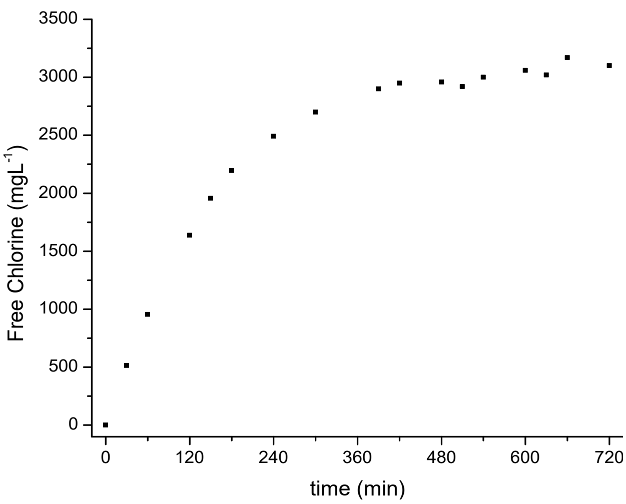


**Figure 2** Evolution of free chlorine during electrolysis at an applied current of 1A

These preliminary results reveal that electrobleaching works under alkaline pH like conventional hypochlorite-based bleaching, but at lower average active chlorine concentration.

Table 1 shows the change in whiteness index of raw cotton fabrics after two hours of processing for different kind of treatments. Note that the amount of wetting agent used in the electrochemical treatment is ten times lower than in a conventional treatment.

**Table 1** Whiteness index and tensile strength loss

| Wetting agent concentration | Conventional treatment | Electrochemical treatment Current 0.5 A | Electrochemical treatment Current 1.0 A | Tensile strength loss [%] |
|---|---|---|---|---|
| 0.2 % v./v. | 71±2 | | | 16±2 |
| 0.0 % v./v. | | 35±7 | 57±8 | 6±3 (*) |
| 0.02 % v./v. | | 67.1±0.7 | 72.3±0.3 | 11±2(*) |

(*) This values belong to an electrochemical treatment with an applied DC current of 1.0 A.

A high whiteness index was obtained in the electrochemical process when the wetting agent was used. This value was very similar than that reached in a conventional treatment, but it has the advantage of using a considerably lower concentration of wetting agent. Moreover, a significantly lower amount of bleaching agent is generated, which would imply considerable savings in chemical costs and reduction of wastes.

Another key advantage of the electrochemical method over the conventional one is that the electrolyte can be reused for bleaching of several cotton fabrics in batchwise mode. The bleaching action of hypochlorite is related to the reaction in Eq. 6. Thus, in the electrochemical process the chloride precursor is regenerated during the bleaching action itself, which potentially enables the electrolytic bath to be used indefinitely. To illustrate this behaviour a set of experiments were designed where a series of up to 6 identical cotton fabric samples were sequentially electrobleached in the same electrolyte with no further addition of sodium chloride. Each experiment was carried out for two hours.

Figure 3 shows the evolution of the whiteness index for different cotton fabrics in batchwise mode in the same electrolyte. When working without the wetting agent, acceptable whiteness index is reached only at the fourth fabric.

The rising shape of the WI curve in Figure 3 can be related to the continuous increase in the concentration of electrogenerated active chlorine throughout the whole batch process (Figure 2).

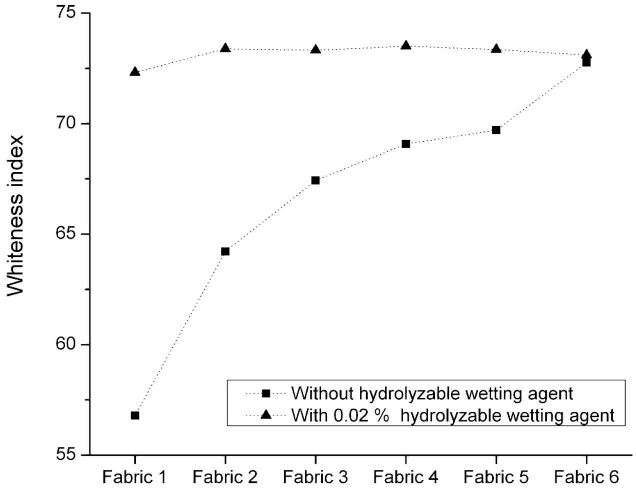


**Figure 3** Whiteness index of different raw cotton fabrics electrobleached in batchwise mode with reutilization of electrolyte. A DC current of 1 A was applied in all treatments

However, when a wetting agent is added, the whiteness index is satisfactory and very similar for all the fabrics. Despite maximum steady free chlorine concentration was not yet achieved until the end of the experiment, the wetting agent enables a facile access of the electrogenerated bleaching agent to the fiber, so enhancing the bleaching rate and providing high whiteness indices.

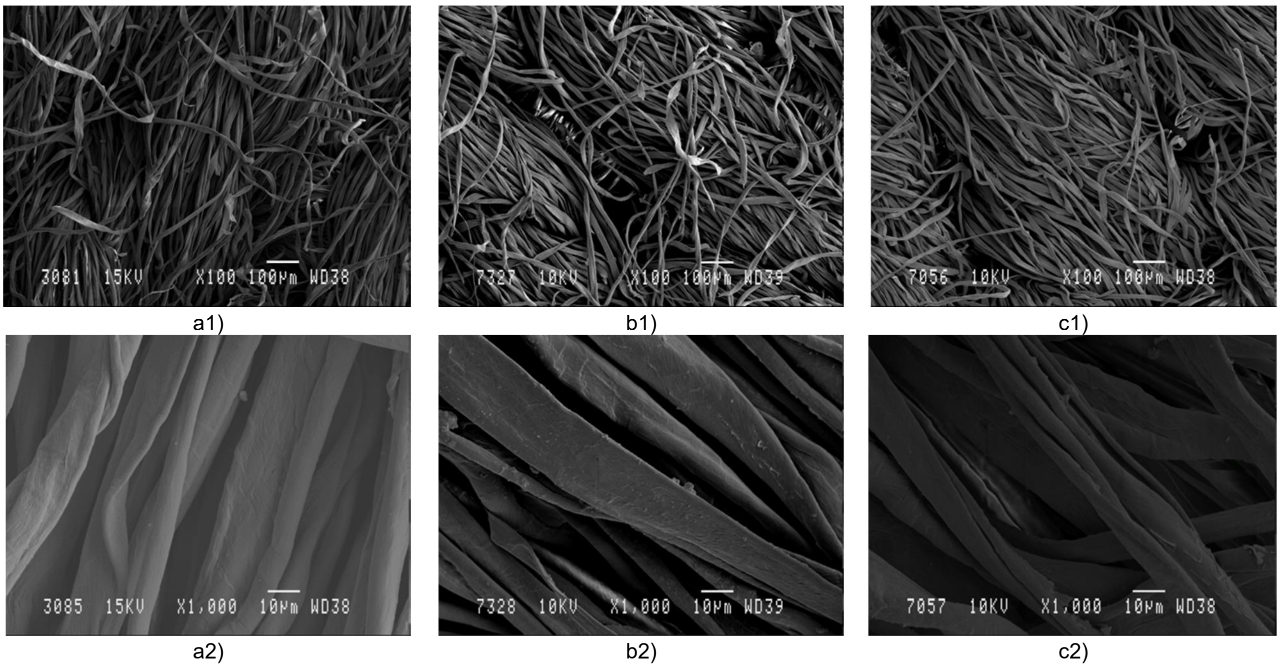


**Figure 4** SEM imaging which represent a1) raw fabric x100, a2) raw fabric x1000, b1) conventional treatment of chemically bleach x100, b2) conventional treatment of chemically bleach x1000, c1) electrochemical treatment (current applied 1.0 A) x 100, c2) electrochemical treatment (current applied 1.0 A) x 1000

SEM imaging of fabrics with electrobleaching treatment did not show any noticeable change in their surface morphology. When these images are compared with those of chemically bleached fabrics we cannot observe any prominent difference between fibers. With both treatments, the fiber appearance of twisted flat ribbons with cellulose fibrils assembled in spiral along the fiber axis and the cross-sectional bilateral structure was preserved (Figure 4, a2-b2-c2). So, the electrochemical treatment produces the same surface properties as the conventional treatment.

It is well known that bleaching treatments reduce traction resistance of the fibers. With the conventional treatment there is a tensile strength loss of 16% (Table 1). On the contrary, lower losses of the tensile strength were measured in electrobleached cotton fabrics (Table 1). So, it is observed how the fabrics submitted to electrolysis had a better traction resistance than those submitted to conventional treatments.

## 4 CONCLUSIONS

Electrochemical technologies have shown to be methodologies of enormous potential for bleaching textiles. Electrobleaching processes based on the generation of a bleaching agent from the electrochemical conversion at an electrode of a dissolved precursor gather unequalled benefits over conventional chemical bleaching methods from economic and environmental points of view: the primary reactant, the electron, is cheap, clean, widely available and easily transferrable; in addition the bleaching species is produced on demand from a harmless precursor and its dosage can be easily set with precise control of the applied current. Therefore, transport, storage and handling of hazardous chemical can be avoided, and chemical cost reduced.

In this paper we show that raw cotton fabrics can be electrobleached by the anodic generation of hypochlorite to reach high wihiteness index, negligible affection to the fiber morphology or to the tensile strength and with the use of low concentration of wetting agents. Furthermore, the bleaching liquor is continuously regenerated which enables the use of the same electrolytic bath in the batch processing of successive cotton samples. This makes electrobleaching a environmentally friendly technology when compared to conventional chemical bleach.

***Acknowledgements:*** *This work was supported by the research project MAT2013-42007-P of Ministerio de Economía y Competitividad (MINECO).*

## 5 REFERENCES

1. Rajeshwar K., Ibanez J.G.: Chapter Five, in: Environ. Electrochem., Elsevier, 1997, pp. 361-497
2. Panizza M., Cerisola G.: Direct and Mediated Anodic Oxidation of Organic Pollutants, Chem. Rev. 109, 2009, pp. 6541-6569
3. Kokot S., Marahusin L., Schweinsberg P.: A Morphological Study of Cotton Fabric Damage by Electro-Generated Oxygen, Text. Res. J. 63, 1993, pp. 313-319
4. Fukatsu K., Kokot S., Schweinsberg D.P.: Bleaching cotton fabric with electrogenerated oxygen-the role of hydroxyl and superoxide radicals, Text. Res. J. 69, 1999, pp. 769-775
5. Fukatsu K., Kokot S.: Bleaching of Cotton Fabric by Electrogenerated Species--Decoloration of Coloring Matter by Electrolysis, Text. Res. J. 70, 2000, pp. 340-346
6. Bechtold T., Maier P., Schrott W.: Bleaching of indigo-dyed denim fabric by electrochemical formation of hypohalogenites in situ, Color. Technol. 121, 2005, pp. 64-68
7. Bechtold T., Turcanu A., Campese R., Maier P., Schrott W.: On-site formation of hypochlorite for indigo oxidation – Scale-up and full scale operation of an electrolyser for denim bleach processes, J. Appl. Electrochem. 36, 2005, pp. 287-293
8. El-Ashtoukhy E.: Electrochemical bleaching of kraft bagasse pulp using a new cell design, Can. J. Chem. Eng. 88, 2010, pp. 126-132
9. Deborde M., von Gunten U.: Reactions of chlorine with inorganic and organic compounds during water treatment-Kinetics and mechanisms: A critical review, Water Res. 42, 2008, pp. 13-51
10. Berenguer R., Marco-Lozar J.P., Quijada C., Cazorla-Amorós D., Morallón E.: Effect of electrochemical treatments on the surface chemistry of activated carbon, Carbon N. Y. 47, 2009, pp. 1018-1027
11. Beralus J.-M., Ruiz-Rosas R., Cazorla-Amorós D., Morallón E.: Electroadsorption of Arsenic from Natural Water in Granular Activated Carbon, Front. Mater. 1, 2014. pp. 1-9
12. López-Bernabeu S., Ruiz-Rosas R., Quijada C., Montilla F., Morallón E.: Enhanced removal of 8-quinolinecarboxylic acid in an activated carbon cloth by electroadsorption in aqueous solution, Chemosphere. 144, 2016, pp. 982-988
13. UNE-EN ISO 7393-1 Calidad del agua Determinación de cloro libre y de cloro total Parte 1: Método por valoración con N,N-dietil-1,4-fenilendiamina, 2000
14. ISO 105-J02:1997 Textiles - Tests for colour fastness - Part J02: Instrumental assessment of relative whiteness, 1997
15. UNE-EN ISO 13934-1 Textiles Propiedades de los tejidos frente a la tracción. Parte 1: Determinación de la fuerza máxima y del alarga- miento a la fuerza máxima por el método de la tira, 2013

# THE INFLUENCE OF NANO-ADDITIVES ON THE FORMATION OF MATRIX-FIBRILLAR STRUCTURE IN THE POLYMER MIXTURE MELTS AND ON THE PROPERTIES OF COMPLEX THREADS

**N.M. Rezanova[1], V.G. Rezanova[1], V.P. Plavan[1] and O.O. Viltsaniuk[2]**

*[1]Kyiv National University of Technologies & Design, N.-Danchenko str. 2, 01011 Kiev, Ukraine*
*mfibers@ukr.net*
*[2]Vinnitsa National Pirogov Memorial Medical University, Pirogov str. 56, 21018 Vinnitsa, Ukraine*
*admission@vsmu.vinnica.ua*

*The influence of concentration of additives silver/silica ($Ag/SiO_2$) and silver/alumina ($Ag/Al_2O_3$) on the processes of structure-formation in the thermodynamically incompatible mixtures of polypropylene/copolyamide (PP/CPA) and the properties of complex threads from nano-filled PP microfibers were researched. Nano-fillers, that were used, show the compatabilization action in the mixture, reducing the value of interfacial tension and increasing the degree of dispersion and deformation of drops of disperse phase. This leads to a decrease in the average diameter of PP microfibers and reduction of mass fraction of films and particles, which the more perfect matrix-fibrillar structure is forming. The researched silver-containing nano-additives provide to complex threads an antimicrobial properties and improve their mechanical properties.*

***Keywords:*** *polymer mixtures, nano-additives, microfibers, interfacial tension, complex threads.*

## 1 INTRODUCTION

Increasing requirements for properties of textile materials and expansion of fields of their use led to search methods of obtaining of fibers and threads with a given set of parameters. The priority way is to develop methods of obtaining of nano-filled ultrafine fibers. The use of substances in nanostate can effectively solve the problem of increasing strength, elasticity, providing incombustibility, electrical, magnetic, optical, sorption, antimicrobial properties, etc. [1, 2]. As nano-fillers are widely used carbon nanotubes, nanoparticles of metals and metal oxides, silica and alumina. In recent years developed bifunctional nano-additives in which nanoparticles of metals or oxides are inflicted on the surface of mineral sorbents [3, 4]. Such substances exhibit antimicrobial activity silver-containing drugs combined with high sorption and anti-toxic properties. Their use minimizes consumption of silver, hence the reduction in toxicity and cost of silver-containing drugs. Reducing the diameter of individual filaments in complex threads to micro- and nanoscale improves product quality and reduces material consumption of production. Super-thin synthetic fibers can be obtained by different methods: melt - spinning, melt - blowing, processing of polymer mixture melts and electrospinning. Formation of microfibers and complex threads by processing of polymer mixture melts allows you to adjust their properties as by characteristics of the nano-fillers, and through their influence on fiber-formation of the component of the dispersed phase in the matrix [5-8]. Materials from ultrafine fibers retain all the positive properties inherent to products made of synthetic fibers: strength, shape stability and high durability. At the same time, because of the very small diameter of the individual filaments in the tissues of them, can form many air voids. Thanks to them, there is a free exchange of air between the skin and the environment, and such fabrics have high hygienic properties (fabric is "breathing") [9].

Purpose of the work is to research the influence of bifunctional nano-additives on the processes of structure-formation in molten mixtures of polypropylene/copolyamide as well as their impact on the properties of complex threads from microfibers.

## 2 EXPERIMENTAL

### *2.1 Materials used*

To obtain complex threads from polypropylene microfibers was used a mixture of polypropylene/copolyamide (PP/CPA) content 30/70 wt.%. Characteristics of input polymers are given in the work [6]. To modify PP microfibers were chosen bifunctional inorganic antimicrobial substances in nanostate - silver/silica ($Ag/SiO_2$) and silver/alumina ($Ag/Al_2O_3$), their characteristics are shown in Table 1.

**Table 1** Characteristics of nano-additives

| Name | Specific surface of oxide [m$^2$/g] | The average particle size [nm] | Content of Ag [μg/m$^2$] | Specific surface of nano-additive [m$^2$/g] |
|---|---|---|---|---|
| silver/silica | 320 | 17 | 16.3 | 296 |
| silver/alumina | 145 | 10 | 9.5 | 134 |

The concentration (*C*) $Ag/SiO_2$ and $Ag/Al_2O_3$ was in mixtures (0.5÷3.0) wt.% from mass of polypropylene. Nano-additives were received by restoring with glucose of ions $Ag^+$, deposited on the surface of pyrogenic silica ($SiO_2$) and alumina ($Al_2O_3$) from a water-alcohol solution of silver nitrate. The used additives combine bactericidal activity of silver and sorption properties of base components.

### 2.2 Methods used

Nano-filled composition were prepared with the help of the combined worm-disk extruder brand LGP-25, at this the additives previously were entered into polypropylene. The impact of nano-additives on fiber-formation of PP in matrix of CPA was evaluated using an optical microscope brands MBD by the method described in the [6]. At this were determined the mass fraction of the PP, which is spent on the formation of different types of structures (microfibers, particles, films) and the average diameter of microfibers. The kinetics of disintegration of liquid jets of PP (microfibers) in the CPA matrix was studied using a microscope equipped with a heating table. Longitudinal sections of the extrudates of mixtures were placed on it and were photographed the various stages of the process of destruction of the jets when heated. The radii (*R*) of jets and the distances between the centers of drops (*r*), which formed, were determined from the micrographs. The results were treated by the classical theory of Tomotika and were calculated the coefficient of instability (*q*), lifetime (decay) ($t_l$), adjusted decay ($t_l/R$) of jets and the value of interphase tension ($\gamma_{\alpha\beta}$). The complex threads were formed on research-industrial extrusion machine with 1000% spinneret extractor hood and were stretched at 150°C with multiplicity 6. Complex threads from nano-filled PP microfibers were obtained by extraction of the matrix polymer with solvent inert with respect to fiber-forming polymer. The strength at break (*P*) and modulus of elasticity (*E*) of complex thread was determined as described in [6]. Research of antibacterial activity of nano-filled threads from PP microfibers was made on the World Health Organization recommended test-strains of microorganisms and fungi by standard methodics [10, 11]. Suspensions of microorganisms were prepared using the device Densi-La-Meter (Czech Republic). Antibacterial activity of samples of microfibers was examined by two methods. The first method consisted in the diffusion of the active substance into the nutrient medium (method of "wells"). To do this, threads from PP microfiber were kept in saline (in a ratio 1:5) for 2 hours at 37°C, then the resulting liquid is poured into the wells of culture medium placed in a Petri dish. Microbial load amounted to $1.10^7$ bacterial cells per 1 ml of medium and is established by the standard of McFarland. For the study was taken 18-24 hours culture of microorganisms. The antimicrobial activity of modified PP threads was determined by the diameter of the zone delayed the growth of microorganisms around the hole (*D*), in millimeters. According to the second method were studied the features of the growth of microorganisms on the surface of microfibers by playback of contamination of cultures. The threads were placed in casein-soy broth at a ratio of $1.10^7$ of colony-forming units per milliliter [CFU/ml], incubated in an thermostat during 48 hours, after this, was made seeding on agar and was counted the number of microorganisms grown on nutrient medium. The criterion of evaluation was the decrease of number of viable colonies of cells of microorganisms in the corresponding period of time after the contamination, which is defined as the logarithm of the number of colonies.

## 3 RESULTS AND DISCUSSION

Formation of microfibers by processing molten polymer mixture is a special type of structure-formation in which is happening process of deformation and merging of drops polymer of dispersed phase into microfiber. They must maintain its stability in the channel of the forming hole and after the exit from it. Deformation, coalescence of drops, the thermodynamic instability of jets and the degree of compatibility of ingredients on the interphase area are effective factors to create the desired structure of the polymer dispersion. The final morphology is the result of a balance between the processes of deformation and desintegration on the one hand, and coalescence - the other. It is known that during the flow the dispersion medium is acting on drop dispersed therein with power that can deform it, provided that there is sufficient interaction between two polymers of mixture in the transition layer. From the fundamental relationships that describe thermodynamic equilibrium in dispersed systems, follows, that the most effective factor, that allows you to adjust the parameters of the phase structure, is the affinity of components. The value of surface tension at the interphase area is an indirect characteristic of degree of compatibility of polymers.

Compatibilization effect of nano-additives in polymer mixtures is described in several papers and it is associated with increasing of affinity between macromolecules of components at the interphase area [5-7].

Experimental results on the effects of nano-additives silver/silica and silver/alumina on decay of PP liquid jets in the matrix of CPA evidence their significant impact on the value of interphase tension throughout all the range of concentrations that were studied: $\gamma_{\alpha\beta}$ falls from 2.60 mN/m for the initial mixture to 0.47 and 0.27 mN/m for mixtures filled with $Ag/SiO_2$ and $Ag/Al_2O_3$ respectively (Table 2).

At this compatibilization effect depends upon the concentration of nano-additives and it is the maximum for the nano-filler content of 0.5 wt.%. Further increase in the concentration of $Ag/SiO_2$ and $Ag/Al_2O_3$ leads to an increase the value of interfacial tension. Extreme dependence $\gamma_{\alpha\beta} = f(C)$ is due to the fact that upon reaching its critical amount the additive is allocated in a separate phase, and its surface activity decreases. The efficiency of nano-additives depends on their chemical nature: the maximum reduction $\gamma_{\alpha\beta}$ occurs when into the mixture melt is entered additive based on alumina. This result is due to fact that in polymer mixtures compatibilization action is determined by selective localization of nanoparticles at the interphase area. Thus the effect is the higher, the greater the difference between polymer-philic of the components of mixture [5, 12]. Higher hydrophilic of surface of aluminas is probably contributes to more intense pushing of them to the interphase area.

The liquid jet (cylinder) is thermodynamically unstable and breaks up into drops in the event of appearance on its surface excitation of wave nature, provided that the amplitude of the wave coincides with the radius of the jet. Its decay time (lifetime) is directly proportional to the diameter of the initial cylinder and inversely proportional to the value of surface tension. So, other things being equal, decrease of interfacial tension value provide stability of jets smaller diameters that contribute to the formation of more thin microfibers. Data presented in Table 2, confirm a significant increase of the lifetime and adjusted lifetime of polypropylene microfibers in nano-filled mixtures PP/CPA and reduction of unstability coefficient, compared with initial mixture. Stability of microfibers depends upon the concentration of nano-additives: value $t_l/R$ is maximum when their content is 0.5 wt.%. Changing the value of interfacial tension between the components is one of the factors regulating the morphology of polymer dispersions. The performed investigations of the microstructure of extrudates of initial and nano-filled mixtures showed, that addition of bifunctional nano-fillers into the mixture PP/CPA does not change the nature of structure-formation of polymer of dispersed phase in the matrix. For all studied compositions there is formation of a matrix-fibrillar morphology (Table 3).

**Table 2** Characteristics of decay kinetics PP microfibers in the matrix of CPA

| Nano-additive | | $\gamma_{\alpha\beta}$ | q | $t_l$ [s] | $t_l/R$ [s/μm] |
|---|---|---|---|---|---|
| name | content [wt.%] | | | | |
| without additives | | - | 0.0348 | 32.6 | 24.5 |
| $Ag/Al_2O_3$ | 0.5 | 0.27 | 0.0187 | 57.4 | 46.3 |
| | 1.0 | 0.32 | 0.0193 | 55.2 | 38.9 |
| | 1.5 | 0.41 | 0.0224 | 51.8 | 36.4 |
| | 3.0 | 0.51 | 0.0241 | 49.1 | 33.5 |
| $Ag/SiO_2$ | 0.5 | 0.47 | 0.0198 | 50.9 | 32.9 |
| | 1.0 | 0.54 | 0.216 | 47.5 | 31.6 |
| | 1.5 | 0.65 | 0.0252 | 45.1 | 30.5 |
| | 3.0 | 0.73 | 0.0265 | 41.8 | 28.8 |

**Table 3** Influence of nano-additives on microstructure of extrudates of mixture PP/CPA

| Nano-additive | | Microfibers | | Films [wt.%] | Particles [wt.%] |
|---|---|---|---|---|---|
| name | content [wt.%] | d [μm] | [wt.%] | | |
| without additives | | 3.8 | 90.3 | 7.0 | 2.7 |
| $Ag/Al_2O_3$ | 0.5 | 1.9 | 96.8 | 1.3 | 1.9 |
| | 1.0 | 2.2 | 95.1 | 3.5 | 1.4 |
| | 1.5 | 2.5 | 94.0 | 4.7 | 1.3 |
| | 3.0 | 2.8 | 93.7 | 5.2 | 1.1 |
| $Ag/SiO_2$ | 0.5 | 2.4 | 95.1 | 3.6 | 1.3 |
| | 1.0 | 2.7 | 94.2 | 4.6 | 1.2 |
| | 1.5 | 3.2 | 93.9 | 5.2 | 0.9 |
| | 3.0 | 3.4 | 92.8 | 6.3 | 0.9 |

Researched nano-additives improve process of fiber-formation PP in matrix of CPA: reduces the average diameter of microfibers and reduces mass fraction of films and particles in comparison with the initial mixture. At this the ratio between the types of structures and diameters of microfibers depends upon the concentration of nano-additives and their chemical nature. The positive effect of nano-fillers on fiber-formation is due to the stabilizing effect of nanoparticles on the finest PP microfibers by increasing the lifetime of the liquid jet and the reduction of the interfacial tension (Table 2).

Mechanical properties of complex threads, formed of the investigated mixtures, are shown in the Figure 1.

Adding of nano-fillers into the structure of PP microfibers leads to improvement of quality threads: their tensile strength and modulus of elasticity are increasing. This dependence is the logical and it is due to a number of factors. First, the addition of high-modulus nano-disperse additives increases the strength and resistance to deformation due to the effect of filling. Secondly, reducing the diameters of filaments in complex threads also helps to strengthen them. We have previously shown that the maximum mechanical properties have yarns, in which microfibers are the predominant type of structure [6, 7]. At this, presence of films impairs quality of threads. For nano-fillers concentration in a mixture of more then 1.5 wt.% the growth rate slowed down, which may be due to the process of aggregation of nanoparticles. Effect of modification by the additive $Ag/SiO_2$ is more pronounced versus $Ag/Al_2O_3$, due to its larger specific surface area. It is known that silica provide a significant improvement of mechanical properties of filled compositions. At this reinforcing action of silica correlates with the size of its specific surface area ($S_{BET}$): module increases when $S_{BET} \geq 50$ m$^2$/g, and the degree of reinforcement increases with increasing of specific surface [13].

Test results of antimicrobial activity of saline after withstanding of complex threads from nano-filled PP microfibers in it are shown in Table 4.

According to the methodic [10] were evaluated the antimicrobial effect by the following criteria: $D<10$ - microorganism is insensitive to the drug; $10<D<15$ - low sensitivity; $15<D<25$ - microorganism is sensitive to the drug. The obtained data indicate, that PP microfibers filled with nanoparticles $Ag/Al_2O_3$ and $Ag/SiO_2$, are showing insignificant antimicrobial activity towards all studied test-strains of microorganisms and fungi - the diameters of delay of their growth around the holes lie within (12.3÷14.7) mm. At the same time, we know that the antibacterial activity of the initial $Ag/SiO_2$ is high - about 10 times higher compared to silver ions [3]. Low sensitivity of saline solution in this case may be due to the fact that silver nanoparticles are in the pores of base oxide and are slowly diffusing into it.

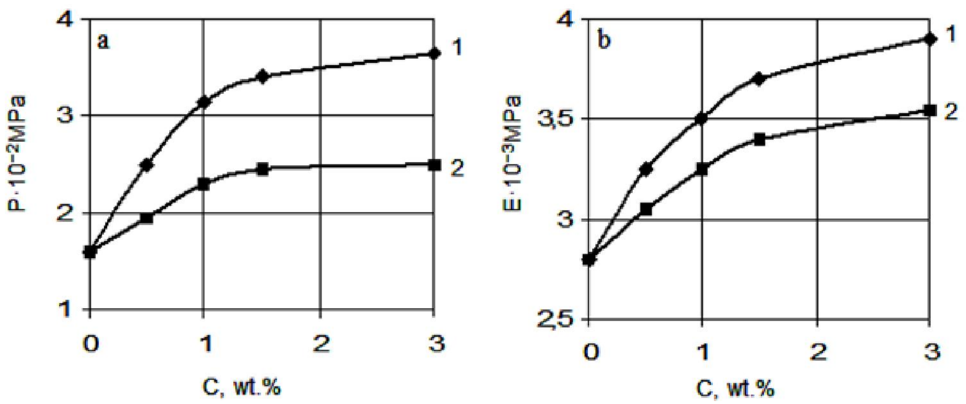


**Figure 1** The impact of the concentration of nano-additives on the strength P (a) and elastic modulus E (b) of threads from PP microfibers: 1– $Ag/SiO_2$; 2 – $Ag/Al_2O_3$

**Table 4** Antimicrobial activity of nano-filled threads, defined by the method of diffusion in agar

| Name and composition of the mixture [wt.%] | Diameters of the zones stunted growth [mm] | | | | | |
|---|---|---|---|---|---|---|
| | *Staphylococcus aureus ATCC 25923* | *Escherícha coli ATCC 25922* | *Pseudomonas aeruginosa ATCC 27853* | *Proteus vulgaris ATCC 4636* | *Basillus subtilis 6633* | *Cadida albicans ATCC 885/653* |
| **PP/CPA 30/70** | **the growth of microorganisms and fungi** | | | | | |
| PP/CPA/$Ag/Al_2O_3$ 30/70/0.5 | 14.1±0.9 | 14.7±0.2 | 13.0±0.5 | 12.9±0.6 | 14.0±0.4 | 13.9±0.8 |
| PP/CPA/$Ag/SiO_2$ 30/70/3.0 | 13.9±0.8 | 13.0±0.4 | 12.8±1.1 | 12.3±0.7 | 14.2±0.1 | 13.6±1.0 |

**Table 5** Antibacterial activity of nano-filled complex threads, defined by contamination method

| Exposition [days] | Δ [CFU/ml] | | | | | |
|---|---|---|---|---|---|---|
| | **PP/Ag/$Al_2O_3$** | | | **PP/Ag/$SiO_2$** | | |
| | *Staphylococcus aureus ATCC 6538* (5.60)* | *Pseudomonas aeruginosa ATCC 9027* (5.60)* | *Cadida albicans ATCC 885/653* (5.60)* | *Staphylococcus aureus ATCC 6538* (5.74)* | *Pseudomonas aeruginosa ATCC 9027* (5.65)* | *Cadida albicans ATCC 885/653* (5.60)* |
| Initial seeding | 0.98 | 0.95 | 0.95 | 1.06 | 0.96 | 0.98 |
| 2 | 3.21 | 2.21 | 2.21 | 3.27 | 2.26 | 2.43 |
| 7 | not found | 3.91 | 4.0 | 4.05 | 3.65 | 3.30 |
| 14 | microorganisms and fungi are not found | | | | | |

* logarithm of the microbial load [CFU/mL]

Antibacterial action of nano-filled complex threads from PP microfibers, which is defined by the method of contamination as the difference (*Δ*) between the values of logarithms of microbial load and number of viable colonies of cells of microorganisms through an appropriate time period, is shown in the Table 5. This value after two days shall be not less than 2, and after 7 days - not less than 3. In the future, the number of viable bacteria colonies should not grow.

For studies were selected complex threads formed from mixtures containing 0.5 wt.% Ag/$Al_2O_3$ and 3.0 wt.% Ag/$SiO_2$. The results show that the modified threads exhibit high antimicrobial and antifungal activity towards *Staphylococcus* reference strains of microorganisms and fungi of the genus *Cadida* (Table 5). Complex threads filled with nanoparticles Ag/$Al_2O_3$ are more effective compared with Ag/$SiO_2$ because alumina itself has high antimicrobial activity to some strains of microorganisms that is shown in the work [14].

## 4 CONCLUSIONS

It was established, that the addition of nano-fillers silver/silica and silver/alumina into the mixture polypropylene/copolyamide provides reduction of surface tension at the interphase zone, increasing of lifetime and reduction of instability of liquid jets of PP in matrix of CPA. Compatibilization action of additives depends upon their chemical nature and content. Nanoparticles Ag/$Al_2O_3$ are more effective compared to the Ag/$SiO_2$ and have the maximum impact on phase morphology of modified mixture at concentration of 0.5 wt.%, which corresponding to a minimum value of interfacial tension. Reducing the average diameter of the microfibers and increase their mass fraction due to a decrease spending for the formation of new surfaces and the stabilizing effect of nanoparticles on the finest microfiber PP by increasing the lifetime of almost 2 times.

It is shown that the complex threads of nano-filled PP microfibers are characterized by high tensile strength and elastic modulus that is connected with the effect of filling and with decreasing diameters of filaments. Modification of threads with silver-containing nano-additives provides them with anti-microbial properties and ability to protect against pathogenic organisms. The developed complex threads from nano-filled PP microfibers can be used to create new materials for medical purposes.

## 5 REFERENCES


1. Andrady A.L.: Science and technology of polymer nanofibers, John Wiley & Sons, Inc., Hoboken, New Jersey, USA, 2008, 404 p., ISBN-10: 0471790591
2. Biomedical Applications of Polymeric Nanofibers, R. Jayakumar, S.V. Nair (Eds.), New York: Springer, 2012, XII, 288 p., ISBN 978-3-642-27147-2
3. Egger S., Lehman R.P., Height M.J., Loessner M.J., Schuppler M.: Antimicrobial Properties of a Navel Silver-Silica Nanocomposite Material, Applied and Environmental Microbiology 75(9), 2009, pp. 2973-2976
4. Bohatyrov V.M., Oranskaya E.I., Galaburda M.V., Gerashhenko I.I., Osolodchenko T.P., Yusypchuk V.I.: Silica nanocomposites with compounds of silver, copper, zinc and their antimicrobial properties, Chemistry, Physics and Technology of Surface 7(1), 2016, pp. 44-58, (in Russian)
5. Li W., Karger-Kocsis J., Schlarb A.K.: Dispersion of $TiO_2$ Particles in PET/PP/$TiO_2$ and PET/PP/PP-g-MA/$TiO_2$ Composites Prepared with Different Blending Procedure, Macromol. Mater. Eng. 294, 2009, pp. 582-589
6. Rezanova N.M., Plavan V.P., Rezanova V.G., Bohatyrov V.M.: Regularities of producing of nano-filled polypropylene microfibers, Vlakna a Textil (Fibres and Textiles), 23(4), 2016, pp. 3-8
7. Tsebrenko M., Rezanova V., Tsebrenko I.: Polypropylene microfibers with filler in nano state, Chemistry & Chemical Technology 4(3), 2010, pp. 253-260
8. Sangroniz L., Palacios J.K., Fernandez M., Eguiazabal J.I., Santamaria A., Muller A.J.: Linear and non-linear rheological behavior of polypropylene/polyamide blends modified with a compatibilizer agent and nanosilica and its relationship with the morphology, European Polymer Journal 83, 2016, pp. 10-21
9. Krichevskij G.E.: Nano-, bio- and chemical technologies and production of a new generation of fibers, textiles and clothing, Moscow: Izvestiya, 2011, 528 p, (in Russian)
10. Volyanskyj Yu.L., Grytsenko I.S., Shyrobokov V.P.: Studying of the specific activity of antimicrobial

medical drugs: Methodic guidelines, Kyiv, State Pharmacological Center, 2004, 39 p., (in Ukrainian)

11. Determination of the sensitivity of microorganisms to antibacterial drugs, Methodic guidelines, Kyiv, MOZ of Ukraine, 2007, № MB 9.9.5-143-2007, (in Ukrainian)
12. Xiu H., Bai H.W., Huang C.M., Xu C.L., Li X.Y., Fu Q.: Selective localization of titanium dioxide nanoparticles at the interface and its effect on the impact toughness of poly(L-lactide)/poly(ether)urethane blends, eXPRESS Polymer Letters 7(3), 2013, pp. 261-271
13. Manson J., Sperling H.: Polymer blends and composites, New York: Plenum Press, 1976, 440 p.
14. Williams M.: Ions, not particles, make silver toxic to bacteria: News Releases, 2012, Access mode: http://news.rice.edu/2012/07/11/ions-not-particles-make-silver-toxic-to-bacteria-3

# THE INFLUENCE OF STRETCH FABRIC MECHANICAL PROPERTIES ON CLOTHING PRESSURE

**Nareerut Jariyapunya[1], Blažena Musilová[1], Jelka Geršak[2] and Smita Baheti[3]**

[1]*Department of Clothing,* [3]*Department of Textile Evaluation, Faculty of Textile Engineering, Technical University of Liberec, Studentská 2, 461 17 Liberec, Czech Republic*
[2]*Research and Innovation Centre for Design and Clothing Science, Faculty of Mechanical Engineering, University of Maribor, Smetanova 17, SI-2000 Maribor, Slovenia*
*nareerut.j@en.rmutt.ac.th, blazena.musilova@tul.cz, jelka.gersak@um.si*

***Abstract:*** *The stretch fabric is selected to be for sportswear which is considered to be of high importance to produce tight-fitting clothing for comfortable properties and body fitting to human body. The pressure comfort of clothing not only decreases size of pattern construction which has influence on the value of pressure but also the mechanical properties of stretch fabrics that change the value of the pressure when wearing on the body. The purpose of this research is to study the mechanical properties of eight stretch knitted fabrics with different elastic composition and to design 3D pattern construction which could eventually decreased 10% of pattern according to European standard size 38 clothing. The result of mechanical properties using OptiTex software represents the tension properties of fabric generated on the surface of the simulation model and uses for comparing 10 critical point marks of the body. Moreover, the pattern construction from 3D simulation was made into eight stretch fabric prototypes in order to measure the pressure of model and prototypes by PicoPress pressure tester. Besides, their pressure results were then compared between a real mannequin and lady human body.*

***Keywords:*** *Stretch fabric, tension of clothing, pattern construction, pressure comfort, tight-fitting clothing*

## 1 INTRODUCTION

The 3D simulation should not only be used for creating pattern but also to simulate for fabric properties. There are three major contributions to the 3D simulation of clothing; the pattern construction, body measurements of the model and the mechanical properties of fabric. R. Nemčoková measured the fabrics using the Kawabata Evaluation System for Fabrics (KES FB-Auto) and also applied the Design Concept3D software to enable the visualization of these models which showed the pressure, curvature, strain or tension and the elongation related to the mechanical properties of fabrics [1]. According to the pressure in wearing sportswear, it can be classified as high pressure sportswear, moderate and low pressure sportswear. In many cases their production requires automatic 2D digital customized apparel pattern generation system. Special technology is required that allows to us modification of pattern dimensions due to changing mechanical properties of a stretch fabric. Thus value of pattern design curves should be calculated using regression equations that each of them consists of the sum of characteristics that influence a pattern shape [2].

Stretch fabric for tight-fitting has been providing comfortable movement, minimizing the risk of injury or muscle fatigue, and reducing friction between body and clothing [3]. Patterns construction for tight-fitting garments which very closely contour the human body and therefore the physical movement is made, the comfort performance level changes and different parts of the body stretch very differently [4]. According to J. Geršak adjustment adapting an initial pattern of a tight-fitting garment is often done by decreasing the pattern-pieces [5]. The garment pattern-pieces are often, in practice, reduced by subjectively evaluating fabric elasticity, using only a manual elongation test. A simple and ordinary body movement expands the skin by about 10–50% [6]. Pressure garments are defined as custom made elastic garments that exert pressure on the body by virtue of the fact that they are made smaller than the body they are designed to fit [7, 8].

Accounting for garment pressure and comfort sensations at the waist, they have observed that in the lower garment pressure range (0-15 gf/cm$^2$) no sense of discomfort is there. In the medium range of garment pressure (15-25 gf/cm$^2$) negligible or only slight discomfort is perceived. But in higher pressure range, i.e. when the garment pressure exceeds 25 gf/cm$^2$, extreme discomfort is perceived Makabe H. et al [9]. The Reduction Factor method reduces all of the size measurements by a standard amount, typically between 10 and 20% [7, 8], regardless of the fabric used. Krzywinski et al. evaluate elastic properties of a fabric, wearing tests will determine the necessary load to match adequate garment fit with required comfort during wear. Investigations have shown that the feeling of comfort when wearing tight garments is reached at fabric elongation occurring at a load of 1.5 or 2.0 N $(5\ cm)^{-1}$ [10].

Ganssauge et al, Frydrych et al and Bereck et al used Fabric Assurance by Simple Testing (FAST) system to find out their mechanical properties [11-13]. N. Jariyapunya et al, compared the mechanical properties of knitted fabrics and measured them using (KES FB-Auto). The obtained results showed that the knitted structures have significantly influenced on the total hand value (THV) [14].

PicoPress sensor was used by Vinckx et al to measure the interface pressure occurred from the compression of elastic garment on a cylinder [15].

## 2 EXPERIMENTAL APPARATUS

Eight commercially produced knitted fabrics with different types of stretch knitted fabrics were varied in percentages for their elastic compositions and structurers as shown in the Table 1. The experiment on mechanical properties of the stretch fabrics had been tested by Fabric Assurance by Simple Testing (FAST) system to find out their mechanical properties such as relaxation shrinkage, hygral expansion, formability, extensibility, bending rigidity, shear rigidity, thickness, surface thickness and weight. The experiment preparation, pre-conditioning of more than 24 hours and testing were carried out under standard atmospheric conditions of 20±2°C temperatures and 65±5% relative humidity.

### *2.1 Mechanical properties of knitted fabrics*

The (FAST) system in Figure 1 illustrating the measuring principle of system in 3 separate tests including the FAST-1 compression meter in Figure 1(a), the FAST-2 bending meter in Figure 1(b) and the FAST-3 Extension meter in Figure 1(c)

The FAST-1 compression meter provides a direct measure of fabric thickness at 2 $gf/cm^2$ (196 Pa) and 100 $gf/cm^2$ (9.81 kPa) can be calculated fabric surface thickness as shown by the following formula 1:

$$ST = T2 - T100 \tag{1}$$

where *ST* is surface thickness [mm], *T2* is average thickness [mm] at 2 $gf/cm^2$ and *T100* is average thickness [mm] at 100 $gf/cm^2$.

The FAST-2 bending meter provides a direct measure of fabric bending length in either the wale or course direction. Bending rigidity is calculated from the bending length and fabric mass per unit area by formula 2:

$$B = W \times c^3 \times 9.81 \times 10^{-6} \tag{2}$$

where *B* is bending rigidity [μN.m], *W* is mass per unit area [$g/m^2$] and *c* is bending length [mm].

The FAST-3 Extension meter provides a direct measure of fabric extension under selected loads with wale and course directions. Shear rigidity is calculated from formula 3 which using extension on the bias at 5 gf/cm should be calculated:

$$G = 123 \div EB5 \tag{3}$$

where *G* is shear rigidity [N/m] and *EB5* has extension on the bias at 5 gf/cm.

Extensibility is measured at loads 100 gf/cm in wale and course directions of stretch fabric by using tensile tester because the fabric specimens had very high extension value with loading at *E100* (100 gf/cm) from FAST-3 Extension meter.

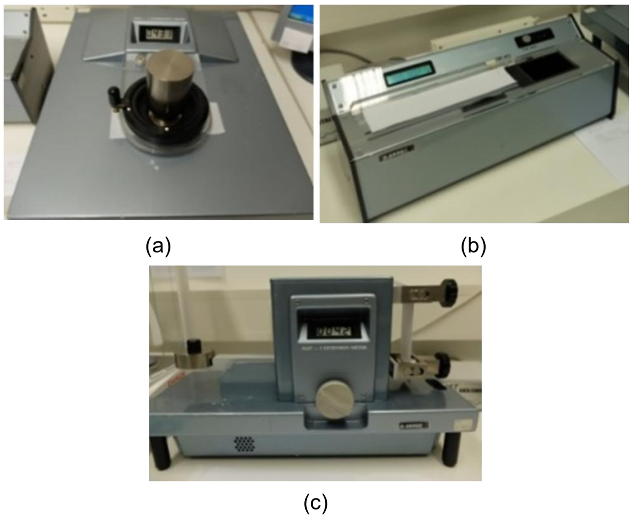

**Figure 1** Fabric Assurance by Simple Testing (FAST) system (a) FAST-1 compression meter, (b) FAST-2 bending meter and (c) FAST-3 Extension meter

**Table 1** Characteristics of stretch knitted fabrics

| Fibre composition | Weight [$g/m^2$] | Thickness [mm] | Structure |
|---|---|---|---|
| 1) 92% PA, 8% Lycra | 164.19 | 0.50 | Single Jersey |
| 2) 80% PA, 20% Elastane | 197.59 | 0.57 | Single Jersey |
| 3) 80% PA, 20% Lycra | 180.52 | 0.59 | Interlock |
| 4) 38% Outlast, 52% PES, 10% Spandex | 150.84 | 0.67 | Mesh |
| 5) 85% PA(6,6), 15% Elastane | 287.34 | 0.59 | Single Jersey |
| 6) 69% PA(6,6) Micro, 31% Elastane | 133.53 | 0.46 | Single Jersey |
| 7) 53% PA(6,6) Tactel Micro, 23% PA(6), 24% Elastane | 148.03 | 0.50 | Rib |
| 8) 78.5% PA, 21.5% Elastane | 131.75 | 0.36 | Single Jersey |

### 2.2 3D modeling and virtual 3D pattern simulation

The 3D simulated model will be determining the parametric model of female human body in accordance with standard European size body measurement of 38 and calculating the body measurement from the real rigid mannequin which is performed at Department of Clothing, Technical University of Liberec. This model simulation considers mainly on the upper part of female body in steady standing state as shown in the Figure 2(a). Moreover, the simulated model from European body standard size 38 used in the OptiTex was based on the height of 168 cm.

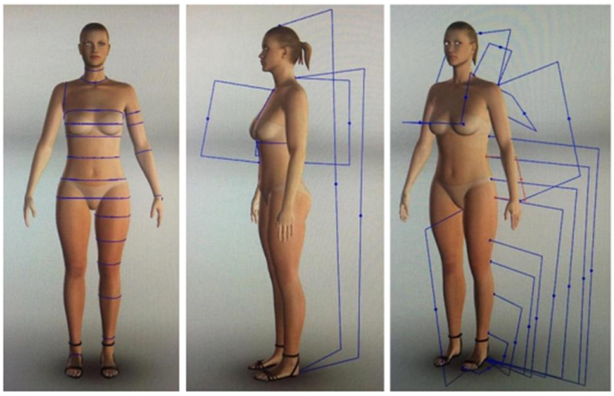

(a)

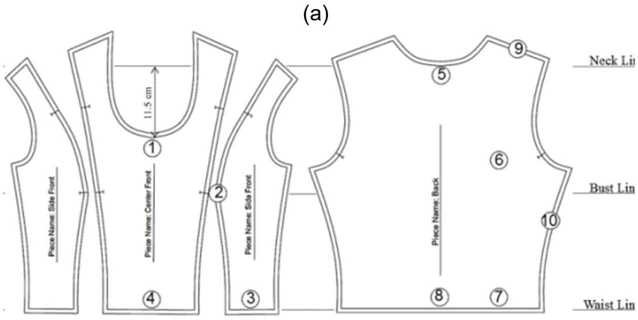


(b)

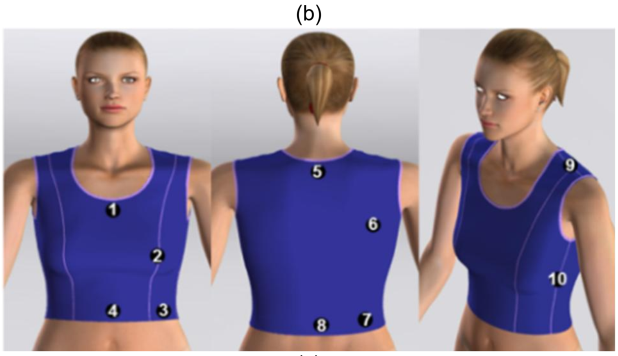

(c)

**Figure 2** Virtual pattern construction (a) Simulation model, (b) 2D Pattern and (c) Virtual draping simulation on the model

The pattern design system (PDS) designed from basic pattern construction that decreased the size of each pattern circumference approximately 10% in accordance with standard European size body measurement of 38 as in Figure 2(b) and mark 10 critical points which have extreme extension of clothing in order to determine those points for measuring tension and pressure value. The virtual sewed and draped on 3D model as in the Figure 2(c) determined grain line in wale direction on pattern pieces before simulating draping on the model.

**Table 2** The 3D simulation model body measurement

| | Circumference [cm] | | Length [cm] | |
|---|---|---|---|---|
| 1 | Under bust | 72.00 | Should slope | 4.68 |
| 2 | Waist | 70.00 | Cross shoulders | 38.10 |
| 3 | Hips | 96.00 | Bust height | 24.00 |
| 4 | Bust | 88.00 | Under bust height | 114.00 |
| 5 | Over bust | 84.00 | Out seam | 104.21 |
| 6 | Armscyet | 36.00 | Inseam | 79.50 |
| 7 | Neck | 29.00 | Armscye depth | 14.09 |
| 8 | Base neck | 36.00 | Bust to bust point | 20.00 |

### 2.3 Tension evaluation

The results of mechanical properties of stretch knitted fabrics measured by (FAST) system and converted properties for clothing simulation will be used in OptiTex 3D simulation to evaluate the tension map of clothing. The mechanical property requirements of stretch fabrics are extensibility, bending rigidity, shear rigidity, surface thickness, friction and weight. FAST tests are used for fabric definition in simulation software.

### 2.4 Clothing pressure

Eight clothing prototypes of stretch fabrics were sewed by a specialist from LISCA Company to control size of clothing at tolerant ±1/8 inch to produce clothing. These clothing were used to determine clothing pressure which had been measured by the pressure tester from PicoPress. The pressure was later compared between mannequin and human body by covering the cloths on the models. Then the pressure at the 10 critical marks of the body was measured as shown in the Figure 2(b and c).

## 3 RESULTS AND DISCUSSION

Parameters of elastic knitted fabric properties that resulted from OptiTex software simulation had been used to determine the tension map on the virtual mannequin are as follows: from Table 3, results of mechanical properties of fabric measure by FAST system were shown. Simulation of 3D tension map on stretch fabric distribution could help input parameter factors to evaluate amount of physical tension influencing on the clothing. Figure 3 illustrates gradient of 8 stretch knitted fabrics simulated by 3D tension map. The highest tension value was sample 5 with tension value of 24.47 fg/cm. and the lowest was sample 7 of 6.42 fg/cm. From the result, only one size of 2D pattern construction has been used according to Figure 2(b) and those images have shown each colour gradient depending on the range of the value of tension more or less. Therefore, they could not be compared to other images which illustrated the difference colour of tension distribution of clothing on the model simulation where the highest tension to the lowest tension from red, orange, yellow, green, light blue and dark blue respectively. However, the best solution for comparing the value of tension from eight stretch fabrics was to determine 10 mark points that refers from Figure 2(c) to find out the value of tension on each mark point.

The value of the stretch fabric tension from 10 different positions on the body as shown in Figure 2(b and c) had been compared with eight types of stretch fabrics in Figure 4. Obviously, second point mark had shown the highest tension value at bust position which has the most extreme extension of clothing when wearing. While the fabric made from 85% PA (6,6), 15% Elastane of sample 5, had the highest tension value because the percentage of extensibility in course direction was the lowest at 30.30%. The lesser the extension is applied on the fabric, the higher the tension is.

Besides, the first point mark, fifth point mark and ninth point mark had very low the value of tension at centre front neck, centre back neck and shoulder respectively. From the result, the tension value was very low at the pattern curve area which resulted in the circle shape of pattern. In case of the shoulder area, it showed lower value of tension due to the fact that, in course direction, the fabric had less extension which resulted in low value of tension from three mark points.

**Table 3** The Elastic knitted parameter from FAST system

| Parameter | | Fabric sample | | | | | | | |
|---|---|---|---|---|---|---|---|---|---|
| | | 1 | 2 | 3 | 4 | 5 | 6 | 7 | 8 |
| Bending rigidity [μN.m] | X (Wale) | 1.6 | 2.2 | 2.1 | 1.6 | 13.0 | 0.7 | 0.5 | 2.2 |
| | Y (Course) | 2.0 | 3.1 | 1.5 | 3.0 | 3.8 | 0.9 | 1.7 | 0.9 |
| Extensibility [%] | X (Wale) | 22.90 | 48.13 | 28.43 | 63.60 | 29.21 | 140.01 | 122.47 | 93.55 |
| | Y (Course) | 70.86 | 58.66 | 85.14 | 38.89 | 30.30 | 89.27 | 119.00 | 116.59 |
| Shear rigidity [N/m] | | 17.4 | 29.2 | 22.4 | 17.8 | 95.8 | 14.3 | 11.7 | 14.5 |
| Friction | | 0.204 | 0.218 | 0.073 | 0.286 | 0.359 | 0.339 | 0.301 | 0.306 |
| Surface thickness [mm] | | 0.124 | 0.075 | 0.290 | 0.275 | 0.105 | 0.094 | 0.105 | 0.048 |
| Weight [g/m$^2$] | | 164 | 198 | 181 | 151 | 287 | 134 | 148 | 132 |

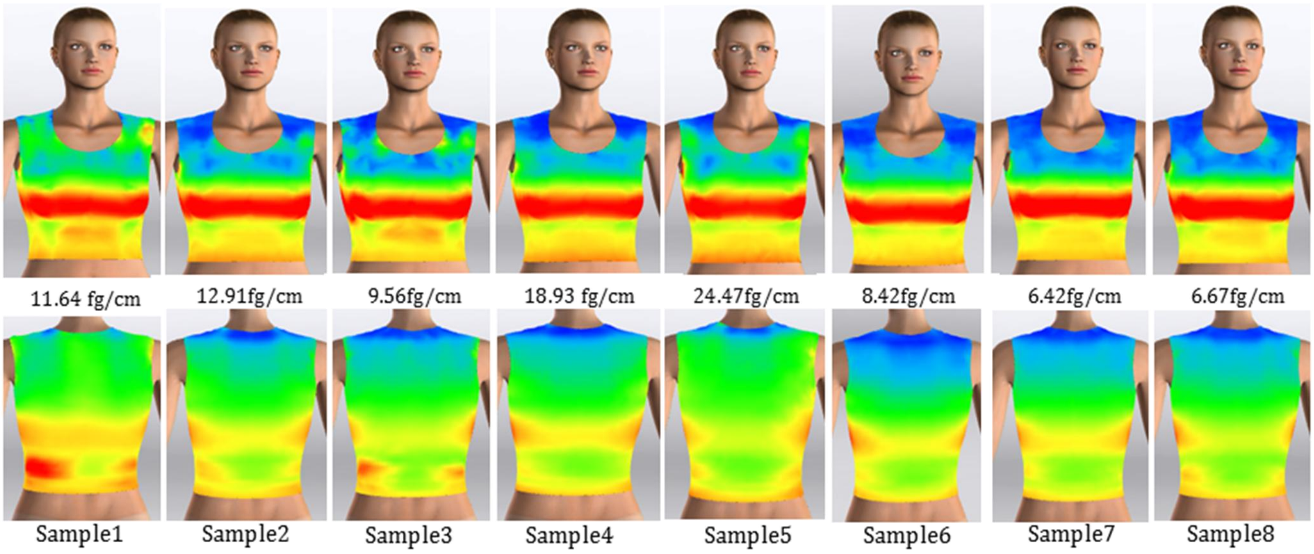


**Figure 3** Tension map gradient with different 8 stretch fabric samples

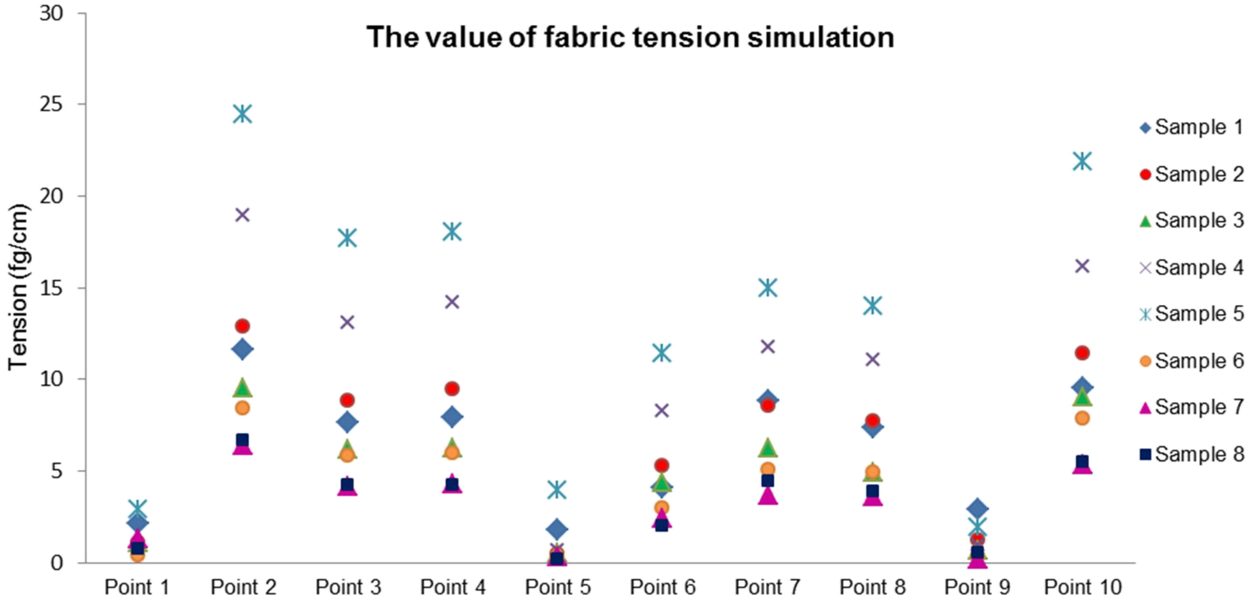


**Figure 4** A graph of the value of fabric tension with 10 different positions

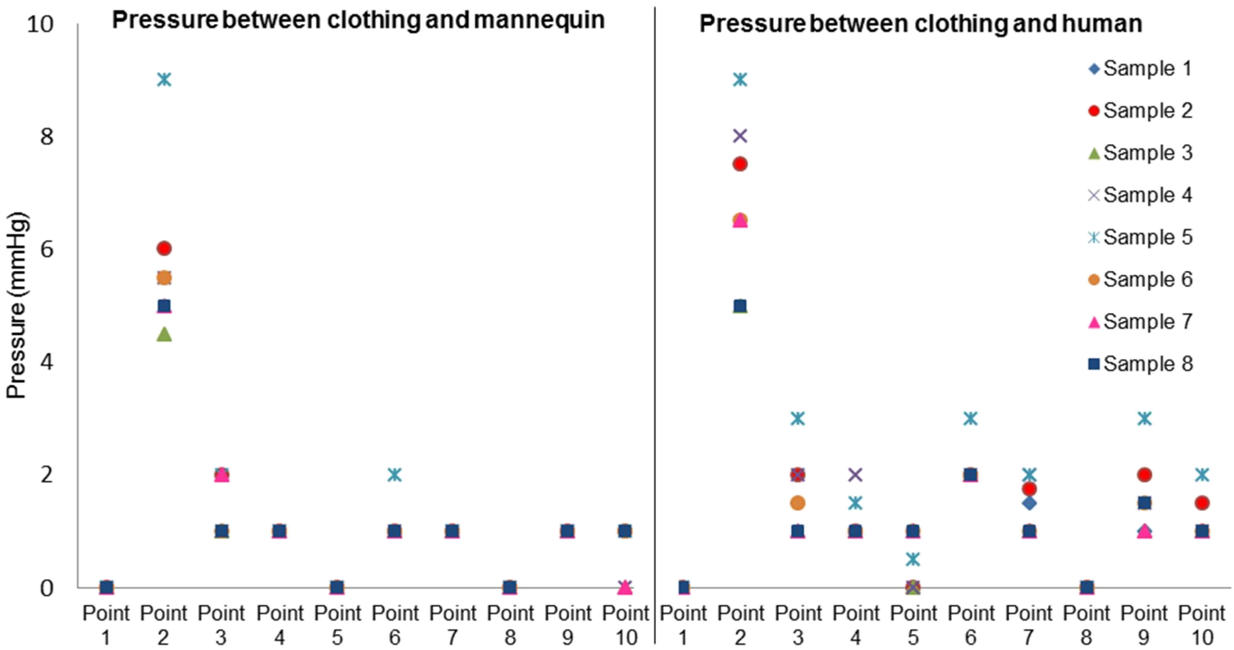


**Figure 5** A graph of pressure on mannequin and human comparing with 10 different positions of the body

In Table 4, the values of tension and extensibility at course direction were analyzed to find out their correlation values which were carried out based on the value of tension with different position of the body. The equations from linear regression were determined when Y is dependent variable of the value of tension and X is independent variable of the extensibility at course direction. It could be concluded that when $R^2$ value are almost strong correlation except those three points of 1$^{st}$ , 5$^{th}$ and 9$^{th}$ that mention the reasons above.

**Table 4** The correlation between tension and extensibility at course direction from 10 mark points

| Mark point | Equation from linear regression | Correction ($R^2$) |
|---|---|---|
| Point 1 | y = -0.0125x + 2.2736 | 0.26 |
| Point 2 | y = -0.1811x + 26.16 | 0.88 |
| Point 3 | y = -0.1334x + 18.624 | 0.86 |
| Point 4 | y = -0.1416x + 19.574 | 0.89 |
| Point 5 | y = -0.0255x + 2.9798 | 0.43 |
| Point 6 | y = -0.0902x + 11.982 | 0.84 |
| Point 7 | y = -0.1141x + 16.638 | 0.91 |
| Point 8 | y = -0.1066x + 15.303 | 0.89 |
| Point 9 | y = -0.0157x + 2.2877 | 0.31 |
| Point 10 | y = -0.161x + 23.096 | 0.88 |

Owing to 3D pattern construction simulated by OptiTex, eight prototypes of clothing had been produced with different types of stretch fabrics. Besides, clothing pressure had also been measured by the pressure tester from PicoPress. Figure 5 illustrates pressure graph between prototypes and a real mannequin where 10 point marks were compared on the body in both left and right side. While, Figure 5 also presents a graph which shows the measurement of pressure on a female human who has bust circumference of 90 cm. and waist circumference of 73 cm. The results of pressure tested by PicoPress tester from graph below shows similar trend where point mark number 2 reaches highest peak demonstrated in the line graphs.

## 4 CONCLUSION

It could obviously be seen after finding the tension value that stretch fabric value of course direction had an inverse influence on tension value; nevertheless, the extensibility value of wale had no influence on tension value. The results can be concluded that the highest tension value is at bust position and the highest tension is sample number 5, 85% PA (6,6), 15% Elastane at 24.47 fg/cm while the extensibility value is the lowest at 30.30% in course direction. Therefore, the lesser extensibility at course direction is, the higher the value of tension will be, which undeniably corresponded to linear regression and the correlation ($R^2$). At different positions except point mark 1, 5 and 9, $R^2$ were high while others are low. At the same time, the pressure value between a real mannequin and actual body are quite similar. Sample 5 was considered to have high pressure value while sample 7 and 8 had least when wearing which correlated to the percentage of stretch fabric in course direction. This could be concluded that the higher extensibility is the lesser pressure and also lower the value of tension will be on clothing and vice versa.

***Acknowledgement:*** *The authors would like to extend sincere appreciation to the Department of Clothing, Faculty of Textile Engineering, Technical University of Liberec and This work was supported by "SGS 21147" , Univ.-Prof. Dr. SC. Jelka Geršak, The Research and Innovation Centre for Design and Clothing Science, Faculty of Mechanical Engineering, University of Maribor. Department of Textile Engineering, Faculty of Engineering, Rajamangala University of Technology Thanyaburi as well as Dr. Danijela Klemenčič from LISCA Company in Slovenia.*

## 5 REFERENCES

1. Nemčoková R.: 3D Designing of the Product and the Effect of Mechanical and Physical Properties on the Shapes of Pattern, Vlákna a texti (Fibres and Textiles) 20(3), 2013, pp. 22-27
2. Musilová B. and Nemčoková R.: Implementing Mass Customization into Clothing Production, Vlákna a texti (Fibres and Textiles) 20(4), 2013, pp. 12-19
3. Taya Y., Shibuya A. and Nakajima T.: Evaluation method of Clothing Fitness with Body – Part 4: Evaluation by Waveform Spacing between Body and Clothing Journal Textile Machinery Society of Japan 48(11), 1995, pp. 261-269
4. Voyce J., Dafniotis P. and Towlson S.: Elastic Textiles, Textiles in Sport, Wood Head Publications, Cambridge, UK, 2005
5. Geršak J.: Design of clothing manufacturing processes, Woodhead publishing series in textile, 2013, 125
6. Voyce J., Dafniotis P. and Towlson S.: Elastic Textiles, In: Shishoo, R. (ed.), Textiles in Sport, WoodHead Publications, Cambridge, UK, 2005, 205
7. Macintyre L. and Baird M.: Pressure garments for use in the treatment of hypertrophic scars – a review of the problems associated with their use, 32, 2006, pp. 10-15
8. Macintyre L. and Baird M.: Pressure garments for use in the treatment of hypertrophic scars – an evaluation of current construction techniques in NHS hospitals, BURNS 31(1), 2005, pp. 11-14
9. Makabe H., Momota H., Mitsuno T. and Ueda K.: Effect of covered area at the waist on clothing pressure, Sen-iGakkaishi 4109, 1993, pp. 513-521
10. Krzywinski S., Tran Thi N. and Röder H.: Schnittgestaltung für körpernahe Bekleidung aus Maschenwarenmit Elastangarnen, Maschen-Industrie 6, 2002, pp. 36-39
11. Ganssauge D., Lehmann K.H., Angenadel A..: Wie Beeinflussen Typische Gewebemerkmale den Griff Einer Ware Melliand Textilberichte 6: s. 1998, 427-435
12. Frydrych I., Objective Evaluation of Handle Textile Rewiew (Prz. Wlok.) 4, 1997, pp. 9-12 (in Polish)
13. Bereck A., Dilldohner S., Mitze H., Weber B., Riegel D., Riegel M., Pieper J.M., Brakelmann A.: Eine neue, einfache Methode zur Messungder Weichnen textiler Flächengebilde. Teil 2. Einfluss der Ausrüstung auf die Gewebeweichheit Textilveredlung 32(9/10), 1997, pp. 216-222
14. Jariyapunya J., Musilová B. and Koldinská M.: Evaluating the Influence of Fiber Composition and Structure of Knitting Fabrics on Total Hand Value (THV), Applied Mechanics and Materials, ISSN: 1662-7482, Vol. 848, 2016, pp 211-215
15. Vinckx L., Boeckx W. and Berghmans J.: Analysis of the pressure perturbation due to the introduction of a measuring probe under an elastic garment, Medical and Biological Engineering and Computing 28(2), 1990, pp. 133-138

# EXPERIMENTAL INVESTIGATION OF MULTIAXIAL STRESS OF THE SEWING SEAM AND CREATING ITS NUMERICAL MODEL

**Natalia Kovalova[1], Petr Kulhavý[2], Josef Voséhlo[3] and Antonin Havelka[1]**

[1]*Department of Clothing*
[2]*Department of Machine Elements and Mechanisms*
[3]*Department of Nonwovens and Nanofibrous Materials*
*Faculty of Textile Engineering, Technical University of Liberec, Studentská 1402/2, Liberec, Czech Republic*
natalia.kovalova@tul.cz

***Abstract:** The presented work is based on experiments determining the strength of sewing seams in car seat covers. In order to understand the behavior of the seam on the car seat, it is necessary to create the conditions that will be close to real stresses. This experiment has been carried out on a designed device that simulates multiaxial stress. In this study, four different sizes of spun polyester and polyamide threads are used to sew the textile material (used for car seat cover) by a lockstitch sewing machine. By using the device made for measuring the multiaxial strain the average load of seam strength were obtained. After the experiments a theoretical calculation of the stress by finite element method (FEM) is follow. The carried models were drawn in Creo parametric and FEM analysis has been conducted in the software ANSYS. Based on the measurements of the individual components (strength of the material, threads in the loop…) and entire assembly has been compiled to make a numerical model.*

***Keywords:** technical textiles, seam strength, multiaxial stress, numerical model.*

## 1 INTRODUCTION

Sewing process is an important part of assembling some technical textile products. During the product usage, sewn seams and materials are subjected to variable loads leading to various deformations and some zones of them are put under intensive stretching [1]. The main prerequisites for a successful construction of a product, is the knowledge of mechanical properties of the used materials [2]. Determining the mechanical properties of technical textiles is very important mainly because of its applications in practice. In addition, in some cases, human life may be in danger due to a malfunction of these products (such as parachutes, airbags, safety belts ...) [3].

Automotive textiles represent the most valuable world market for technical textiles and within this segment there is a broad spectrum of products comprising novel textile structures with performance properties and attractive design [4]. The materials used to sewing the car seat cover are made for different materials, produced by different manufacturing methods and are subjected of mechanical loads during a processes of sewing and using [5]. The shape of car seat cover changes when it is loaded in use. The sewed textile material undergoes continuous stress on material and it is mostly visible at the seams. The most common include mechanical tensile stress. There are methods for detecting deformation and mechanical properties of materials, which are primarily focused on measuring material strength, seam strength and tensibility. The mechanical properties of the thread are very important for its performance and durability. Sewing thread requires high elasticity and for satisfactory performance [6]. The mechanical performance of threads is governed by the properties of constituent fibers and their arrangement. The friction, bending, and compression during the sewing process cause damage/pull-out of surface fibers resulting in a loss in mechanical properties [7].

Currently, for determining the strength of the seam the conventionally standard experimental methods, which are implemented as transversal uniaxial and biaxial stress in quasi-static mode. On the other side is not fixed standard method of measurement for determining the seams strength at multiaxial loading. For this purpose an instrument is fabricated that is part of tensile testing machine and serves to the determination of multiaxial sewing seam strength.

## 2 EXPERIMENTAL

### *2.1 Materials*

Material, needle and sewing thread have a direct influence on the quality of the seam. Selection the appropriate number and tip of the needle is important. Sewing thread selection depends on the thickness and composition of the material. Consequently, all these technical parameters should be compatible. In order to investigate the effect of different sewing threads on seam strength, four different threads were used for specimens preparing. Parameters are shown in Table 1.

**Table 1** Parameters of the sewing thread

| Property | Type B (Nm 30) | Type C (Nm 40) | Type H (Nm 30) | Type M1 (Nm 40) |
|---|---|---|---|---|
| Material | PA 6.6 | PA 6.6 | PES | PES |
| Density [tex] | 104 ± 15 | 77 ± 9 | 90 ± 5 | 77 ± 8 |
| Twist [t/m] | 340 ± 40 | 400 ± 50 | 370 ± 35 | 400 ± 40 |

Sandwich-type of fabric was use for preparing samples for testing mechanical properties of sewing seam under multiaxial loading. Exactly parameters of fabric are shown in Table 2.

**Table 2** Fabric parameters

| Parameter | Value |
|---|---|
| Width [mm] | 1520 ± 30 |
| Weight [g/m$^2$] | 560 ± 40 |
| Thickness [mm] | 6.4 ± 0.5 |
| Lamination [kg/m$^2$] | 35 (ESTERFOAM) |
| Material [g/m$^2$] | 100% PES |
| Backing [g/m$^2$] | 55 (65%PES/35%CO) |

### 2.2 Used method

A device which is part of the tensile testing machine used to measure sewing seam strength under the multi-axial stress was used. In this case the essential requirement is applied pressure at seam sample, and therefore it is necessary to choose the appropriate settings of the tensile machine. Instrument for measuring seam strength under multiaxial strain is presented in Figure 1. This device is consists of: clamping block, connector for fixing hemisphere, hemisphere, hook clamp, jaws, cylinder head screw, welded construction (pedestal).

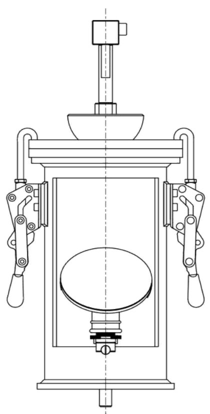

**Figure 1** 2D view of created device

Measuring device for seam strength under multiaxial stress is characterized by the stress in the seam occurs due to pushing of a spherical cap with a constant speed. In testing, the hemisphere moves vertically downward to the seam rupture with constant velocity of 100 mm/min. In order to minimize the shape instability of the knitted fabric, all samples were prepared in standard laboratory environmental conditions for 24 hours.

### 2.3 Theoretical seam strength

Theoretical transverse seam strength is the maximum value that can be achieved. Real transversal seam strength ($F_s$) is less than theoretical because the strength of the sewing thread decreases during the formation of stitch. It is characterized by the coefficient of the damage of the thread, which is the rest of the strength of the thread after the sewing.

$$F_s = 2 \cdot 10^{-4} \cdot (h \cdot b + 10) \cdot F_t \cdot F_{rts} \cdot F_{rtl} \cdot \alpha \tag{1}$$

where: $F_s$ - real strength of the seam [N],
$F_t$ - strength of the thread [N],
$F_{rts}$ - relative strength of the thread after sewing [%],
$F_{rtl}$ - relative thread strength in the loop [%],
$h$ - density of the stitch [cm$^{-1}$],
$b$ - width of the sample [cm],
$\alpha$ - coefficient of the seam.

## 3 MODEL SECTION

The first step before modeling was to explore how actually is going seam rupture. For a better comprehension the principle of the seam rupture and course of the experiments were monitored by using high-speed cameras i-SPEED 3. The examples of the seam rupture observation under multiaxial loading are shown below in the Figure 2. On the images, seam rupture places are clearly visible with a recording speed of 10 000 fps.

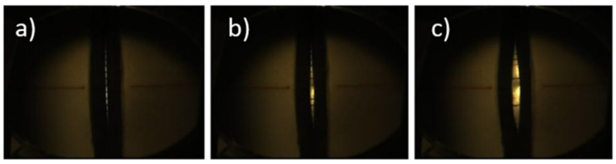


**Figure 2** Seam rupture place under multiaxial loading

### 3.1 CAD model

During the model creation it is necessary to pay attention to the model thread and fabric especially with regard to future numerical calculation. The seams with PA 30 threads were chosen to modelling. For creating a CAD model of the thread is the main parameter find out the most appropriate forming and carrier curve, which will be able to respond to sudden changes in the direction vectors and in the radius of curvature [2]. Defining thread model are shown in Figure 3.

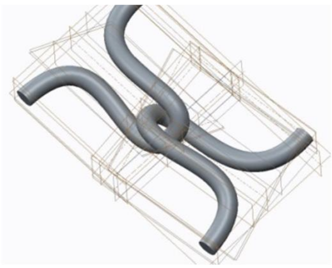

**Figure 3** Thread loop CAD model

The entire model has been verified by tracking global interferences of all parts, where any intersection no contact could not occur. To check geometry of the whole assembly this way is really necessary, especially in terms of solving the future numerical contact model.

### *3.2 Numerical model*

The created CAD geometry was imported into the commercial numerical software ANSYS. For thus geometrically complicated assembly was necessary to recreate a mesh with using a combination of the sweep method and the triangular polygons type of 187. Have been introduced the boundary conditions of the assembly (Figure 4).

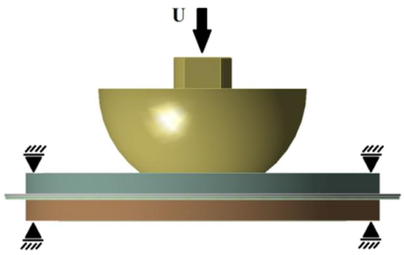


**Figure 4** The defined boundary conditions

In fixing jaws, the model was firmly fix in all directions and rotations. The displacement to a maximum value of 54.4 mm has been introduced into the impactor. The determined value corresponds to mean values of the measured displacements during which breach of threads in real samples occurred.

## 4 RESULTS AND DISCUSSION

The outputs of tensile experiment sewing seam strength under multiaxial stress are view in the Figures 5 and 6.

The outputs of the experiment of sewing seam strength in car seat covers revealed that seams with PA 30 threads have the highest strength and elongation and can be the most important for sew covers in comparison to other threads. According to (1) theoretical seam strength under multiaxial stress was calculated. Appropriate results are shown in Table 3.

The difference between theoretical and experimental seam strength in Figure 7 are shown.

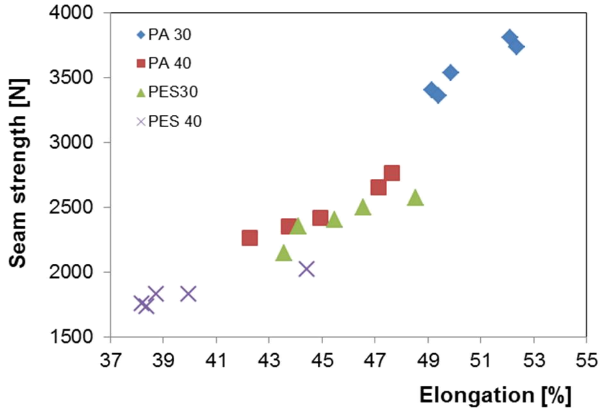


**Figure 5** Comparison between seam strength and elongation

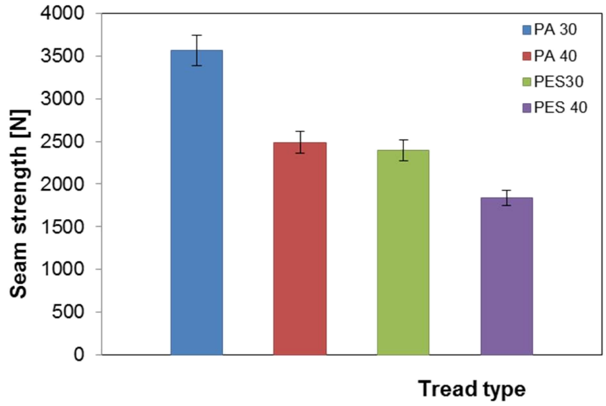


**Figure 6** The average of seam strength depend of the thread type

**Table 3** Calculation of the theoretical seam strength using prediction function

| Thread type | $F_t$ [N] | $F_{rtl}$ [%] | $F_{rts}$ [%] | $F_{st}$ [N] | $F_{sr}$ [N] |
|---|---|---|---|---|---|
| PA 30 | 70.7 | 69.6 | 95.8 | 3857 | 3566 |
| PA 40 | 52.5 | 68.0 | 91.8 | 2680 | 2489 |
| PES 30 | 59.6 | 60.6 | 87.7 | 2592 | 2395 |
| PES 40 | 48.6 | 67.6 | 88.2 | 2373 | 1837 |

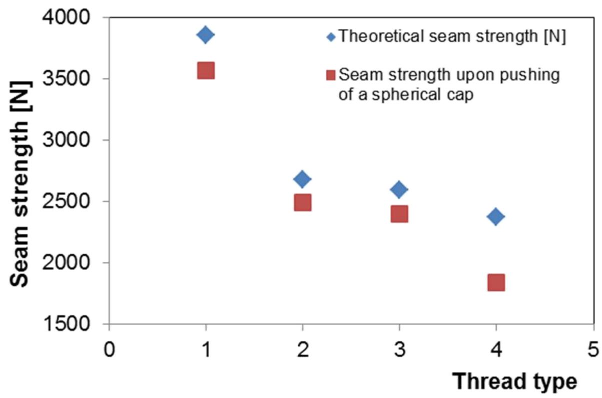


**Figure 4 -** Comparison between theoretical and real seam strength

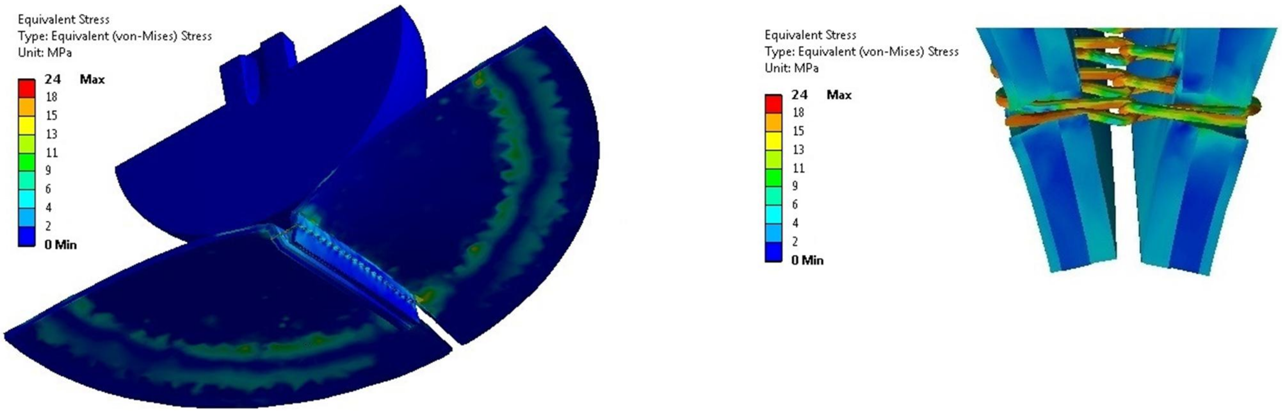


**Figure 5** Sectional view and detail of the observed von-Mises stress in the symmetric half of model

After the calculation of theoretical seam strength by using prediction function, the results showed the different between theoretical and experimental seam strength. Constantly, the values suggested that prediction function is usable for calculation of the theoretical seam strength under multiaxial stress.

The maximum Von Mises stress critical areas threads connection was observed. These results are shown on Figure 8.

The calculated values of force from the ANSYS were selected and export to excel. Further, the data from the program and the measured data of the experiment were compared. Simulated values correspond to the experimental values with a deviation of 8% in the force and 10% in the displacement (Figure 9).

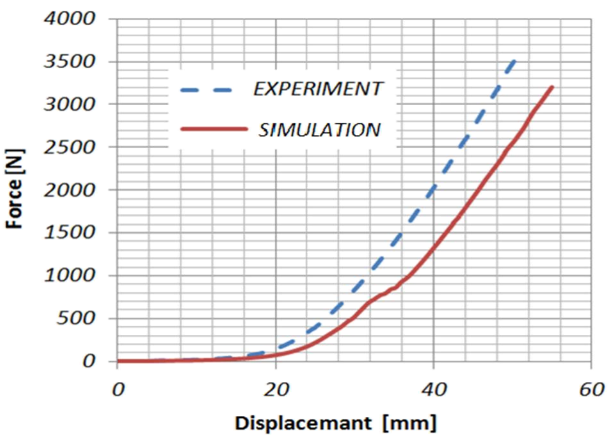


**Figure 6** The comparison of force and displacement between the real experiment and simulation

## 5 CONCLUSIONS

In this study, the method of sewing seam strength measurement has been proposed with following findings:

- The device for seam strength measurement under multiaxial stress was developed. It is very useful because of anisotropy of sandwich structure, seam strength of car seat covers could be investigated experimentally by using this special apparatus.
- Seam rupture place is located in the middle of the seam because of forces distribution and shape of forcing element. This consequence was discovered by monitoring the experiment by using a high speed camera.
- Theoretical seam strength by using prediction function was calculated. After the calculation, values of real (actual) seam strength and theoretical (nominal) seam strength were compared.
- Design CAD model with the sewing seam was imported to software Ansys 14.0 Workbench, where the model has been subjected to a simulation of pushing of a spherical cap. In the result we can see the real cause of breaking seam. Discontinuity occurs in the seam region, because the seam strength is less then material strength.

These results provide a better understanding of the mechanical properties of sewing seam, especially in technical textiles because this study was conducted in the field of car seat covers. Future research is needed an improvement of the apparatus for measuring the strength of a seam in the multiaxial strain, correction of the seam numerical model, because it helps to shorten the development cycle, which consists in preparing the samples-prototypes, testing them and re-sampling.

*ACKNOWLEDGEMENT: This work was supported by the Ministry of Education of the Czech Republic within the SGS project no.21145 on the Technical University of Liberec.*

## 6 REFERENCES


1. Germanova-Krasteva D., Petrov H.: Investigation on the seam's quality by sewing of light fabrics, International Journal of Clothing Science and Technology 20), 2008, pp. 57-64
2. Kulhavý P., Kovalova N., Vosáhlo J.: Numerical Model of the Static Loading of a Stitched Seam in the Composite Cover of Car Seat, Applied Mechanics and Materials 827, 2016, pp. 137-140
3. Dosedělová I.: Determination of sewn seam impact strength, In Acta Technica Corviniensis - Bulletin of Engineering, Scientific supplement of Annals of Faculty Engineering Hunedoara – International Journal of Engineering, Romania, Fascicule 4, 2009. ISSN: 1584-2665 [print], ISSN: 1584-2673 [CD-Rom]
4. The textile institute, Ed. by R. Sishoo, Textile advances in the automotive industry, Boca Raton [u.a.]$NCRC Press: Woodhead, 2008, ISBN 9781845693312
5. Kulhavý P., Kovalova N. a Vosáhlo J.: Methods of creating a numerical model of a real seam based on experimental data, EAN 2015-53rd Conference on Experimental Stress Analysis, Cesky Krumlov; Czech Republic, 2015, pp. 195-202
6. Midha V.K., Chatopadhyay R., Kothari V.K.: Studies on the Changes in Tensile Properties of Sewing Thread at Different Sewing Stages, Tex. Res. J. 79(13), 2009, pp. 1155-1167
7. Mazari A., Havelka A.: Sewing needle temperature of an Industrial lockstitch machine, Industria Textila, 65(6), 2014, pp. 335-339

# IMAGE ANALYSIS FOR CHARACTERIZING TENSILE DEFORMATION OF KNITTED FABRIC

**Smita Baheti[1], Nareerut Jariyapunya[2] and Maros Tunak[1]**

[1]*Department of Textile Evaluation*
[2]*Department of Clothing*
*Faculty of Textile Engineering, Technical University of Liberec, Studentska 2, Liberec, Czech Republic*
smita.baheti@hotmail.com

**Abstract:** *Elastic fabrics are considered to be of high importance to produce garments with comfortable fitting to the human body. However, the compression resulting from the tight-fitting of such clothing tends to generate high-pressure and discomfort while wearing them. In order to design comfortable knitted garments, it is necessary to predict their distribution of elastic behavior across different body sizes. The standard tensile testing methods are not sufficient to explain distribution of these elastic properties. When digital image analysis technique is adjusted to the standard tensile test method, more detailed study and additional results can be obtained. This work presented the digital image analysis method for the measurement of local deformations of knitted fabrics during tensile testing. The distributions of elastic properties of fabric under different levels of stretching were determined. The image analysis approach was selected to calculate the gradient deformation tensor under the extension ranging from 10 to 40% in respective course, wale and bias directions. The gradient deformation tensors were obtained by analysis of movements of dots painted on the specimen. In this way, the outcome of this work will help to construct knitted fabric structures with appropriate pressure distribution for comfortable body fitting.*

**Keywords:** *Knitted fabric, Comfortable body fitting, Image analysis, Threshold, Segmentation, Gradient deformation tensor*

## 1 INTRODUCTION

The development of the garment industry and social life positively influence the efficiency of clothes. The clothing can enhance the interactions between the body and the environment which in turn causes physical, physiological, and psychological comfort [1]. Consumers are keen to wear clothes which have the best comfort and performance. As specific example, the inherent benefits of stretch to comfort properties are increasingly utilized for applications in body fit garments used in sports. However, the optimization of stretch potential of such garments during pattern design is difficult to implement. The detailed measurement of critical material properties such as strain limit, strength coefficients, anisotropy coefficients, etc are required in order to optimize the design of patterns and manufacture of garments. Therefore, the deformation characteristics are very important from comfort aspects as it allows free movement of the wearer [2].

The measurement of deformations has always been an important topic in the evaluation of material properties, such as material strengths or fracture parameters. The most commonly used method for finding the material properties is tensile test. However, this system only provides an average strain over the specimen gauge length and is not applicable to post diffuse necking [3]. In other words, standard investigation methods are not always sufficient when analyzing the complex behavior of textile materials and new solutions need to be explored. The digital image analysis is a state of art technique that can be used for accurate strain measurement. By using the universal tensile test supplemented with an image analysis system, it is possible to capture not only the overall fabric deformation, but also the formation of localized deformation zones. Image analysis is well suited for the characterization of material properties due to faster data acquisition. It also has advantages of full field, non-contact, and high accuracy for displacement and strain measurements [4]. However, the drawback of this method is its sensitivity towards the surface of the research object. In addition, the digital camera characteristics, camera place and direction toward the object, the distance between the object and camera, and illumination conditions are important parameters to avoid the occurrence of image analysis errors [5, 6].

This work presents an investigation on local textile deformations during the tensile testing of knitted fabrics in course, wale and bias directions using image analysis technique. The grid pattern of black dots was applied on the specimen surface before the test and used as the reference points for image analysis [7, 8]. The concept of gradient deformation tensor was employed to estimate the relative displacement of marked points on textile surface under different stretch loading of 10, 20, 30 and 40% extension. Later, the obtained results were validated with simulated images generated by MATLAB image processing tool box. In this way, the image analysis method was successfully employed for estimation of deformation properties of elastic knitted fabrics for adequate fitting of garments to the required comfort.

## 2 EXPERIMENTAL METHODS

### *2.1 Capture of images under tensile deformation*

The elastic fabric containing 80% Polyamide (PA) and 20% Lycra was used for the experiment. The specimens were cut in course, wale and bias directions with dimensions of (length x width) of 30 cm x 5 cm. The samples were conditioned for 24 hours before actual testing in standard atmosphere of 21±1°C temperature and 65±2% relative humidity. The digital image analysis was applied for the standard textile tension test ASTM D 4964-96. The tensile force was applied at a speed of 100 mm/min and the gauge length was fixed at 20 cm. For the image acquisition and analysis, the specimen was applied with dot pattern of black color and the distance between the dots kept at 1 cm both in X axis and Y axis all over the fabric surface. Figure 1 shows the images of stretched textile specimen captured by a digital camera with resolution 4000x3000 pixels, ISO 200, aperture f2.2, shutter speed 1/15 s and distance to camera of 50 cm. The sequences of deformed images at every step of 10% of specimen elongation are shown in Figure 2 (a-d). A special algorithm is developed in MATLAB 7.10 (R 2010a) to automatically track the motions of the dots and compute their centroid coordinates in a sequence of images before and after particular extension percentage.

**Figure 1** Experimental setup for tensile test and image analysis

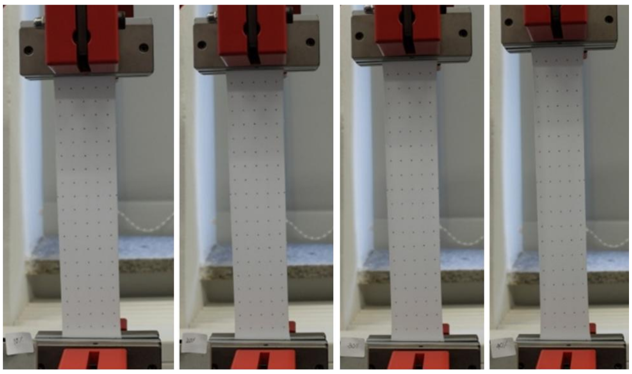

(a) 10% (b) 20% (c) 30% (d) 40%

**Figure 2** Captured images under different extension percentage

### *2.2 Concept of gradient deformation tensor*

The concepts of gradient deformation tensor are introduced to quantify the change in shape of infinitesimal line elements in a solid body. Figure 3 shows the straight line drawn on the undeformed configuration of a solid. However, after the deformation, the line becomes as a smooth curve.

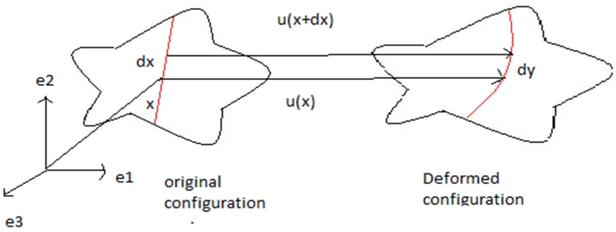


**Figure 3** Concept of gradient deformation tensor

When we focus attention on a line segment *dx*, much shorter than the radius of curvature of this curve, the segment would be straight in the undeformed configuration and almost straight in the deformed configuration. Thus, no matter how complex a deformation we impose on a solid, infinitesimal line segments are merely stretched and rotated by a deformation. If we know the displacement field in the solid, we can compute *dy* from the position vectors of its two end points:

$$dy_i = x_i + dx_i + u_i(x_k + dx_k) - (x_i + u_i(x_k)) \tag{1}$$

Expand $u_i(x_k + dx_k)$ as a Taylor series:

$$u_i(x_k + dx_k) \approx u_i(x_k) + \frac{\partial u_i}{\partial x_k} dx_k \tag{2}$$

$$dy_i = dx_i + \frac{\partial u_i}{\partial x_k} dx_k = \left(\partial_{ik} + \frac{\partial u_i}{\partial x_k}\right) dx_k \tag{3}$$

We identify the term in parentheses as the deformation gradient, so:

$$dy_i = F_{ik} dx_k \tag{4}$$

In general, deformation gradient tensor is given by:

$$F = I + \nabla u \tag{5}$$

or in Cartesian components:

$$F_{ik} = \partial_{ik} + \frac{\partial u_i}{\partial x_k} \tag{6}$$

$$F = \begin{pmatrix} 1+u_{11} & u_{21} \\ u_{21} & 1+u_{22} \end{pmatrix} \tag{7}$$

Where $\nabla u$ is the displacement gradient tensor, also expressed as $\frac{\partial u_i}{\partial x_k}$ and $I$ is the identity tensor described by the Kronekor delta symbol as:

$$\partial_{ik} = \begin{Bmatrix} 1, i = k \\ 0, i \neq k \end{Bmatrix} \tag{8}$$

## 3 RESULTS AND DISCUSSION

### *3.1 Improvement of image quality*

The acquired digital images were processed to remove the noise and improve the quality of images before calculation of gradient deformation tensor. Figure 4 shows the sequence of operations performed for image processing. Segmentation is the process in which an image is divided into constituent objects or regions of similar attributes. Segmentation extracts the desired object of interest from the background. Thresholding is a process of converting a gray-scale input image to a binary image. The purpose of thresholding is to extract those pixels from image which represent an object. In present work ISODATA thresholding was employed [9].

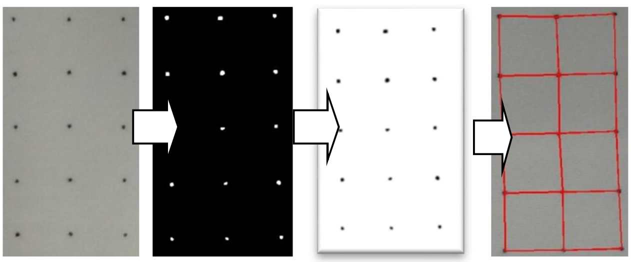

RGB image Compliment Thresholding Centroid

**Figure 4** Image processing steps

### *3.2 Validation of results with simulated images*

In order to confirm the accuracy of calculated gradient deformation tensor values, the results were validated with simulated images generated by MATLAB image processing tool box. Figure 5 (1-d) shows the simulated images for no extension, 30% extension in course, wale and bias directions respectively. The simulated images show that the gradient tensor deformation values also change in similar percentage with respect to the applied extension. This successfully validated the concept of image analysis for determination of elastic distribution properties of knitted fabrics.

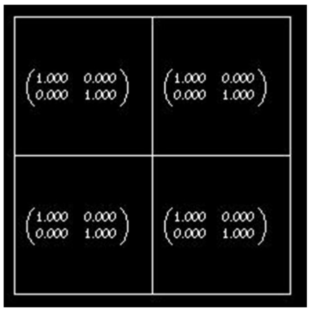

(a) No extension

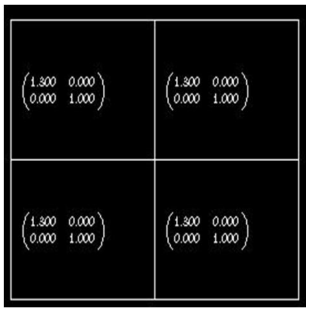

(b) 30% extension in course direction

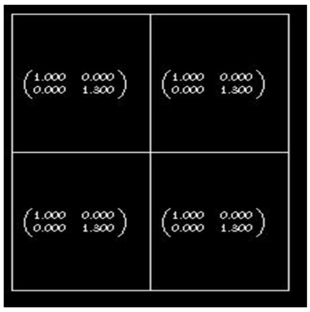

(c) 30% extension in wale direction

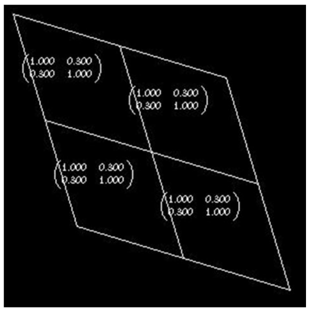

(d) 30% extension in bias direction

**Figure 5** Simulated images from MATLAB image processing toolbox

### *3.3 Determination of gradient deformation tensor in course direction*

The measurements of each grid point were obtained from gradient deformation tensor theory under the extension of 10, 20, 30 and 40%. The values of specimen local displacements in the longitudinal and perpendicular to the tension directions were estimated calculating the variation of each grid point height and width at every step of specimen elongation. Figure 6 (a-f) shows the calculated values of gradient deformation tensor for 0, 10, 20, 30 and 40% extension in course direction of knitted fabrics. It is clear that the images get stretched along with the points marked on them under different extension. The calculated gradient deformation tensor values were also found to change in similar percentage for each case, which proved accurate estimation of image analysis.

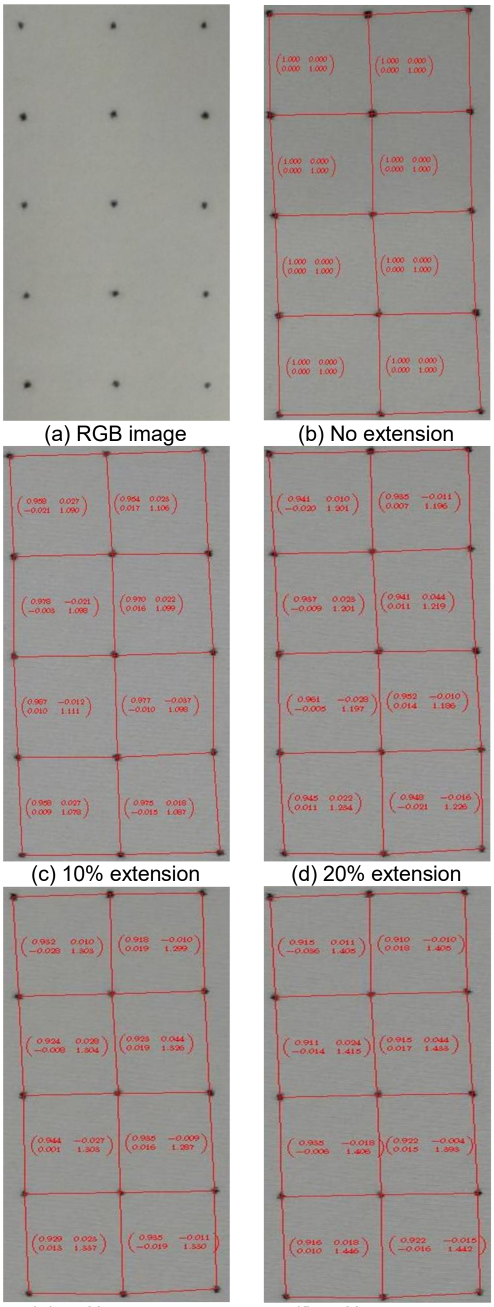

(a) RGB image (b) No extension (c) 10% extension (d) 20% extension (e) 30% extension (f) 40% extension

**Figure 6** Gradient deformation tensor for course direction extension

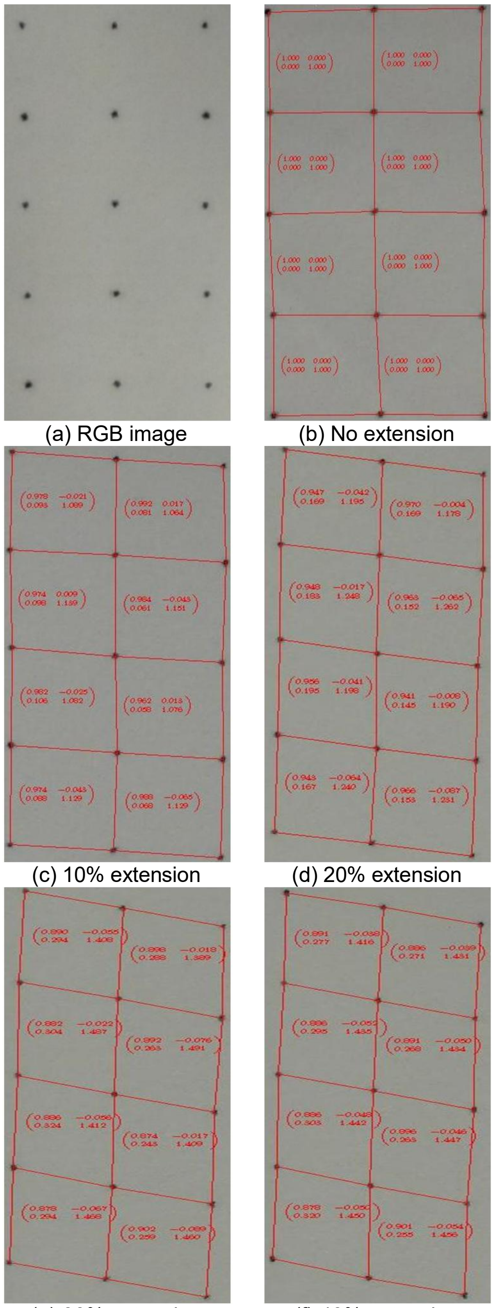

(a) RGB image (b) No extension (c) 10% extension (d) 20% extension (e) 30% extension (f) 40% extension

**Figure 7** Gradient deformation tensor for bias direction extension

### *3.4 Determination of gradient deformation tensor in bias direction*

Figure 7 (a-f) shows the calculated values of gradient deformation tensor for 0, 10, 20, 30 and 40% extension in bias direction of knitted fabrics. The calculated gradient deformation tensor values were found to change in similar percentage for each case, however not in similar pattern as in course and wale wise extension. This is due to different properties of knitted fabrics in bias directions in comparison to course and wale directions as a result of different loop structures.

At the end, the results of gradient tensor deformation co-ordinates for course and bias direction extension are summarized in Table 1.

**Table 1** Results of gradient tensor deformation

| | Extension [%] | $u_{11}$ | $u_{12}$ | $u_{21}$ | $u_{22}$ |
|---|---|---|---|---|---|
| | 0 | 1.000 | 0.000 | 0.000 | 1.000 |
| Bias direction | 10 | 0.978 | 0.021 | 0.098 | 1.089 |
| | 20 | 0.947 | 0.047 | 0.169 | 1.169 |
| | 30 | 0.890 | 0.055 | 0.294 | 1.406 |
| | 40 | 0.891 | 0.088 | 0.277 | 1.389 |
| Course direction | 10 | 0.958 | 0.027 | 0.001 | 1.090 |
| | 20 | 0.941 | 0.010 | 0.020 | 1.201 |
| | 30 | 0.932 | 0.010 | 0.028 | 1.308 |
| | 40 | 0.915 | 0.011 | 0.036 | 1.405 |

## 4 CONCLUSION

In this work, a robust and straight forward non-contacting method based on gradient deformation tensor concept was described. The estimation of knitted fabric extension deformation properties using image analysis of distinct dots applied on the test specimen was performed. This was done by using the camera images captured during the tensile testing of samples. The image analysis algorithm of gradient deformation tensor was developed to automatically track the motions of the dots and compute their centroid coordinates in a sequence of images before and after particular extension percentage. The validation of obtained results with simulated images obtained from MATLAB image processing toolbox showed accurate implementation of gradient deformation tensor concept for determination of elastic distribution properties of knitted fabrics. In this way, the outcome of this study will help to construct knitted fabric structures with appropriate pressure distribution for comfortable body fitting.

***ACKNOWLEDGEMENT:*** *This work was supported under the student grant scheme (SGS-21147) by Technical University of Liberec.*

## 5 REFERENCES

1. Meskuotiene A., Dargiene J., Domskiene J.: Metrological performance of the digital image analysis method applied for investigation of textile deformation, Textile Research Journal 85, 2015, pp. 71-79
2. Pazireh E., Gharehaghaji A. A., Haghighat E.: Study on the comfort of knitted elastic fabrics based on compressive deformation behavior, Journal of Engineered Fibers and Fabrics 9, 2014, pp. 83-89
3. Zhong T., Hu H.: Formability of weft-knitted fabrics on a hemisphere, Autex Research Journal 7, 2007, pp. 245-251
4. Jang L., Smith L., Gothekar A., Chen X.: Measure of strain distribution using digital image correlation (DIC) for tensile tests 2010, pp. 1-27
5. Sze Wei K., Saravanan K., Ridzuan Bin Abdul Latif M.: Development of an optical strain measurement method using digital image correlation, Asian Journal of Scientific Research 6, 2013, pp. 411-422
6. Dargiene J., Domskiene J.: Errors related to image analysis technique applied for the investigation of textile local deformations, Fibers and Polymers 14, 2013, pp. 1574-80
7. Striz B.: Mechanika Textilii, Cast 1. Zaklady mechaniky Kontinua [Scriptum] Liberec: Technical University of Liberec 2002, ISBN 80-7083-458-7
8. Rychnavska E.: Assessment of the impact of material properties of car seats during manufacturing process, Diploma Thesis, Technical University of Liberec 2010
9. Gonzalez R. C., Woods R. E.: Digital image processing, Prentice Hall Publishers 2002

# MOISTURE TRANSPORT PHENOMENA OF FUNCTIONAL UNDERWEARS

**Sajid Hussain[1], Viera Glombikova[1], Antonín Havelka[1], Hafsa Jamshaid[2], Syeda Sidra Batool[3] and Muhammad Zaman Khan[4]**

*[1]Department of Clothing, Faculty of Textile Engineering, Technical University of Liberec, Liberec, Czech Republic*
*[2]Department of Knitting, National Textile University, Faisalabad, Pakistan*
*[3]School of Textile and Design, University of Management and Technology, Lahore, Pakistan*
*[4]Department of Material Engineering, Faculty of Textile Engineering, TU of Liberec, Liberec, Czech Republic*
*sajid.hussain@umt.edu.pk; viera.glombikova@tul.cz; antonin.havelka@tul.cz; hrntu@hotmail.com; sidra.batool@umt.edu.pk; zamankhan017@yahoo.com*

***Abstract:*** *Moisture management property has a vital role in any kind of fabric used for inner layer or outer layer of garment. Moisture transportation from the skin to environment through textile material decides the comfort level of that fabric. Every human body sweats during different kinds of activities like walking, running or during exercise. But the main feature is that how efficiently a textile material transports liquid moisture out of the body to environment in order to make the wearer feel comfortable. This review paper reports the concept of moisture management, moisture management of different fibers, moisture management improvement in case of using different fiber blend, moisture management of spun and filament yarns and moisture management of different knitted fabric structures.*

***Keywords:*** *Wetting, wicking, functional underwears, moisture transportation, water vapor permeability, moisture transport properties, micro denier filament.*

## 1 INTRODUCTION

### *1.1 Moisture transport phenomena*

Moisture vapour permeability

It is the tendency of a textile material to transfer amount of sweat or moisture which is produced from human body during walking, running or playing some sports. There are different factors which are effective on moisture vapour permeability [1].

Moisture transportation of fabrics is one vital factor that affects the physiological comfort of textile structures. The moisture transfer behavior of textiles mainly depends mainly on the capillary capability and moisture absorbency of their fibers [2, 3].

The moisture transportation and quick drying behavior of knitted fabrics depend mainly upon the capillary action and moisture absorbency of their respective fibers. These characteristics are important in sport textiles next to the skin [4]. In these situations, textiles can absorb large amounts of sweat, draws liquid moisture to the outer surface in order to keep the body dry. In order to analyses these properties in sport clothing, it is necessary to evaluate the wicking behavior and immediate drying capability of functional knitted fabrics. Liquid transmission mechanisms include capillary wicking, which are determined by effective capillary pore distribution, surface tension, while the drying rate of a textile material is related to the macro molecular structure of the fibers [5-7].

Wetting and wicking

Wetting of a fabric surface is the result of its contact with a specified liquid under some conditions. There are two processes involved. Wettability of a textile material is the tendency of a surface to get interaction with a specific liquid [8, 9].

Then wicking process is performed after wetting of textile materials. Process of wetting can be divided into two sub processes. First one is essentially mechanical, is the escape of air from the substrate, and the other, mainly physio chemical, is the rate at which specific mass of material is wetted [10, 6].

### *1.2 Functional underwears*

Functional underwears maintains the temperature of human body under different climates. During alpine skiing and snowboarding [11], athletes experience alternating phases of physical activity and in these state functional underwear create an environment that maintains stable body climate in order to prevent the body from overheating or cooling down too much [2, 12]

Similarly in case of summer, when exercising or exposing to hot environment, fabrics may become wet because of continuous sweating. It is the ability of human body to transfer the heat and moisture outside in order to cool the body by means of sweating. Absorption of sweat, sweat spreading, and drying of a fabric determines the thermophysiological comfort property of the garment [13].Fabrics having good moisture transport properties and fabric drying properties are necessary for sportswear, underwear or other type of clothing which have direct contact with human skin [6, 12].

## 2 LITERATURE REVIEW

During continuous body movement like walking running or exercise, a person perspires and the cloth weared next to skin will get wet. The sports wears experience a barrier for quick transfer of excessive heat resulting in a rise in core body temperature and skin temperature which increases the speed of sweating. Due to the, fabric becomes wet and a person who has weared that fabric feels fatigue. There should be a fabric that has two types of properties [14].

First of them is the ability of perspiration evaporation from the surface of human skin and second one is to transfer moisture through the textile material to the environment in order to make the wearer comfortable. Sometimes moisture management refers to the transportation of both moisture vapour and liquid away from the body. The quicker a fabric can wick moisture, the more surface area the moisture covers on the fabric. In this way , quicker will be evaporation of the sweat and wearer will feel dry and comfortable [14].

Better moisture properties can be achieved by selecting the best fibers, yarns and knitted fabrics and fabric treatments. Moisture management properties of knitted fabrics can also be enhanced by using Multi-channelled or profiled fibers, micro-denier fibers, micro-porous fibers as well as suitable blends of hydrophobic and hydrophilic fibers. Similarly other properties like yarn structure, fineness, blend ratio and twist level also affects the knitted fabric moisture management properties. That is why fabric structure also plays an important role in improvement of moisture management properties of knitted fabrics [15-17].

Thermal comfort properties of knitted fabrics are influenced by the fibre, yarn and fabric properties. Fibre type, yarn manufacturing technology, yarn linear density; yarn twist, yarn hairiness, knitted fabric thickness, fabric tightness factor, fabric porosity and fabric finish are some of the factors, which play major role in determining the comfort properties of fabrics [18].

### *2.1 Moisture flow through different fibers*

*Cotton*

Cotton is composed of long chains of natural cellulose having carbon, hydrogen and oxygen. High moisture absorbency, high wet modulus its soft touch are some of important properties of cotton fibre [19].

Fabrics prepared by organic cotton provide better thermal comfort properties as compared to conventional cotton [20, 21]. Cotton fabric has good water absorbing property. It absorbs moisture from the human skin more quickly than synthetic fibers, and is generally more comfortable in normal conditions especially in summer. Cotton fabric keeps absorbed water inside its structure and its moisture transfer property is not very good especially during exercise in a humid and warm environment [22, 23].

*Polyester*

In the polyester fabrics, the water molecules are not absorbed due to their hydrophobic nature even polyester contributes to the wetness comfort by transporting the liquid quickly [24].

Channelled polyester fibers have ability of quick drying and moisture absorption properties having strong capillary effect, On the other side, hollow polyester fibers have higher thermal insulation properties due to the entrapping of air within the fiber structure [25].

Dacron is a four channel polyester fiber. It is observed that the fabrics prepared by Dacron improve the speed of evaporation of perspiration. Fabric prepared by this fiber is a superior fabric for wicking action, drying time, moisture absorption and transport [26, 27].

*Polypropylene*

Polypropylene having hydrophobic nature cannot wick liquid moisture. However, moisture vapour can be forced through polypropylene fabric by body heat generated. Polypropylene has the advantage of providing insulation when it is wet. Polypropylene is a good performer in moisture management due to its hydrophobic nature and due to its good thermal characteristics, it keeps the wearer warm in cold weather and cold in warm weather [28, 5, 29].

*Coolmax*

Coolmax by DuPont is either tetra-channel or hexa channel polyester, which has excellent wicking properties and that is why Coolmax pulls or "wicks" moisture away from the skin to the outer layer of the fabric. Presence of grooved sections allows moisture to escape by capillary action and that is why wearer feels comfortable because of fast drying [5, 30-32].

*Wool*

Wool is the second most important natural fibre. It is composed of protein: a mixture of chemically linkage amino acids that are the natural constituents of all living organisms. Protein in the wool fibre has a helical chain structure with strong inter- and intra-chain hydrogen bonding that is responsible for many of its unique properties. High extensibility of wool, natural crimp in fiber and its ability to trap air has a remarkable effect of comfort and warmth, which makes it an ideal insulating material [19, 27, 2].

Fabrics prepared by wool have excellent one way liquid transport capacity from the inner surface to the outer surface. Wool fabrics have high ability to manage the transportation of liquid moisture and highly suitable for skin layer for the active wear fabrics [33].

*Modal*

Modal is referred to high wet modulus and alkali resistance viscose fibers. Modal fibers possess lower elongation but higher wet modulus as it has high rate of polymerization. Modal is used for high quality woven and knitted materials. Modal is about 50 percent more water absorbent per unit volume than cotton. It has soft and smooth against the skin [34].

Knitted fabrics produced from 100% micro modal yarns with single jersey structure have the highest water vapor permeability. This fiber type is the best option to get superior water vapor permeability [35].

*Bamboo*

Bamboo has high water absorption and fast drying rate due to high amount of micro cracks and grooves in the fiber structure. Bamboo has ability to take up three times its weight in water. Bamboo has ability to wick water away from the human body three to four times quicker than cotton, keeping the wearer drier, cooler and comfortable [36-38].

Structure of bamboo fibers has vital property to make bamboo fabrics more breathable and thermal regulating than cotton, wool or some of synthetic fabrics. Bamboo knitted fabrics have high air and water permeability [34].

Bamboo yarns can be easily woven and knitted in any type of design and pattern. Bamboo has a thermal-regulating characteristic that keep wearer cool when climate is hot and warm when climate is cold. Clothes made of bamboo have a unique wicking ability that prevents fatigue under perspiration [33].

*Tencel*

TENCEL® fibers have sub microscopic channels between individual fibrils for best moisture wicking and moisture transportation. These fibers may be considered as hygroscopic nano-multifilaments. Even Tencel has higher moisture absorption capacity, but the moisture transportation and drying rate of Tencel fabrics are comparable with those of fabrics made from synthetic fibers [39-41].

*Nylon*

Killat N from Kanebo Ltd is a nylon hollow filament. The hollow portion of Nylon fiber is about 33 percent of the cross section of each filament that is why it gives better water absorbency and warmth retentive property. The yarn is spun as bi-component filament yarn with soluble polyester copolymer as the core portion and nylon as the skin portion [26, 42].

### *2.2 Moisture flow through different fiber blends*

Blending of different fibers has an important role in moisture-related properties of clothing [16, 43]. Moisture transmission through blended fiber assemblies is a complex phenomenon. Knitted structures should have good water vapour as well as liquid moisture transport property, in order to provide the thermo-physiological clothing comfort. The clothing should take up the moisture from the skin as well as transmit it to the atmosphere [44, 45].

Water vapour permeability and absorbency of the textile material has positive impact with the increased hydrophilicity of the material. A moisture absorbent material can absorb water vapour from the humid air in direct contact with the human skin and releases it in dry air. The quick response or rates greatly effects the thermo regulatory comfort properties, but hydrophilic fibers involvement has a positive effect on the liquid moisture transmission behaviour [44].

In case of blending wool with bamboo or wool with polyester gives better moisture management properties in case of knitted fabrics as compared to 100% bamboo and 100% wool fabrics [27].

As the bamboo content increases in the blended yarn, rate of moisture absorption is increased but decrease in wetting time of fabric, moisture spreading speed of sweat, maximum wetted radius and overall moisture management capacity of single jersey bamboo/cotton knitted fabrics [16].

In this study thermal conductivity value of knitted structures reduces as the blend ratio of bamboo fibre increases in the blended yarn. The water vapour permeability shows incredible increment as the blend ratio of bamboo fibre increases. If the blend proportion of cotton and bamboo is the same, then the thermal conductivity reduces, but the water vapour permeability increase as the yarn becomes the finer one [18].

Blending of polyester fibers with cotton improves moisture management properties. The spreading speed of polyester blended cotton fabrics was higher than that of 100% cotton fabric [46, 47].

### *2.3 Comparative effect of different fibers on moisture transportation*

Both fabric test results show higher air and less water vapor permeability for polyester than that for cotton fabrics. It is not confirm whether different sportswear knitted fabrics induce differences in the thermos-physiological responses during the exercise and after high intensity exercise in warm and humid environment [22].

Chen et al. [54] found that the antibacterial properties of fabrics prepared by bamboo are significantly higher than common viscose fabric. The reason is that bamboo fabric quickly absorbs and evaporates water molecules due to its favorable structure and that bacteria cannot survive in such a kind of dry environment. Xu, et al. [40] investigated that bamboo fibers exhibits good water retention power due to the many voids in cross section of fiber and bamboo fibers and conventional viscose fiber have better ability to absorb and release water than Tencel. Gericke and Jani studied properties of fabrics prepared by regenerated bamboo, cotton and viscose rayon yarns. According to the results, regenerated bamboo fibers made fabrics are very comfortable and have excellent moisture management properties [34].

A double-faced knitted fabric was constructed with polypropylene yarn for the inner surface and cotton yarn for the outer surface. Polypropylene having in inner layer easily transfers the generated sweat keeping a dry feeling. So it is recommended for summer, active, and sportswear, because of high moisture management property and high level of comfort in the wet condition [48].

In a comparison between the polypropylene and polyester in combination with other functional fibers, the functional knitted fabrics made with polypropylene face yarn are worse in wicking ability and better in drying capability than fabrics using a face polyester yarn [5].

### *2.4 Effect of yarn properties on moisture transportation*

Yarn structure plays an important role in moisture management properties of clothing. Structural arrangement not only affects the mechanical properties of yarns but also helps to regulate moisture management behavior of clothing that influences its comfort properties. Basic objective of generating micro pores in a fiber assembly is to provide better thermos-physiological comfort properties by enhancing the breath ability and resulting in improving moisture management behavior of textile structure. The transport of liquid in a fabric can take place through the available inter yarn spacing and through the inter fibre space in yarn. Generation of inter and intra yarn spaces in fabric results in better moisture transportation [49].

Moisture transportation through spun and filament yarns

Fiber fineness plays an important role in moisture and thermal properties of knitted fabrics. Knitted fabrics having yarns made from micro-denier fibers (e.g. micro-polyester, micro-nylon, micro-modal, micro-Tencel, micro-wool) show better moisture management properties as compared to those fabrics made from higher denier fibers [50].

Yarns which are made from micro-denier fibers have more capillaries per yarn cross-section. These extra capillaries per cross section improve moisture management and higher specific surface area for quicker drying [51-53].

Yarns having more filaments have more capillaries which enable structures to transport more liquid water. Low stitch density and higher thickness of knitted fabrics could enhance the water drop absorbency at transverse section. Fine fabrics having dense knitting structure could accelerate the dry rate. More the pores in structure could result in faster dry speed [54].

Knitted fabrics made from hydrophobic fibers with non-circular or channelled shaped fibers show better moisture management properties than those made from fibers of round cross-sections [1, 55]. Overall moisture management capacity (OMMC) of plaited knitted fabrics is considerably better due to increasing filament shape factor [56, 57].

Filament shape factor is calculated by the ratio of perimeter of filament cross section shape and perimeter of a circular shape which have same cross sectional area. Knitted fabrics made from filaments of higher shape factor show better one-way moisture transport capacity and very quickly moisture absorption rate, especially when these fabrics are present in the next-to-skin fabric layer [56, 45].

Fibers, having multi-channelled area, have been found to have increment in the horizontal and vertical wicking capacity of knitted fabrics [2]. Similarly micro-pores in the fiber structure also improve the moisture management properties of knitted fabrics. Polyester fiber with a micro-porous honeycomb structure was developed in order to improve moisture absorption and quick drying properties of knitted structures [7].

Knitted fabrics prepared by hollow fibers also provide better moisture transportation through enhanced capillary action as compared to conventional solid fibers [28].

The comparison of vortex and ring yarn knitted fabrics shows that the fabrics prepared by vortex yarn showed poor wicking and total moisture absorbency. Water vapour transmission properties for vortex yarn fabrics found to have improved as compared to the fabrics made up of ring spun yarns [43, 49].

### *2.5 Effect of different knitted fabric structure on moisture transport properties*

Thermo-physiological comfort properties of single layered fabrics are not better than double layered fabrics. Each layer has distinct function to perform; the layer next to the skin wicks away the perspiration quickly to the outer layer, which absorbs it and evaporates it quickly to the atmosphere. It takes away body heat and keeps the human body cool. On the inside a man-made textile material having good moisture transfer properties and good capillary action e.g. polypropylene, polyester, nylon, acrylic or is used [58, 59].

Whereas on the outside, a material which is a good absorber of moisture, e.g. cotton, wool, viscose rayon or their blends can be placed [13, 28, 29]. In a comparative study of single jersey and rib knitted fabrics prepared from cotton, viscose and polyester, it has been seen that polyester fabrics show best overall moisture management properties as compared to cotton and viscose [31, 24].

As there is no any water-bonding groups in polyester, polyester fibers perform better moisture wicking and cellulosic fibers like cotton are slow in transportation of moisture because of the hydrogen bonding with water molecules [24, 9].

In comparison to combined pattern fabrics, fleecy knitted structures have been found to give significantly greater initial water absorption rate and one-way moisture transport capacity [60, 61]. Double-layered knitted fabrics having yarns of same or different fibers (i.e. cotton-cotton, polypropylene-cotton, and cotton-polypropylene) on the both sides of knitted fabrics have been compared for overall moisture management properties. Fabric with polypropylene on inner-side and cotton on outer-side shows the best moisture management properties [48, 62].

An irregular pique knitted fabric was developed on a double knit machine having superior wicking and moisture management properties. The fabric was constructed with a non-microfiber yarns of polyester, nylon or polypropylene on the inner fabric side, and microfilament yarns on the outer fabric side in order to prove siphon to wick away the moisture form the wearer's skin [63].

Plaited single-jersey knitted fabrics of wool-polyester and wool-bamboo show better moisture management properties as compared to 100% wool, 100% bamboo or 100% polyester fabrics [27].

Moisture absorption properties are higher in knitted fabrics having float stitches as compared to the fabrics with all knit stitches. One-way moisture transport index and overall moisture management capacity (OMMC) is lower in single jersey structures in comparison with the knitted structures having float stitches [64, 31].

A moisture management knitted structure with denier differential mechanism was developed in which the yarns in the next-to-skin fabric layer are made from courser denier as compared to those yarns in the outer fabric layer. Moisture transported from the next-to-skin knitted fabric layer to the outer knitted layer due to an increment in surface area in the outer layer [63].

In another case, plaited double-knit structure has been constructed having inner layer comprising fine polyester yarns of coarser individual filaments, and outer layer having coarser spun polyester yarns prepared by finer denier fibers. This composite fabric was claimed to provide best wicking of the sweating away from the wearer's body to the outer side [57].

Knitted structures having combined construction and in plain and plaited single jersey having laid-in yarns construction of different fibrous contents in outer-layer has different values of moisture management properties. The most effective factor for moisture transport was the knitted fabric structure: fleecy fabrics can transport moisture more effectively compared to plain knitted fabrics [60].

Single jersey knitted structures has lower values of thermal conductivity and thermal resistance along with higher relative water vapour permeability than 1×1 rib knit structures and interlock knitted fabrics [8, 65].

These knitted structures also give a warmth feeling due to their lower thermal absorptivity values. That is why due to better moisture management and thermal properties, single jersey structured fabrics are better and should be selected for active sportswear and for summer apparel products. If we compare for single jersey, 1×1 rib and interlock fabrics, organic cotton will be better as compared to ordinary cotton to use for a warmer feeling [20, 21].

Increase in the fabric cover factor decreases the air permeability and improves the wicking ability especially in one hour measurements. It is determined that the fabric tightness is effective on different knitting structures in case of moisture management properties. The knitted structures having float stitches and the knitted structures which were fleece derivations have high values of OMMC values. If wearer is performing some physical activity in a hot weather, human body temperature will rise quickly and wetness will start. The knitted fabrics used in these weathers should have high wicking properties and good moisture management properties so that they transport liquid outside without the process of absorption. The structures having float stitches will be more suitable under these conditions [64].

## 3 SUMMARY

Moisture transport properties of all knitted structures can be improved by better selection of textile fibrous materials, suitable yarns and knitted structures. Multi-channelled fibers, micro-denier fibers, hollow fibers as well as blends of natural and synthetic fibers has quite effective for improvement of moisture transport and quick drying properties of knitted structures.

Yarn structure, yarn fineness, yarn blend ratio and yarn twist level also affect the knitted structure moisture transport properties. Along with the properties of fibers, fiber blends, yarn structure and yarn characteristics, it is very important that how this fabric is knit in the fabric.

Fabric structure seems to be much more important for effective achievement of moisture management properties. Major consideration in the knitted fabric structure is that which layer we are using next-to skin and are mostly more hydrophobic and better wicking yarns which absorb less amount of moisture, and the outer fabric layer of knitted structure has yarns which pull the moisture outwards and facilitate quicker evaporation. Selection of all these parameters can be important for making a knit structure of best moisture management properties.

## 4 REFERENCES


1. Varshney R.K., Kothari V.K., Dhamija S.: A study on thermophysiological comfort properties of fabrics in relation to constituent fibre fineness and cross-sectional shapes, J. Text. Inst. 101(6), 2010, pp. 495-505
2. Fangueiro R., Gonçalves P., Soutinho F., Freitas C.: Moisture Management Performance of Multifunctional Yarns Based on Wool Fibers, Indian J. Fibre Text. Res. 34, 2009, pp. 315-320
3. Sharabaty T., Biguenet F., Dupuis D., Viallier P.: Investigation on moisture transport through polyester/cotton fabrics, Indian J. Fibre Text. Res. 33(4), 2008, pp. 419-425
4. Jhanji Y., Gupta D., Kothari V.K.: Moisture management properties of plated knit structures with varying fiber types, J. Text. Inst, 106(6), 2015, pp. 663-673
5. Fangueiro R., Filgueiras A., Soutinho F., Meidi X.: Wicking Behavior and Drying Capability of Functional Knitted Fabrics, Text. Res. J. 80(15), 2010, pp. 1522-1530
6. Duru S.C., Candan C.: Effect of Repeated Laundering on Wicking and Drying Properties of Fabrics of Seamless Garments, Text. Res. J. 83(6), 2012, pp. 591-605
7. Wang F., Zhou X., Wang S.: Development processes and property measurements of moisture absorption and quick dry fabrics, Fibres Text. East. Eur. 73(2), 2009, pp. 46-49
8. Yanılmaz M., Kalaoğlu F.: Investigation of wicking, wetting and drying properties of acrylic knitted fabrics, Text. Res. J. 82(8), 2012, pp. 820-831
9. El Messiry M., El Ouffy A., Issa M.: Microcellulose particles for surface modification to enhance moisture management properties of polyester, and polyester/cotton blend fabrics, Alexandria Eng. J. 54(2), 2015, pp. 127-140
10. Patnaik A., Rengasamy R.S., Kothari V.K., Ghosh A.: Wetting and Wicking in Fibrous Materials, Text. Prog. 38(1), 2006, pp. 1-105
11. Schindelka B., Litzenberger S., Sabo A.: Body climate differences for men and women wearing functional underwear during sport at temperatures below zero degrees celsius, Procedia Eng. 60, 2013, pp. 46-50
12. Weder M., Rossi R.M., Chaigneau C., Tillmann B.: Evaporative cooling and heat transfer in functional underwear, Int. J. Cloth. Sci. Technol. 20(2), 2008, pp. 68-78
13. Liya Zhou, Xunwei Feng, Yanfeng Du, and Yi Li: Characterization of Liquid Moisture Transport Performance of Wool Knitted Fabrics, Text. Res. J. 77(12), 2007, pp. 951-956
14. Senthilkumar M., Sampath M.B., Ramachandran T.: Moisture Management in an Active Sportswear: Techniques and Evaluation-A Review Article, J. Inst. Eng. Ser. E 93(February), 2013, pp. 61-68
15. Paper C.: Liquid Moisture Management in Knitted Textiles – A Review Liquid Moisture Management in Knitted Textiles – A Review, no. MARCH, 2015
16. Prakash C., Ramakrishnan G.: Effect of blend proportion on moisture management characteristics of bamboo/cotton knitted fabrics, J. Text. Inst. 104(January), 2013, pp. 1320-1326
17. Cil M.G., Nergis U.B., Candan C.: An Experimental Study of Some Comfort-related Properties of Cotton--Acrylic Knitted Fabrics, Text. Res. J. 79(10), 2009, pp. 917-923
18. Majumdar A., Mukhopadhyay S., Yadav R.: Thermal properties of knitted fabrics made from cotton and regenerated bamboo cellulosic fibres, Int. J. Therm. Sci. 49(10), 2010, pp. 2042-2048
19. Pritchard M., Sarsby R.W., Anand S.C.: Handbook of Technical Textiles, 2000
20. Islam M., Rokon A.A., Rubel M.C., Ahmed M., Islam A.: Investigation on Comfort Properties of Conventional Cotton and Organic Cotton of Knitted Fabric Structures, Manuf. Sci. Technol. 2(3), 2014, pp. 62-66
21. An S.K., Gam H.J., Cao H.: Evaluating Thermal and Sensorial Performance of Organic Cotton, Bamboo-Blended, and Soybean-Blended Fabrics, Cloth. Text. Res. J. 31(3), 2013, pp. 157-166
22. Brazaitis M., Kamandulis S., Skurvydas A., Daniusevičiute L.: The effect of two kinds of T-shirts on physiological and psychological thermal responses during exercise and recovery, Appl. Ergon. 42(1), 2010, pp. 46-51
23. Dai X.Q., Imamura R., Liu G.L., Zhou F.P.: Effect of moisture transport on microclimate under T-shirts, Eur. J. Appl. Physiol. 104(2), 2008, pp. 337-340
24. Öner E., Atasağun H.G., Okur A., Beden A.R., Durur G.: Evaluation of moisture management properties on knitted fabrics, J. Text. Inst. 5, 2013, pp. 1-9
25. Oğlakcıoğlu N., Çay A., Marmaralı A., Mert E.: Characteristics of Knitted Structures Produced By Engineered Polyester Yarns and Their Blends in Terms of Thermal Comfort. 10(1), 2015, pp. 32-41
26. Soundri S.G.M., Kavitha S.: Textiles in sports, Int. J. Sci. 4(1), 2015, pp. 1010-1014
27. Troynikov O., Wardiningsih W.: Moisture management properties of wool/ polyester and wool/bamboo knitted fabrics for the sportswear base layer, Text. Res. J. 81, 2011, pp. 621-631
28. Ozdil N., Anand S.: Recent Developments in Textile Materials and Products Used for Active wear and Sportwear, Electron. J. Text. Technol. 8(3), 2014, pp. 68-83
29. Schneider A.M., Hoschke B.N., Goldsmid H.J.: Heat Transfer through Moist Fabrics, Text. Res. J. 62(2), 1992, pp. 61-66
30. Chaudhari S.S., Chitnis R.S., Ramkrishnan R.: Waterproof breathable active sportswear fabrics, Man-Made Text. India 47(5), 2004, pp. 166-174

31. Öner E., Okur A.: Thermophysiological comfort properties of selected knitted fabrics and design of T-shirts, J. Text. Inst. 106(12), 2015, pp. 1403-1414
32. Lizák P., Mojumdar S.C.: Thermal properties of textile fabrics, J. Therm. Anal. Calorim. 112(2), 2013, pp. 1095-1100
33. Liquid moisture transport performance of wool knitted fabrics for skin. 2009
34. S. Heat and T. Processes: Eco Friendly Fabrics., pp. 6-44
35. Badr A.A., El-Nahrawy A., Hassanin A., Morsy M.S.: Comfort and Protection Properties of Tencel/Cotton Blends, Beltwide Cotton Conferences, New Orleans, LA, January 6-8, 2014, pp. 1009-1020
36. Lipp-Symonowicz B., Sztajnowski S., Wojciechowska D.: New commercial fibres called 'bamboo fibres' - Their structure and properties, Fibres Text. East. Eur. 84(1), 2011, pp. 18-23
37. Mahish S.S., Patra A.K., Thakur R.: Functional properties of bamboo/polyester blended knitted apparel fabrics, Indian J. Fibre Text. Res. 37(3), 2012, pp. 231-237
38. Prakash C., Ramakrishnan G., Koushik C.V.: A study of the thermal properties of single jersey fabrics of cotton, bamboo and cotton/bamboo blended-yarn vis-a-vis bamboo fibre presence and yarn count, J. Therm. Anal. Calorim. 110(3), 2012, pp. 1173-1177
39. Abu-Rous M., Ingolic E., Schuster K.C.: Visualisation of the Nano-Structure of Tencel®(Lyocell) and Other Cellulosics as an Approach to Explaining Functional and Wellness Properties in Textiles, Lenzinger Berichte 85, 2006, pp. 31-37
40. Xu Y., Lu Z., Tang R.: Structure and thermal properties of bamboo viscose, Tencel and conventional viscose fiber, J. Therm. Anal. Calorim. 89(1), 2007, pp. 197-201
41. Schuster K.C., Suchomel F., Männer J., Abu-Rous M., Firgo H.: Functional and comfort properties of textiles from TENCEL® fibres resulting from the fibres' water-absorbing nanostructure: A review, Macromol. Symp. 244, 2006, pp. 149-165
42. Jhanji Y., Gupta D., Kothari V.K.: Comfort properties of plated knitted fabrics with varying fibre type, Indian J. Fibre Text. Res. 40(1), 2015, pp. 11-18
43. Oglakcioglu N., Celik P., Bedez Ute T., Marmarali A., Kadoglu H.: Thermal Comfort Properties of Angora Rabbit/Cotton Fiber Blended Knitted Fabrics, Text. Res. J. 79(10), 2009, pp. 888-894
44. Das B., Das A., Kothari V., Fanguiero R., Araujo M.D.: Moisture Flow through Blended Fabrics – Effect of Hydrophilicity, J. Eng. Fiber. Fabr. 4(4), 2009, pp. 20-28
45. Manshahia M., Das A.: Moisture management of high active sportswear, Fibers Polym. 15(6), 2014, pp. 1221-1229
46. Achour N.S., Hamdaoui M., Ben Nasrallah S., Perwuelz A.: Investigation of Moisture Management Properties of Cotton and Blended Knitted Fabrics, 9(7), 2015, pp. 891-895
47. Nazir A., Hussain T., Zia Q., Afzal M.A.: Improving thermo-physiological comfort of polyester/cotton knits by caustic and celluloses treatments, Autex Res. J. 14(3), 2014, pp. 200-204
48. Supuren G., Oglakcioglu N., Ozdil N., Marmarali A.: Moisture management and thermal absorptivity properties of double-face knitted fabrics, Text. Res. J. 81(13), 2011, pp. 1320-1330
49. Sharma N., Kumar P., Bhatia D., Sinha S.K.: Moisture Management Behaviour of Knitted Fabric from Structurally Modified Ring and Vortex Spun Yarn, J. Inst. Eng. Ser. E 97(2), 2016, pp. 123-129
50. Sampath M.B., Mani S., Nalankilli G.: Effect of filament fineness on comfort characteristics of moisture management finished polyester knitted fabrics, J. Ind. Text. 41(2), 2011, pp. 160-173
51. Karthik P., Arunkumar H., Sugumar S.: Moisture Management Study on Inner and Outer Layer Blended Fleece Fabric, Int. J. Eng. Res. Technol. 1(7), 2012, pp. 1-13
52. Sampath M.B., Aruputharaj A., Senthilkumar M., Nalankilli G.: Analysis of thermal comfort characteristics of moisture management finished knitted fabrics made from different yarns, J. Ind. Text. 42(1), 2011, pp. 19-33
53. Sampath M.B., Vasantha Kumar R..: Influence of moisture management finish on comfort characteristics of microdenier polyester knitted fabrics, Shodhganga@INFLIBNET Centre, 2014, xxi, 187, http://hdl.handle.net/10603/15507
54. Chen Q., Tang K.P.M., Ma P., Jiang G., Xu C.: Thermophysiological comfort properties of polyester weft-knitted fabrics for sports T-shirt, J. Text. Inst. 108(8), 2017, pp. 1421-1429
55. Su C.-I., Fang J.-X., Chen X.-H., Wu W.-Y.: Moisture Absorption and Release of Profiled Polyester and Cotton Composite Knitted Fabrics, Text. Res. J. 77(10), 2007, pp. 764-769
56. Manshahia M., Das A.: Thermophysiological comfort characteristics of plated knitted fabrics, J. Text. Inst. 105(5), 2014, pp. 509-519
57. Torres-Velazquez P.E.L.: Plaited Double-Knit Fabric with Moisture Management and Improved Thermal Insulation, 1(12), 2007
58. Govindachetty G., Sidhan P., Venkatraman K.C.: Thermo-physiological Comfort Properties of Polyester and Polyester/Acrylic blended Synthetic Fabrics treated with Herbal Finishes, J. Eng. Fiber. Fabr. 9(3), 2014, pp. 115-119
59. Wardiningsih W.: Study of Comfort Properties of Natural and Synthetic Knitted Fabrics in Different Blend Ratios for Winter Active Sportswear, Master of Technology thesis, RMIT University, Melbourne, 2009
60. Baltušnikaite J., Abraitienė A., Stygienė L., Krauledas S., Rubežienė V., Varnaitė-Žuravliova S.: Investigation of Moisture Transport Properties of Knitted Materials Intended for Warm Underwear, Fibers Text. East. Eur. 106(4), 2014, pp. 93-100,
61. Zhuang Q., Harlock S.C., Brook D.B.: Transfer Wicking Mechanisms of Knitted Fabrics Used as Undergarments for Outdoor Activities, Text. Res. J. 72, 2002, pp. 727-734
62. Bivainyte A., Mikučioniene D.: Influence of shrinkage on air and water vapour permeability of double-layered weft knitted fabrics, Medziagotyra 18(3), 2012, pp. 271-274

63. Wolfson M.I. , Dippert W.H.: Moisture Management Support Garment with a Denier Differential Mechanism, 1(12), 2002
64. Oner E., Okur A.: The effect of different knitted fabrics' structures on the moisture transport properties, J. Text. Inst. 104(11), 2013, pp. 1164-1177
65. Uçar N., Yılmaz T.: Thermal Properties of 1x1 2x2 3x3 Rib Knit Fabrics," Fibres Text. East. Eur. 12(3), 2004, pp. 34-38

# INSTRUCTIONS FOR AUTHORS

The journal ,,**Vlákna a textil**" (**Fibres and Textiles**) is the scientific and professional journal with a view to technology of fibres and textiles, with emphasis to chemical and natural fibres, processes of fibre spinning, finishing and dyeing, to fibrous and textile engineering and oriented polymer films. The original contributions and works of background researches, new physical-analytical methods and papers concerning the development of fibres, textiles and the marketing of these materials as well as review papers are published in the journal.

**Manuscript**

The original research papers are required to be written in English language with summary. The advertisements will be published in a language according to the mutual agreement.

The first page of the manuscript has to contain:

*The title of the article* (16 pt bold, capital letters, centred)

The full *first name* (s) and also *surnames* of all authors (11 pt, bold, centred).

*The complete address* of the working place of the authors, e-mail of authors (9 pt, italic, centred)

*Abstract* (9 pt, italic)

*Key words* (9 pt, italic)

***The manuscript*** has to be written in A4 standard form, in **Arial, 10 pt**.

The text should be in ***double-column format*** *(width 8.1 cm)* ***in single line spacing***.

*Page margins:* up and down 2.5 cm; left and right 2.0 cm.

***Do not number the pages and do not use footnotes. Do not use business letterhead.***

*Figures, tables, schemes and photos (centered)* should be numbered by Arabic numerals and titled over the table and under the figure or picture.

Photos and schemes have to be sufficiently contrastive and insert in text as pictures.

***Figures, tables, schemes and photos, please, send in separate file.***

*Mathematical formulae* should be centred on line and numbered consecutively on the right margin.

*Physical and technical properties* have to be quantified in SI units, names and abbreviations of the chemical materials have to be stated according to the IUPAC standards.

*References* in the text have to be in square brackets and literature cited at the end of the text. References (9 pt), have to contain names of all authors.

[1] Surname N., Surname N.: Name of paper or Chapter, In Name of Book, Publisher, Place of Publication, YYYY, pp. xxx-yyy

[2] Surname N., Surname N.: Name of paper, Name of Journal Vol. (No.), YYYY, pp. xxx-yyy

[3] Surname N., Surname, N.: Title of conference paper, Proceedings of xxx xxx, conference location, Month and Year, Publisher, City, Surname N. (Ed.), YYYY, pp. xxx-yyy

[4] Surname N., Surname N.: Name of Paper, Available from http://www.exact-address-of-site, Accessed: YYYY-MM-DD

The final template of manuscript is available on **http://www.vat.ft.tul.cz**

Authors are kindly requested to deliver the paper (in Word form) to be published together with information about at least 3 recommended reviewers from institutions others than the parent (name, e-mail, institution, department) by e-mail: marcela.hricova@stuba.sk

Address of the Editor Office:

**Marcela Hricová**

Faculty of Chemical and Food Technology,

Slovak University of Technology in Bratislava

Radlinskeho 9

812 37 Bratislava,

Slovakia